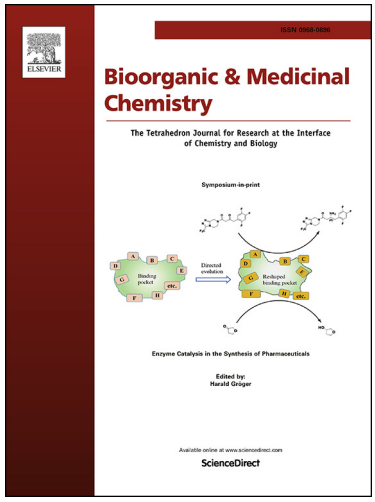

Synthesis, molecular docking, and QSAR study of bis-sulfonamide derivatives as potential aromatase inhibitors

Ronnakorn Leechaisit, Ratchanok Pingaew, Veda Prachayasittikul, Apilak Worachartcheewan, Supaluk Prachayasittikul, Somsak Ruchirawat, Virapong Prachayasittikul

PII: S0968-0896(19)31002-8
DOI: https://doi.org/10.1016/j.bmc.2019.08.001
Reference: BMC 15040

To appear in: *Bioorganic & Medicinal Chemistry*

Received Date: 14 June 2019
Revised Date: 30 July 2019
Accepted Date: 1 August 2019

Please cite this article as: Leechaisit, R., Pingaew, R., Prachayasittikul, V., Worachartcheewan, A., Prachayasittikul, S., Ruchirawat, S., Prachayasittikul, V., Synthesis, molecular docking, and QSAR study of bis-sulfonamide derivatives as potential aromatase inhibitors, *Bioorganic & Medicinal Chemistry* (2019), doi: https://doi.org/10.1016/j.bmc.2019.08.001

Synthesis, molecular docking, and QSAR study of bis-sulfonamide derivatives as potential aromatase inhibitors

Ronnakorn Leechaisit[a], Ratchanok Pingaew[a,*], Veda Prachayasittikul[b,*], Apilak Worachartcheewan[b,c,d], Supaluk Prachayasittikul[b], Somsak Ruchirawat[e,f], Virapong Prachayasittikul[g]

[a]*Department of Chemistry, Faculty of Science, Srinakharinwirot University, Bangkok 10110, Thailand*

[b]*Center of Data Mining and Biomedical Informatics, Faculty of Medical Technology, Mahidol University, Bangkok 10700, Thailand*

[c]*Department of Community Medical Technology, Faculty of Medical Technology, Mahidol University, Bangkok 10700, Thailand*

[d]*Department of Clinical Chemistry, Faculty of Medical Technology, Mahidol University, Bangkok 10700, Thailand*

[e]*Laboratory of Medicinal Chemistry, Chulabhorn Research Institute, and Program in Chemical Biology, Chulabhorn Graduate Institute, Bangkok 10210,Thailand*

[f]*Center of Excellence on Environmental Health and Toxicology, Commission on Higher Education (CHE), Ministry of Education, Thailand*

[g]*Department of Clinical Microbiology and Applied Technology, Faculty of Medical Technology, Mahidol University, Bangkok 10700, Thailand*

---

*Corresponding authors:

E-mail: ratchanok@swu.ac.th (R. Pingaew)

Tel: 662-649-5000 ext 18253; Fax: 662-260-0128

E-mail: veda.pra@mahidol.ac.th (V. Prachayasittikul)

Tel: 662-441-4376; Fax: 662-441-4380

Abstract

A library of bis-sulfonamides (**9-26**) were synthesized and tested for their aromatase inhibitory activities. Interestingly, all bis-sulfonamide derivatives inhibited the aromatase with IC_{50} range of 0.05-11.6 μM except for compound **23**. The analogs **15** and **16** bearing hydrophobic chloro and bromo groups exhibited the potent aromatase inhibitory activity in sub-micromolar IC_{50} values (i.e., 50 and 60 nM, respectively) with high safety index. Molecular docking revealed that the chloro and bromo benzene sulfonamides (**15** and **16**) may play role in the hydrophobic interaction with Leu477 of the aromatase to mimic steroidal backbone of the natural substrate, androstenedione. QSAR study also revealed that the most potent activity of compounds was governed by van der Waals volume (GATS6v) and mass (Mor03m) descriptors. Finally, the two compounds (**15** and **16**) were highlighted as promising compounds to be further developed as novel aromatase inhibitors.

Keywords: Sulfonamide; Bis-sulfonamide; Xylylenediamine; Aromatase inhibitor; Molecular docking; QSAR

1. Introduction

Estrogens (estrone, 17β-estradiol) are steroidal sex hormones which are biosynthesized by the conversion of their corresponding androgens (androstenedione, testosterone). This conversion reaction is catalyzed by the key rate-limiting enzyme called aromatase (CYP19), a member of the cytochrome P450 family.[1-7] Estrogens have been noted for their promoting roles in cancer cell growth, recurrence, and mestastasis of the hormone-dependent breast cancers. A reduction of estrogen levels by targeting the aromatase inhibition is one of effective current therapeutic strategies for management of breast cancer. Several aromatase inhbitors (AIs) have been developed including steroidal AIs and nonsteroidal AIs. Although clinical success stories have been noted for these available AIs, coping with their side effects (such as bone loss and cardiovascular disease) and potential resistance in prolonged use are still challenging.[8-11] Therefore, the search for novel classes of AIs still remains an essential on-going research issue.

Sulfonamides have been proven to be interesting scaffold that hold a wide range of biological activities including anticancer, antimicrobial, antimalarial, and antiviral activities.[12-16] This is owing to their potential structural features which are capable of multiple interactions with various biological targets.[16] Furthermore, sulfonamides are generally stable, easy to synthesize, while providing maximized pharmacological profiles such as oral absorption and low side effects.[13] Bis-sulfonamide comprising two groups of sulfonamide that could act as apoptotic inducing agents by disrupting anionic homeostasis of cell in cancer treatment.[17] Significantly, sulfonamide pharmacophore is found in AIs (**1**-**5**) [18-24] as shown in Figure 1 in which the molecular docking study revealed that both oxygen and nitrogen atoms of such sulfonamide group could form hydrogen bond with the target protein.[20-24]

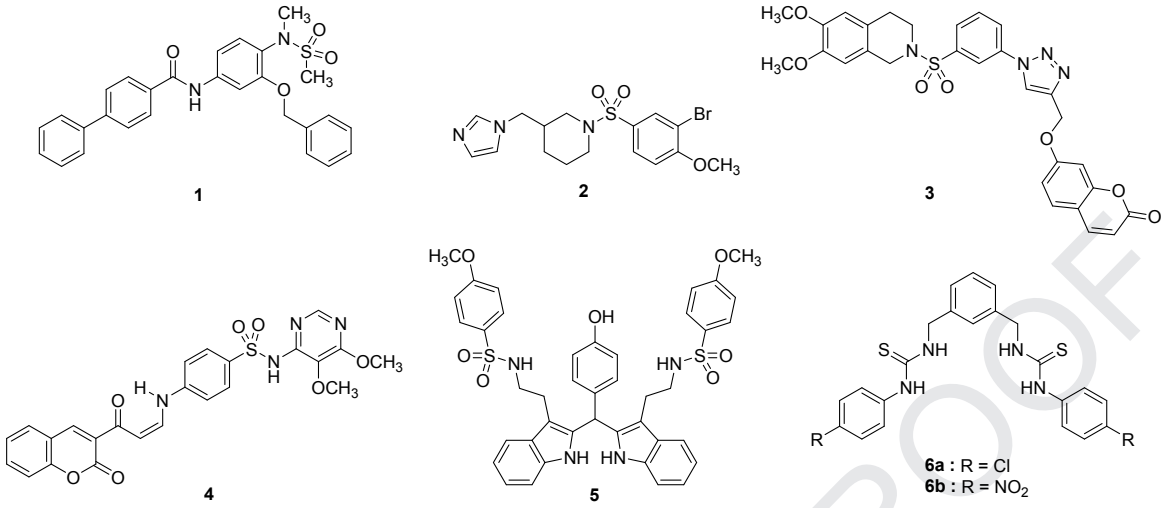

Figure 1. Representative aromatase inhibitors containing sulfonamide (**1**-**5**) and thiourea (**6**) moieties

Recently, our group has reported that bis-thioureas derived from *meta*-xylylenediamine exert aromatase inhibitory activity such as compounds **6a** and **6b** with IC_{50} = 5.5 and 0.8 μM, respectively.[25] The molecular docking study revealed that phenyl xylenyl thiourea moiety could mimic steroidal backbone of androstenedione (ASD) through hydrophobic interaction. In this article, it could be hypothesized that the replacement of thiourea moiety with a bioisosteric sulfonamide group might provide the compound with aromatase inhibitory activity.

To seek for a novel class of AIs, the design, synthesis and investigation on aromatase inhibitory activities of bis-sulfonamide derivatives (**9**-**26,** Scheme 1) have been studied. In addition, computational approaches, including molecular docking and QSAR, were further carried out to provide beneficial information for guiding the rational design and discovery of new potential AIs.

2. Results and discussion

2.1 Chemistry

Bis-sulfonamides (**9**-**21**, **23**, **24**) representing various substituents (R) on sulfonyl part were readily synthesized by alkylations of *meta*- or *para*-xylylenediamine **7a,b** with the corresponding sulfonyl chlorides **8a-m** in the presence of sodium carbonate in dichloromethane at room temperature. However, bis-sulfonamides (**25**, **26**) were obtained by the alkylations of *meta*-phenylenediamine **7c** with the appropriate sulfonyl chlorides **8a-m** in

refluxing pyridine (Scheme 1). Aminosulfonamide **22** was derived from the reduction of nitrosulfonamide **21** using stannous chloride in refluxing ethanol.

Structures of the desired bis-sulfonamides (**9-26**) were confirmed based on their NMR, IR and HRMS spectra. ^{1}H NMR spectra of compounds (**9-26**) typically showed a symmetrical signal of two sulfonamide parts ($NHSO_2Ar$), and a characteristic singlet or doublet signal of methylene proton at δ in the range of 3.8–4.1 ppm was appeared in compounds **9-24**. In addition, infrared spectra of the synthesized compounds displayed strong N–H absorptions at 3200–3400 cm^{-1}, and all bis-sulfonamides had molecular ion peaks corresponding to their molecular formula. ^{1}H NMR data of known compounds **9**, **11-13**, **16** and **19** are consistent with that reported in the literature[17].

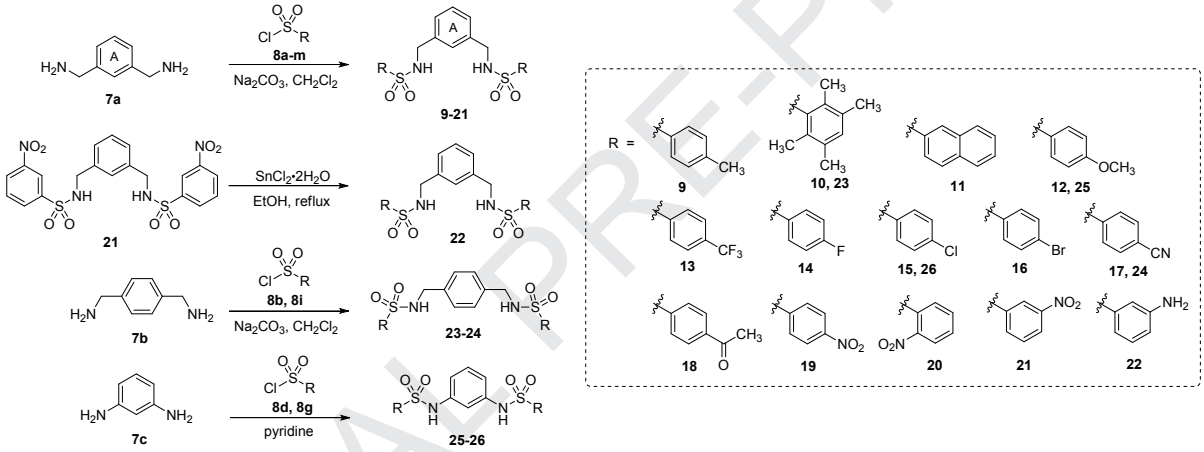

Scheme 1. Synthesis of bis-sulfonamide derivatives (**9-26**)

2.2 Aromatase inhibitory activity / Structure-activity relationship

Eighteen bis-sulfonamide derivatives (**9-26**) were evaluated for their abilities to inhibit the aromatase using letrozole (IC_{50} = 1.9 nM) as the reference drug. An overview about the effects of these inhibitors on the aromatase activity have been provided in Table 1. The investigated bis-sulfonamides comprised three different ring A (*meta*-xylylenediamine ring (**9-22**), *para*-xylylenediamine ring (**23-24**), and *m*-phenylenediamine ring (**25-26**)) as a core part on the nitrogen of sulfonamide whereas the sulfonyl groups of these sulfonamides bearing various R groups as substituted benzene and naphthalene rings.

Table 1 Aromatase inhibitory and cytotoxic activities (IC_{50}, μM) of bis-sulfonamides (**9-26**).

Compound	Aromatase inhibitory activity	cytotoxic activity		selectivity index[a] (SI)
		T47-D	MRC-5	
9	0.13±0.06	43.93±0.85	Non-cytotoxic	> 865.14
10	3.20±1.07	30.92±0.71	80.89±3.02	25.28
11	0.21±0.11	Non-cytotoxic	Non-cytotoxic	> 460.86
12	11.6±2.1	75.27±2.04	Non-cytotoxic	> 9.04
13	0.43±0.22	75.38±5.29	74.59±7.81	173.47
14	2.19±0.54	–[b]	Non-cytotoxic	> 50.46
15	0.05±0.01	37.47±2.15	68.52±1.08	1370.4
16	0.06±0.02	–[b]	Non-cytotoxic	> 1451.0
17	0.16±0.09	69.28±3.55	Non-cytotoxic	> 669.84
18	0.28±0.01	Non-cytotoxic	Non-cytotoxic	> 356.72
19	0.37±0.01	39.29±2.02	Non-cytotoxic	> 266.80
20	3.67±1.27	75.36±2.15	Non-cytotoxic	> 26.90
21	2.75±1.09	Non-cytotoxic	Non-cytotoxic	> 35.89
22	3.30±0.58	90.61±0.95	Non-cytotoxic	> 33.93
23	>12.5	Non-cytotoxic	16.27±0.86	–
24	0.66±0.16	Non-cytotoxic	92.83±4.24	140.65
25	0.53±0.11	Non-cytotoxic	Non-cytotoxic	> 210.34
26	0.78±0.12	87.22±4.39	63.10±1.24	80.90
Letrozole[c]	0.0019±0.0002	–	–	–
Doxorubicin[c]	–	0.88±0.021	2.19±0.37	–

T47-D = hormone-dependent breast cancer cell line; MRC-5 = normal embryonic lung cell line.
Non-cytotoxic= IC_{50}> 50 μg/mL.
[a] SI = IC_{50} for MRC-5/ IC_{50} for aromatase.
[b] Insoluble in testing medium.
[c] Letrozole and doxorubicin were used as reference drugs.

Results showed that all bis-sulfonamides (**9**-**26**) exhibited the aromatase inhibitory activities with IC_{50} in the range of 0.05-11.6 μM, except for *para*- ring A derivative with R = tetramethyl benzene **23** (inactive, IC_{50} > 12.5 μM).

Bis-sulfonamide **9** with R = 4-$CH_3C_6H_4$ showed the aromatase inhibitory activity with IC_{50} of 0.13 μM. Replacement of the R group of compound **9** with hindered R groups (2,3,5,6-tetramethylbenzene and naphthalene) as seen in compounds **10** and **11** decreased the inhibitory potency in 24.6-fold and 1.6-fold, respectively. It could be implied that steric effect of R groups is responsible for inhibitory potency. Reduction of the activity was noted for compound **12** with R = 4-$OCH_3C_6H_4$ (IC_{50} = 11.6 μM), compound **13** with R = 4-$CF_3C_6H_4$ (IC_{50} = 0.43 μM) and compound **14** with R = 4-FC_6H_4 (IC_{50} = 2.19 μM) compared with the compound **9** (R = 4-$CH_3C_6H_4$). Promisingly, the inhibition of aromatase was dramatically improved when hydrophobic halogen groups (Cl and Br) were introduced as seen in compounds **15** (IC_{50} = 0.05 μM) and **16** (IC_{50} = 0.06 μM). Comparable activity with compound **9** (R = 4-$CH_3C_6H_4$) was noted for bis-sulfonamide **17** with R = 4-CNC_6H_4 (IC_{50} = 0.16 μM) whereas reduction of the potency was seen in compounds **18** (IC_{50} = 0.28 μM) and **19** (IC_{50} = 0.37 μM) having the polar electron withdrawing substituents (4-$COCH_3$ and 4-NO_2) on the benzene ring. When 4-nitro group of the compound **19** was moved to 2- and 3-positions led to compounds **20** and **21** with decreasing 9.9-fold and 7.4-fold aromatase inhibitory potency, respectively. The polar electron donating amino compound **22** (R = 3-$NH_2C_6H_4$) diminished the aromatase inhibitory potency compared with the nitro compound **21**. It could be concluded that in the *meta*-isomer ring A, both of steric and electronic effects influenced the aromatase inhibitory potency. Apparently, the effect of R substituents increased the potency in the following trend: 4-Cl phenyl (**15**) ~ 4-Br phenyl (**16**) > 4-CH_3 phenyl (**9**) > 4-CN phenyl (**17**) > 2-naphthyl (**11**) > 4-CH_3CO phenyl (**18**) > 4-NO_2 phenyl (**19**) > 4-CF_3 phenyl (**13**) > 4-F phenyl (**14**) > 3-NO_2 phenyl (**21**) > 2,3,5,6-tetraCH_3 phenyl

(**10**) > 3-NH_2 phenyl (**22**) > 2-NO_2 phenyl (**20**) > 4-OCH_3 phenyl (**12**). It should be noted that the better activity may require higher lipophilicity with lower polarity as seen in compounds **15** (Cl) & **16** (Br) > **14** (F) and in **9** (CH_3) > **13** (CF_3).

Obviously, replacement of *meta*-xylene ring with *para* counterpart (compounds **10** vs **23** and compounds **17** vs **24**) afforded the compounds with decreased aromatase inhibitory potency. Considering the *meta*-isomers **15** and **26** bearing different hydrocarbon chain length on ring A, the compound **15** (R = 4-ClC_6H_4) displayed higher activity than the compound **26** (R = 4-ClC_6H_4, IC_{50} = 0.78 μM). This could suggest that the *meta*-xylene (**15**) is an appropriate size that can interact with the target site of action.

Previously, *meta*-bis-thioureas **6a** (R = Cl, Figure 1) was reported to exert the aromatase inhibitory activitiy with IC_{50} value of 5.5 μM, whereas 4-nitro compound **6b** (R = NO_2) displayed the most potent activity (IC_{50} = 0.8 μM).[25] In this study, *meta*-bis-sulfonamide **15** (R = 4-ClC_6H_4, Scheme 1) exhibited the most potent activity (IC_{50} = 0.05 μM) when compared with the nitro compound **19** (R = 4-$NO_2C_6H_4$, IC_{50} = 0.37 μM). The results indicated that the replacement of *meta*-bis-thiourea moiety[25] with *meta*-bis-sulfonamide analogs, mostly, provided the compounds with improved activity (Table 1).

2.3 Cytotoxic activity

The bis-sulfonamide derivatives (**9-26**) were assayed for their cytotoxic effects against hormone-dependent breast cancer cell line (T47-D). The results (Table 1) showed that compounds **9**, **10**, **12**, **13**, **15**, **17**, **19**, **20**, **22** and **26** exhibited weak to moderate cytotoxic activity against the breast cancer cells (IC_{50} 30.92-90.61 μM).

These sulfonamides (**9-26**) were also tested against the normal embryonic lung (MRC-5) cell line (Table 1). Most analogs were non-cytotoxic toward the normal cell whereas compounds **10**, **13**, **15**, **23**, **24** and **26** showed low cytotoxic effect. The most active compounds **15** and **16** displayed high safety index with the SI values of 1370.4 and >1451.0, respectively.

Additionally, some of these bis-sulfonamides (i.e., **9**, **12**, **13**, **16**, and **19**) have been reported to induce apoptosis of several types of cancer cells including breast cancer MCF-7 cell line. The apoptosis induction mechanism of these compounds was proposed to be *via* acting as an artificial Cl^- ion transporter leading to the disturbance of intracellular ion homeostasis and excessive production of reative oxygen speices (ROS).[17]

2.4 Molecular docking

Molecular docking was performed to reveal possible binding modes of bis-sulfonamide analogs (**9-26**) and the target aromatase enzyme. The validation of docking protocol was performed by redocking the co-crystallized ligand, ASD, towards its target (aromatase enzyme, PDB ID: 3EQM). The protocol provided acceptable accuracy as indicated by the redocking root mean standard deviation (RMSD) value of 0.705 A° (Figure 2A). The validated protocol was subsequently used for investigation of possible binding modes of the bis-sulfonamides **9-26**. All investigated bis-sulfonamides could bind within the same binding site as shown in Figure 2B. The binding modality of the most potent compound **15** is provided in Figure 2C.

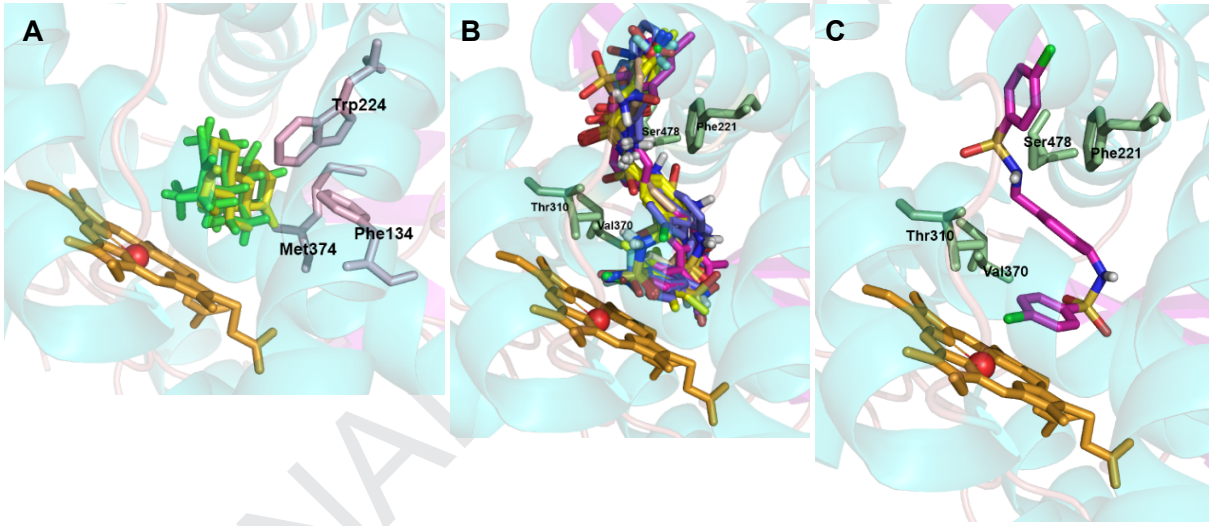

Figure 2. Heme and Fe atom are shown in orange and red, respectively. **(A)** Redocking of the co-crystallized ligand androstenedione (ASD) towards aromatase enzyme providing RMSD value of 0.705 A° (original and redocked poses are shown in green and yellow, respectively). **(B)** Docking poses of all investigated compounds **9-26**. **(C)** Binding modality of the most potent bis-sulfonamide **15**.

According to the experimental IC_{50} values, the active compounds could be classified into three groups. Compounds **15** and **16** (IC_{50} values < 0.1 µM) are considered the highly actives. The compounds with 0.1 < IC_{50} values < 1.0 µM (compounds **9**, **17**, **11**, **18**, **19**, **13**, **25**, **24**, and **26**) are classified as moderately actives. The compounds with IC_{50} values > 1.0 µM are classified as weakly actives (compounds **14**, **21**, **10**, **22**, **20**, and **12**). To elucidate the crucial chemical interactions which are essential for potent aromatase inhibitory activity, a

comparison of the 2D protein-ligand interactions of the bis-sulfonamide representatives from each group was also performed (Figure 3). Herein, the most potent compounds of each group are selected as the representative compounds (compounds **15** and **16** for the highly actives, compound **9** for the moderately active, and compound **14** for the weakly active).

In overview, the interaction diagrams revealed that the representative compounds from all groups shared some common features in forming the hydrogen bonding with Ser478, the π-π interaction with Phe221, and the hydrophobic interactions with Leu477, Phe221, Val370, and Thr310 residues of the enzyme (Figures 3A-3D). In contrast, the unique binding characteristics were observed for the two representative compounds from the highly active group (compounds **15** and **16**) including the hydrogen-bonding formation with His480 and the cation-π interaction with the Fe^{3+} of the enzyme (Figures 3A and 3B). The comparison of binding interactions of these two compounds with that of the natural ASD also revealed that the substitution of the halogen atoms on the terminal benzene rings (R groups) of the bis-sulfonamides (i.e., Cl atom in compound **15**, and Br atom in compound **16**) may play role in the formation of hydrophobic interaction with the Leu477 to mimic steroidal backbone of the ASD (Figures 3A, 3B, and 3E). Additionally, these structural features may facilitate the formation of cation-π interaction between one of the terminal substituted benzene ring (R group) and the Fe^{3+} of the enzyme (Figures 3A, 3B). In summary, molecular docking indicated that the hydrogen-bond formation with His480 as well as the cation-π interaction with Fe^{3+} of the enzyme are suggested to be crucial binding features for the highly potent activities of the halogen bis-sulfonamide analogs **15** and **16**. As the above mentioned, such hydrophobic interaction with Leu477 and Phe221, hydrogen bonding with Ser478, π-π interaction with Phe221, and cation-π interaction with Fe^{3+} of the enzyme, except for H-bond formation with His480, were also observed for the bis-thiourea **6b**.[25] The more potent activity of bis-sulfonamides (**15** and **16**) than bis-thiourea **6b** could be facilitated by the His480 in forming H-bond with the aromatase enzyme.

Accordingly, His480 residue crucial for the aromatase inhibition has been supported by mutagenesis studies[26,27] and the compounds **15** and **16** could mimic nonsteroidal AIs such as letrozole by the characteristic interaction with heme[1,28].

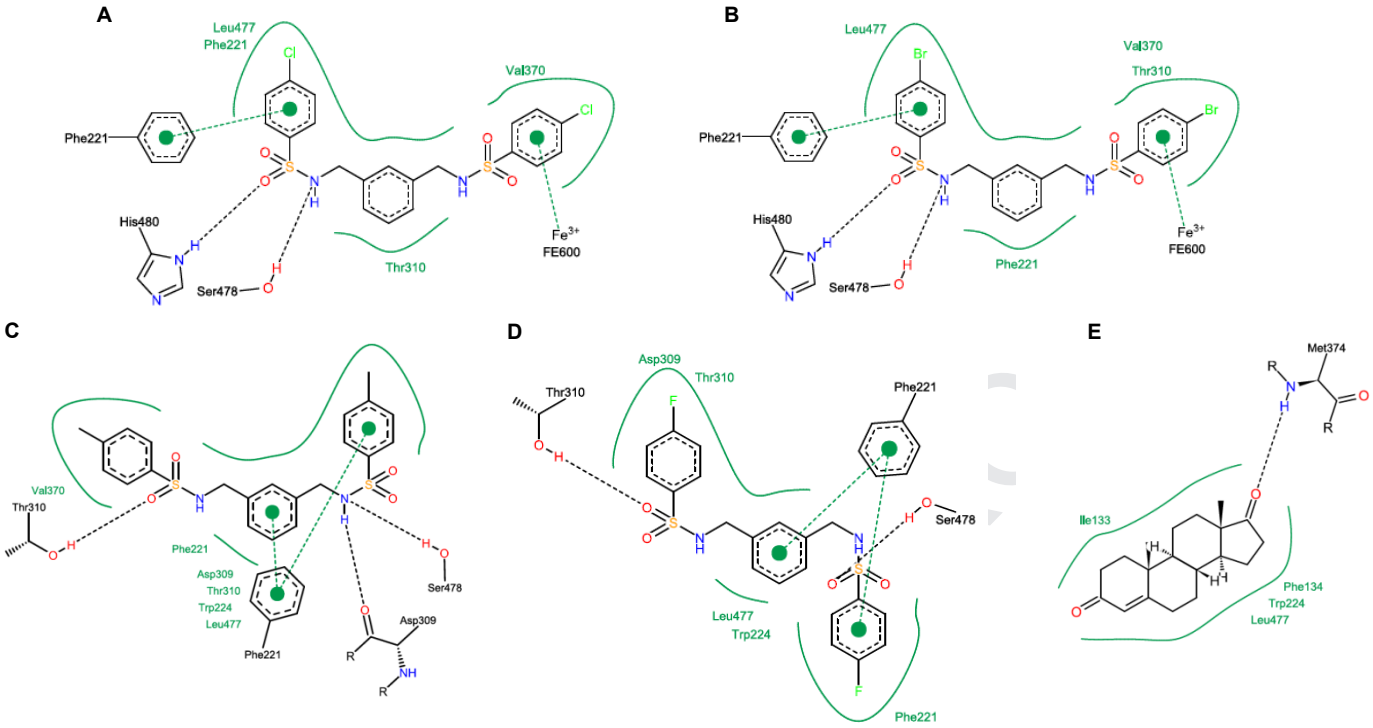

Figure 3. The 2D ligand-protein interactions of the highly active compounds **15** and **16** (A and B), the moderately active compound **9** (C), the weakly active compound **14** (D), and the natural substrate ASD (E).

2.5 QSAR

QSAR modelling was performed to gain insights into structure-activity relationships of the tested compounds (**9-26**, scheme I) and their experimental activities (Table 1). A set of 17 active compounds along with their chemical structures were used as a data set for QSAR analysis. The compounds were drawn, geometrically optimized, and calculated to obtain a large set of descriptors (i.e., molecular descriptors and quantum chemical descriptors). Correlation-based feature selection followed by stepwise multiple linear regression (MLR) was performed to select a final set of important descriptors for QSAR modelling as shown in Table 2. Values of informative molecular descriptors of the compounds in the data set are provided in Table 3.

Table 2 Definition of descriptors used for QSAR modelling

Descriptor	**Type**	**Definition**
Mor03m	3D-MoRSE descriptors	Signal 03 / weighted by mass 3D-MoRSE descriptors
GATS6v	2D autocorrelations	Geary autocorrelation of lag 6 weighted by van der Waals volume

Table 3 The informative molecular descriptor values of compounds **9-26**

Compound	**Mor03m**	**GATS6v**
9	-5.754	1.249
10	-7.546	0.872
11	-4.948	1.581
12	-5.125	0.628
13	-5.761	1.047
14	-5.648	0.588
15	-3.091	1.249
16	-2.644	1.705
17	-5.113	1.269
18	-4.941	1.164
19	-5.22	0.869
20	-5.622	0.872
21	-7.521	0.526
22	-7.498	0.896
23	-8.481	0.974
24	-6.733	1.368
25	-5.927	0.402
26	-6.3	0.925

The QSAR model was successfully constructed using MLR algorithm as shown in equation (1).

$$pIC_{50} = 0.2081(Mor03m) + 0.9138\ (GATS6v) + 0.4406 \qquad (1)$$

The model provided an acceptable predictive performance as indicated by R_{Tr} = 0.7951 and $RMSE_{Tr}$ = 0.4009, and R_{CV} = 0.6759 and $RMSE_{CV}$ = 0.4992 for training and testing sets, respectively. The experimental and predicted activity (pIC_{50}) of the compounds are shown in Table 4 and Figure 4.

Table 4 Experimental and predicted aromatase inhibitory activities (pIC_{50}) of compounds **9-26**

Compound	Experimental	Predicted	Error [a]
9	0.886	0.327	-0.559
10	-0.505	-0.29	0.215
11	0.678	0.906	0.228
12	-1.064	0.204	1.268
13	0.367	0.187	-0.18
14	-0.34	-0.167	0.173
15	1.301	0.794	-0.507
16	1.222	1.601	0.379
17	0.796	0.511	-0.285
18	0.553	0.47	-0.083
19	0.432	0.12	-0.312
20	-0.565	0.116	0.681
21	-0.439	-0.699	-0.26
22	-0.519	-0.248	0.271
23	-[b]	-[b]	-[b]
24	0.18	0.331	0.151
25	0.276	-0.685	-0.961
26	0.108	-0.036	-0.144

[a] Error = Predicted pIC_{50} - Experimental pIC_{50}
-[b] Inactive compound was excluded from the QSAR modelling.

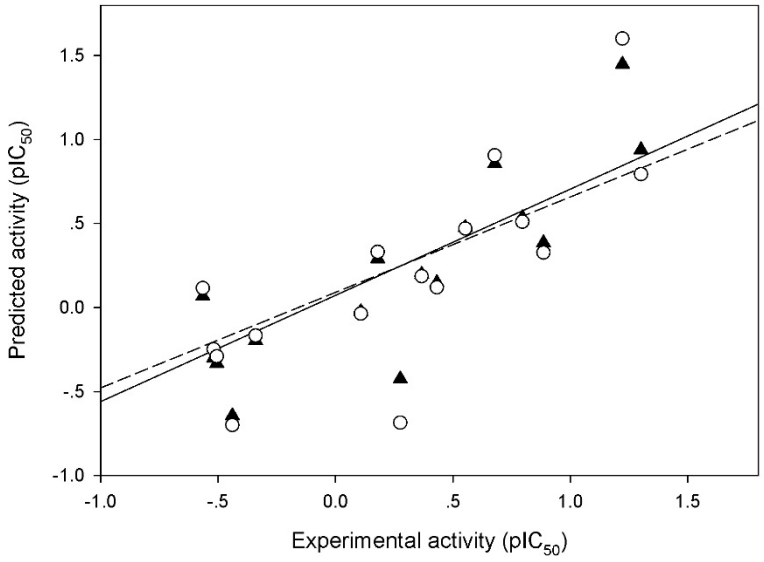

Figure 4. Experimental aromatase inhibitory activities of the tested compounds were plotted against their predicted activities obtained by the constructed QSAR model (experimental versus predicted pIC_{50} values). Closed triangles and solid regression line represented activities of the compounds generated by training set, whereas those of leave-one-out validated testing set are presented by opened circles and dash regression line.

According to the constructed QSAR model, two descriptors including GATS6v (van der Waals volume) and Mor03m (mass) with high regression coefficient values of 0.9138 and 0.2081, respectively, played role in the aromatase inhibitory effect of the compounds.

In overview, the QSAR analysis provided information suggesting the general desired characteristics of the compounds that are in concordance with the experimental findings. Mostly, the more potent compound displayed the higher value of either GATS6v or Mor03m, or both of the two descriptors, depending on the property of substituents and/or substitution patterns on the ring A (Scheme I) i.e., *meta* and *para* isomers. Considering the most potent *meta*-compound **16,** which is considered highly active, possessed the highest values of GATS6v (1.705) and Mor03m (-2.644) when compared to others (Table 3). Additionally, the most potent *meta*-compound **15** had high values of both Mor03m (-3.091) and GATS6v (1.249). In contrast, the rest of compounds with weaker activity and inactive compound (**23**),

mostly, possessed the lower values of both descriptors (Table 3) compared with the most potent compounds (**15** and **16**).

It should be noted that *meta*-isomer **26**, the analog of **15** bearing shorter hydrocarbon chain on ring A, displayed markedly decreased activity (pIC_{50} = 0.108) with lower values of GATS6v (0.925) and Mor03m (-6.300) compared with the most potent compound **15** (pIC_{50} = 1.301, GATS6v = 1.249, Mor03m = -3.091).

In case of moderately active compound **9** ((pIC_{50} = 0.886, R = 4-$CH_3C_6H_4$), it had lower van der Waals volume (GATS6v = 1.249) and mass (Mor03m = -5.754) compared with the most potent compound **16**. Comparing with the most potent compound **15** (Mor03m = -3.091), compound **9** displayed the lower Mor03m value but with the same GATS6v value (1.249).

For the weakly active compound **14** (pIC_{50} = -0.34, R = 4-FC_6H_4), its lower values of both descriptors (GATS6v = 0.588, Mor03m = -5.648) were noted when compared with the most potent 4-Cl (**15**) and 4-Br (**16**) containing compounds with the higher values of GATS6v and Mor03m descriptors. This could be due to the effect of atomic size of these halogens (Br > Cl > F).

In addition, the higher values of both van der Waals volume and mass descriptors involved in the higher activity of compounds such as compounds **9** (R = 4-$CH_3C_6H_4$) > **13** (R = 4-$CF_3C_6H_4$), and **17** (R = 4-CNC_6H_4) > **19** (R = 4-$NO_2C_6H_4$) as shown in Table 3. On the other hands, the higher van der Waals volume was seen in the more potent compounds i.e., **13** > **14** and **19** > **12**, R = 4-$OCH_3C_6H_4$ (Table 3).

The position where both sulfonamides moieties are attached on the central benzene ring A also affects aromatase inhibitory ability of the compound. The compounds possessing the *meta*-bis-sulfonamides exhibited more potent activities when compared to their *para*-derivatives (i.e., tetra-CH_3 derivatives (**10** > **23**) and CN-derivatives (**17** > **24**)). Regarding the QSAR model, the loss of activity of these *para*-compounds (**23** and **24**) could be due to the decreased value of mass descriptor Mor03m (Mor03m: **10** = -7.546, **23** = -8.481, **17** = -5.113, **24** = -6.733, Table 3). The influence of mass descriptor Mor03m was also observed for the benzene sulfonamide ring substituted with NO_2 moiety. Among three NO_2-derivatives (**19**-**21**), the 4-NO_2-substituted compound **19** with the highest Mor03m value provided more potent activity (pIC_{50} = 0.432, Mor03m = -5.22) than those of others i.e., *ortho*-compound **20**

(pIC_{50} = -0.565, Mor03m = -5.622) and *meta*-compound **21** (pIC_{50} = -0.439, Mor03m = -7.521).

3. Conclusions

Eighteen bis-sulfonamides (**9**–**26**) were synthesized by a simple one step sulfonylation of amine compounds using commercially available starting materials. Their aromatase inhibitory activities, molecular docking, and QSAR were investigated. All bis-sulfonamides displayed the aromatase inhibitory activity with IC_{50} range of 0.05-11.6 μM except for compound **23**. Promisingly, the bis-sulfonamides **15** and **16** were shown to be the most potent inhibitors (IC_{50} of 0.05 and 0.06 μM, respectively) with high safety index. The molecular docking revealed that the 4-Cl and 4-Br benzene substitutents (R) on the compounds **15** and **16** may play crucial role in the hydrophobic interaction with Leu477 of the aromatase to mimic steroidal backbone of the natural substrate (ASD). In addition, the QSAR study indicated that both compounds displayed high values of van der Waals volume (GATS6v) and mass (Mor03m) descriptors in governing the aromatase inhibitory activity. In summary, this study demonstrated the integrative approach towards discovering a novel class of aromatase inhibitors where two compounds (**15** and **16**) were highlighted as promising compounds for further development. Additionaly, the computational results would benefits further rational design of the related compounds for therapeutic applications.

4. Experimental section

4.1 Chemistry

Column chromatography was carried out using silica gel 60 (70–230 mesh ASTM). Analytical thin-layer chromatography (TLC) was performed using silica gel 60 F_{254} aluminum sheets. ^{1}H- and ^{13}C- NMR spectra were recorded on a Bruker AVANCE 300 NMR spectrometer (operating at 300 MHz for ^{1}H and 75 MHz for ^{13}C). The following standard abbreviations were used for signal multiplicities: singlet (s), doublet (d), triplet (t), quartet (q), multiplet (m), and broad (br). Mass spectra were recorded on a Bruker Daltonics (microTOF). IR spectra were obtained using a universal attenuated total reflectance attached on a Perkin–Elmer Spectrum One spectrometer. Melting points were determined using a Griffin melting point apparatus and were uncorrected.

*4.2 General procedure for the synthesis of sulfonamides (**9-24**)*

A solution of xylylenediamine **7a,b** (2.5 mmol) in dichloromethane (50 mL) was added in dropwise manner to a stirred mixture of appropriate benzenesulfonyl chloride **8a-m** (5 mmol) and sodium carbonate (10 mmol) in dichloromethane (20 mL). The reaction mixture was stirred at room temperature for 15-24 h (monitored by TLC), and distilled water (20 mL) was added. The organic phase was separated and the aqueous phase was extracted with dichloromethane (2 × 30 mL). The organic extracts were combined and washed with water (30 mL). The organic layer was dried over anhydrous sodium sulfate, filtered and evaporated to dryness under reduced pressure. The crude product was further purified by recrystallized or column chromatography on silica gel to obtain the pure product.

*4.2.1 N,N'-(1,3-phenylenebis(methylene))bis(4-methylbenzenesulfonamide) (**9**)*[17]

From *m*-xylylenediamine **7a** and 4-methylbenzenesulfonyl chloride **8a**. Off-white solid. 80% yield; mp 151-152 °C; IR (UATR) cm^{-1}: 3298, 3268, 1597, 1323, 1152. ^{1}H NMR (300 MHz, DMSO-d_6) δ 2.37 (s, 6H, 2 × CH_3), 3.86 (d, J = 6.3 Hz, 4H, 2 × CH_2NH), 7.06 (s, 1H, Ar*H*), 7.09 (d, J = 7.8 Hz, 2H, Ar*H*), 7.19 (t, J = 7.5 Hz, 1H, Ar*H*), 7.37 (d, J = 8.1 Hz, 4H, Ar*H*), 7.68 (d, J = 8.1 Hz, 4H, Ar*H*), 8.06 (t, J = 6.3 Hz,, 2H, 2 × N*H*). ^{13}C NMR (75 MHz, DMSO-d_6) δ 21.4, 46.5, 126.9, 127.0, 127.2, 128.7, 130.1, 138.1, 143.1. TOF-MS *m*/*z*: 445.1237 (Calcd for $C_{22}H_{25}N_2O_4S_2$: 445.1250).

*4.2.2 N,N'-(1,3-phenylenebis(methylene))bis(2,3,5,6-tetramethylbenzenesulfonamide) (**10**)*

From *m*-xylylenediamine **7a** and 2,3,5,6-tetramethylbenzenesulfonyl chloride **8b**. Off-white solid. 88% yield; mp 170-172 °C; IR (UATR) cm^{-1}: 3311, 1463, 1318, 1143. ^{1}H NMR (300 MHz, DMSO-d_6) δ 2.15 (s, 12H, 4 × CH_3), 2.39 (s, 12H, 4 × CH_3), 3.82 (s, 4H, 2 × CH_2NH), 6.70 (s, 1H, Ar*H*), 6.98 (d, J = 7.3 Hz, 2H, Ar*H*), 7.08 (t, J = 6.6 Hz, 1H, Ar*H*), 7.11 (s, 2H, Ar*H*), 7.90 (s, 2H, 2 × N*H*). ^{13}C NMR (75 MHz, DMSO-d_6) δ 18.0, 20.9, 45.8, 126.7, 127.1, 128.1, 134.6, 135.3, 135.7, 137.8, 139.4. TOF-MS *m*/*z*: 551.2003 (Calcd for $C_{28}H_{36}N_2NaO_4S_2$: 551.2009).

*4.2.3 N,N'-(1,3-phenylenebis(methylene))bis(naphthalene-2-sulfonamide) (**11**)*[17]

From *m*-xylylenediamine **7a** and 2-naphthalenebenzenesulfonyl chloride **8c**. Off-white solid. 72% yield; mp 148-150 °C; IR (UATR) cm^{-1}: 3279, 1592, 1322, 1154. ^{1}H NMR (300 MHz, DMSO-d_6) δ 3.86 (s, 4H, 2 × CH_2NH), 7.00-7.13 (m, 4H, Ar*H*), 7.58-7.70 (m, 4H, Ar*H*), 7.78 (dd, J = 8.6, 1.6 Hz, 2H, Ar*H*), 8.00 (d, J = 7.5 Hz, 2H, Ar*H*), 8.05-8.16 (m, 4H, Ar*H*), 8.39 (s, 2H, Ar*H*). ^{13}C NMR (75 MHz, DMSO-d_6) δ 46.5, 122.7, 126.9, 127.3,

127.8, 127.9, 128.2, 128.6, 129.1, 129.6, 129.7, 132.2, 134.6, 138.0, 138.2. TOF-MS *m*/*z*: 539.1060 (Calcd for $C_{28}H_{24}N_2NaO_4S_2$: 539.1070).

*4.2.4 N,N'-(1,3-phenylenebis(methylene))bis(4-methoxybenzenesulfonamide) (**12**)*[17]

From *m*-xylylenediamine **7a** and 4-methoxybenzenesulfonyl chloride **8d**. Off-white solid. 81% yield; mp 128-130 °C; IR (UATR) cm^{-1}: 3265, 1596, 1325, 1151. ^1H NMR (300 MHz, DMSO-d_6) δ 3.82 (s, 6H, 2 × OC*H*$_3$), 3.86 (s, 4H, 2 × C*H*$_2$NH), 7.03-7.20 (m, 8H, Ar*H*), 7.71 (d, J = 8.8 Hz, 4H, Ar*H*). ^{13}C NMR (75 MHz, DMSO-d_6) δ 46.5, 56.1, 114.8, 126.9, 127.3, 128.6, 129.1, 132.8, 138.1, 162.6. TOF-MS *m*/*z*: 499.0962 (Calcd for $C_{22}H_{24}N_2NaO_6S_2$: 499.0968).

*4.2.5 N,N'-(1,3-phenylenebis(methylene))bis(4-trifluoromethylbenzenesulfonamide) (**13**)*[17]

From *m*-xylylenediamine **7a** and 4-trifluoromethylbenzenesulfonyl chloride **8e**. Off-white solid. 71% yield; mp 176-178 °C; IR (UATR) cm^{-1}: 3267, 1592, 1324, 1138. ^1H NMR (300 MHz, DMSO-d_6) δ 3.94 (d, J = 6.2 Hz, 4H, 2 × C*H*$_2$NH), 7.00-7.14 (m, 4H, Ar*H*), 7.91 (d, J = 8.9 Hz, 4H, Ar*H*), 7.96 (d, J = 8.9 Hz, 4H, Ar*H*), 8.42 (t, J = 6.2 Hz, 2H, 2 × N*H*). ^{13}C NMR (75 MHz, DMSO-d_6) δ 46.0, 123.5 (q, $^1J_{CF}$=271), 126.3 (q, $^3J_{CF}$=4), 126.5, 127.0, 127.4, 128.2, 132.0 (q, $^2J_{CF}$=32), 137.2, 144.7. TOF-MS *m*/*z*: 553.0710 (Calcd for $C_{22}H_{19}F_6N_2O_4S_2$: 553.0685).

*4.2.6 N,N'-(1,3-phenylenebis(methylene))bis(4-fluorobenzenesulfonamide) (**14**)*

From *m*-xylylenediamine **7a** and 4-fluorobenzenesulfonyl chloride **8f**. Off-white solid. 89% yield; mp 247-248 °C; IR (UATR) cm^{-1}: 3285, 1592, 1327, 1153. ^1H NMR (300 MHz, DMSO-d_6) δ 3.92 (s, 4H, 2 × C*H*$_2$NH), 7.03-7.20 (m, 4H, Ar*H*), 7.40 (t, J = 8.9 Hz, 4H, Ar*H*), 7.84 (dd, J = 5.3, 8.6 Hz, 4H, Ar*H*), 8.23 (br s, 2H, 2 × N*H*). ^{13}C NMR (75 MHz, DMSO-d_6) δ 46.5, 116.7 (d, $^2J_{CF}$=23), 126.9, 127.3, 128.6, 130.0 (d, $^3J_{CF}$=9), 137.6, 138.0, 164.5 (d, $^1J_{CF}$=249). TOF-MS *m*/*z*: 475.0569 (Calcd for $C_{20}H_{18}F_2N_2NaO_4S_2$: 475.0568).

*4.2.7 N,N'-(1,3-phenylenebis(methylene))bis(4-chlorobenzenesulfonamide) (**15**)*

From *m*-xylylenediamine **7a** and 4-chlorobenzenesulfonyl chloride **8g**. Off-white solid. 82% yield; mp 157-158 °C; IR (UATR) cm^{-1}: 3279, 1587, 1327, 1159. ^1H NMR (300 MHz, DMSO-d_6) δ 3.92 (d, J = 4.8 Hz, 4H, 2 × C*H*$_2$NH), 7.06 (s, 1H, Ar*H*), 7.07 (d, J = 7.3 Hz, 2H, Ar*H*), 7.16 (t, J = 6.8 Hz, 1H, Ar*H*), 7.62 (d, J = 8.5 Hz, 4H, Ar*H*), 7.77 (d, J = 8.5 Hz, 4H, Ar*H*), 8.28 (br t, 2H, 2 × N*H*). ^{13}C NMR (75 MHz, DMSO-d_6) δ 46.4, 127.0, 127.3, 128.7, 128.9, 129.7, 137.7, 137.8, 140.0. TOF-MS *m*/*z*: 485.0159 (Calcd for $C_{20}H_{19}Cl_2N_2O_4S_2$: 485.0158).

*4.2.8 N,N'-(1,3-phenylenebis(methylene))bis(4-bromobenzenesulfonamide) (**16**)*[17]

From *m*-xylylenediamine **7a** and 4-bromobenzenesulfonyl chloride **8h**. Off-white solid. 88% yield; mp 169-170 °C; IR (UATR) cm^{-1}: 3276, 1574, 1327, 1155. ^{1}H NMR (300 MHz, DMSO-d_6) δ 3.91 (s, 4H, 2 × C*H*$_2$NH), 7.06 (s, 1H, Ar*H*), 7.07 (d, J = 6.8 Hz, 2H, Ar*H*), 7.16 (t, J = 6.8 Hz, 1H, Ar*H*), 7.70 (d, J = 8.6 Hz, 4H, Ar*H*), 7.76 (d, J = 8.6 Hz, 4H, Ar*H*). ^{13}C NMR (75 MHz, DMSO-d_6) δ 46.5, 126.5, 126.9, 127.4, 128.6, 129.0, 132.6, 137.9, 140.6. TOF-MS *m*/*z*: 594.8967 (Calcd for $C_{20}H_{18}Br_2N_2NaO_4S_2$: 594.8967).

*4.2.9 N,N'-(1,3-phenylenebis(methylene))bis(4-cyanobenzenesulfonamide) (**17**)*

From *m*-xylylenediamine **7a** and 4-cyanobenzenesulfonyl chloride **8i**. Yellow solid. 70% yield; mp 154-155 °C; IR (UATR) cm^{-1}: 3284, 2233, 1333, 1159. ^{1}H NMR (300 MHz, DMSO-d_6) δ 3.96 (s, 4H, 2 × C*H*$_2$NH), 7.04 (d, J = 8.0 Hz, 2H, Ar*H*), 7.05 (s, 1H, Ar*H*), 7.12 (t, J = 7.4 Hz, 1H, Ar*H*), 7.90 (d, J = 8.5 Hz, 4H, Ar*H*), 8.02 (d, J = 8.4 Hz, 4H, Ar*H*), 8.29 (br s, 2H, 2 × N*H*). ^{13}C NMR (75 MHz, DMSO-d_6) δ 46.5, 115.2, 118.2, 127.0, 127.4, 127.7, 128.7, 133.8, 137.7, 145.4. TOF-MS *m*/*z*: 489.0650 (Calcd for $C_{22}H_{18}N_4NaO_4S_2$: 489.0662).

*4.2.10 N,N'-(1,3-phenylenebis(methylene))bis(4-acetylbenzenesulfonamide) (**18**)*

From *m*-xylylenediamine **7a** and 4-acetylbenzenesulfonyl chloride **8j**. Off-white solid. 72% yield; mp 270-271 °C; IR (UATR) cm^{-1}: 3292, 1688, 1329, 1159. ^{1}H NMR (300 MHz, DMSO-d_6) δ 2.62 (s, 6H, 2 × C*H*$_3$CO), 3.92 (s, 4H, 2 × C*H*$_2$NH), 7.07 (s, 1H, Ar*H*), 7.05 (d, J = 7.3 Hz, 2H, Ar*H*), 7.13 (t, J = 6.7 Hz, 1H, Ar*H*), 7.88 (d, J = 8.2 Hz, 4H, Ar*H*), 8.08 (d, J = 8.2 Hz, 4H, Ar*H*). ^{13}C NMR (75 MHz, DMSO-d_6) δ 27.5, 46.6, 126.9, 127.3, 128.6, 129.3, 138.2, 139.7, 145.3, 197.8. TOF-MS *m*/*z*: 523.0956 (Calcd for $C_{24}H_{24}N_2NaO_6S_2$: 523.0968).

*4.2.11 N,N'-(1,3-phenylenebis(methylene))bis(4-nitrobenzenesulfonamide) (**19**)*[17]

From *m*-xylylenediamine **7a** and 4-nitrobenzenesulfonyl chloride **8k**. Yellow solid. 80% yield; mp 170-171 °C; IR (UATR) cm^{-1}: 3306, 1526, 1350, 1161. ^{1}H NMR (300 MHz, DMSO-d_6) δ 3.99 (s, 4H, 2 × C*H*$_2$NH), 7.05 (d, J = 8.0 Hz, 2H, Ar*H*), 7.06 (s, 1H, Ar*H*), 7.14 (t, J = 6.5 Hz, 1H, Ar*H*), 8.00 (d, J = 8.9 Hz, 4H, Ar*H*), 8.37 (d, J = 8.9 Hz, 4H, Ar*H*), 8.55 (s, 2H, 2 × N*H*). ^{13}C NMR (75 MHz, DMSO-d_6) δ 46.4, 124.9, 127.1, 127.4, 128.5, 128.8, 137.7, 146.7, 149.9. TOF-MS *m*/*z*: 529.0447 (Calcd for $C_{20}H_{18}N_4NaO_8S_2$: 529.0458).

*4.2.12 N,N'-(1,3-phenylenebis(methylene))bis(2-nitrobenzenesulfonamide) (**20**)*

From *m*-xylylenediamine **7a** and 2-nitrobenzenesulfonyl chloride **8l**. Off-white solid. 70% yield; mp 154-155 °C; IR (UATR) cm^{-1}: 3345, 1535, 1339, 1162. ^{1}H NMR (300 MHz, DMSO-d_6) δ 4.05 (s, 4H, 2 × C*H*$_2$NH), 7.04-7.15 (m, 4H, Ar*H*), 7.69-7.92 (m, 8H, Ar*H*). ^{13}C

NMR (75 MHz, DMSO-d_6) δ 46.8, 124.6, 126.8, 127.3, 128.6, 130.0, 132.8, 134.0, 138.2, 148.0. TOF-MS *m*/*z*: 529.0456 (Calcd for $C_{20}H_{18}N_4NaO_8S_2$: 529.0458).

*4.2.13 N,N'-(1,3-phenylenebis(methylene))bis(3-nitrobenzenesulfonamide) (**21**)*

From *m*-xylylenediamine **7a** and 3-nitrobenzenesulfonyl chloride **8m**. Off-white solid. 74% yield; mp 173-174 °C; IR (UATR) cm^{-1}: 3295, 1531, 1349, 1166. ^1H NMR (300 MHz, DMSO-d_6) δ 3.94 (s, 4H, 2 × C*H*$_2$NH), 6.92-7.10 (m, 4H, Ar*H*), 7.82 (t, J = 7.8 Hz, 2H, Ar*H*), 8.12 (d, J = 7.6 Hz, 2H, Ar*H*), 8.36-8.42 (m, 4H, Ar*H*), 8.48 (br s, 2H, 2 × N*H*). ^{13}C NMR (75 MHz, DMSO-d_6) δ 46.0, 121.3, 126.6, 126.9, 127.0, 128.2, 131.2, 132.5, 137.0, 142.5, 147.7. TOF-MS *m*/*z*: 529.0465 (Calcd for $C_{20}H_{18}N_4NaO_8S_2$: 529.0458).

*4.2.14 N,N'-(1,4-phenylenebis(methylene))bis(2,3,5,6-tetramethylbenzenesulfonamide) (**23**)*

From *p*-xylylenediamine **7b** and 2,3,5,6-tetramethylbenzenesulfonyl chloride **8b**. Off-white solid. 65% yield; mp 225-227 °C; IR (UATR) cm^{-1}: 3279, 1322, 1153. ^1H NMR (300 MHz, DMSO-d_6) δ 2.18 (s, 12H, 4 × C*H*$_3$), 2.41 (s, 12H, 4 × C*H*$_3$), 3.89 (d, J = 6.2 Hz, 4H, 2 × C*H*$_2$NH), 6.99 (s, 4H, Ar*H*), 7.15 (s, 2H, Ar*H*), 7.93 (t, J = 6.2 Hz, 2H, 2 × N*H*). ^{13}C NMR (75 MHz, DMSO-d_6) δ 18.1, 20.9, 45.5, 127.6, 134.7, 135.3, 135.8, 137.1, 139.3. TOF-MS *m*/*z*: 551.2002 (Calcd for $C_{28}H_{36}N_2NaO_4S_2$: 551.2009).

*4.2.15 N,N'-(1,4-phenylenebis(methylene))bis(4-cyanobenzenesulfonamide) (**24**)*

From *p*-xylylenediamine **7b** and 4-cyanobenzenesulfonyl chloride **8i**. Off-white solid. 87% yield; mp 244-245 °C; IR (UATR) cm^{-1}: 3252, 2235, 1335, 1159. ^1H NMR (300 MHz, DMSO-d_6) δ 3.97 (d, J = 6.2 Hz, 4H, 2 × C*H*$_2$NH), 7.09 (s, 4H, Ar*H*), 7.90 (d, J = 8.2 Hz, 4H, Ar*H*), 8.03 (d, J = 8.2 Hz, 4H, Ar*H*). ^{13}C NMR (75 MHz, DMSO-d_6) δ 46.3, 115.1, 118.2, 127.3, 127.7, 128.0, 133.7, 136.9, 145.6. TOF-MS *m*/*z*: 489.0667 (Calcd for $C_{22}H_{18}N_4NaO_4S_2$: 489.0662).

*4.3 General procedure for the synthesis of sulfonamides (**25-26**)*

Benzenesulfonyl chloride (5 mmol) was added to a solution of *m*-phenylenediamine (2.5 mmol) in pyridine (5 mL), and the mixture was stirred under reflux for 6 h then concentrated under reduced pressure. Water (20 mL) was added and extracted with dichloromethane (3 × 20 mL). The organic layer was dried over anhydrous sodium sulfate, filtered and evaporated to dryness under reduced pressure. The crude product was further purified by column chromatography on silica gel to obtain the pure product.

*4.3.1 N,N'-(1,3-phenylene)bis(4-methoxybenzenesulfonamide) (**25**)*

From *m*-phenylenediamine **7c** and 4-methoxybenzenesulfonyl chloride **8d**. Brown solid. 64% yield; mp 155-156 °C; IR (UATR) cm^{-1}: 3256, 1596, 1303, 1150. ^1H NMR (300 MHz, DMSO-d_6) δ 3.79 (s, 6H, 2 × OC*H*$_3$), 6.65 (dd, J = 8.1, 2.0 Hz, 2H, Ar*H*), 6.97-7.07 (m, 5H, Ar*H*), 7.09 (t, J = 1.9 Hz, 1H, Ar*H*), 7.62 (d, J = 8.9 Hz, 4H, Ar*H*), 10.15 (br s, 2H, 2 × N*H*). ^{13}C NMR (75 MHz, DMSO-d_6) δ 56.1, 110.8, 114.7, 115.2, 129.3, 130.1, 131.5, 139.1, 162.9. TOF-MS *m*/*z*: 471.0662 (Calcd for $C_{20}H_{20}N_2NaO_6S_2$: 471.0655).

*4.3.2 N,N'-(1,3-phenylene)bis(4-chlorobenzenesulfonamide) (**26**)*

From *m*-phenylenediamine **7c** and 4-chlorobenzenesulfonyl chloride **8g**. Yellow solid. 66% yield; mp 158-159 °C; IR (UATR) cm^{-1}: 3231, 1608, 1317, 1154. ^1H NMR (300 MHz, DMSO-d_6) δ 6.70 (dd, J = 8.1, 2.0 Hz, 2H, Ar*H*), 7.02 (t, J = 1.9 Hz, 1H, Ar*H*), 7.08 (t, J = 8.1 Hz, 1H, Ar*H*), 7.60 (d, J = 8.8 Hz, 4H, Ar*H*), 7.66 (d, J = 8.8 Hz, 4H, Ar*H*), 10.42 (br s, 2H, 2 × N*H*). ^{13}C NMR (75 MHz, DMSO-d_6) δ 111.6, 116.1, 129.0, 129.8, 130.4, 138.3, 138.5, 138.7. TOF-MS *m*/*z*: 478.9663 (Calcd for $C_{18}H_{14}Cl_2N_2NaO_4S_2$: 478.9664).

*4.4 The synthesis of N,N'-(1,3-phenylenebis(methylene))bis(3-aminobenzenesulfonamide) (**22**)*

A mixture of nitrobissulfonamide **21** (4 mmol) and $SnCl_2{\cdot}2H_2O$ (32 mmol) in absolute ethanol (20 mL) was stirred under reflux for 6 h then concentrated under reduced pressure. Water (20 mL) was added and extracted with EtOAc (3 × 20 mL). The organic extracts were combined and washed with water (20 mL) and brine (20 mL). The organic layer was dried over anhydrous sodium sulfate, filtered and concentrated. The crude product was further purified by column chromatography on silica gel to obtain the pure product.

Yellow solid. 80% yield; mp 148-150 °C; IR (UATR) cm^{-1}: 3467, 3372, 3278, 1598, 1323, 1155. ^1H NMR (300 MHz, DMSO-d_6) δ 3.88 (d, J = 4.5 Hz, 4H, 2 × C*H*$_2$NH), 5.56 (s, 4H, 2 × N*H*$_2$), 6.75 (dd, J = 8.0, 1.9 Hz, 2H, Ar*H*), 6.91 (d, J = 7.8 Hz, 2H, Ar*H*), 7.00 (t, J = 1.9 Hz, 2H, Ar*H*), 7.09-7.26 (m, 6H, Ar*H*), 7.92 (br t, 2H, 2 × N*H*). ^{13}C NMR (75 MHz, DMSO-d_6) δ 46.6, 111.6, 113.7, 117.6, 126.8, 127.1, 128.6, 130.0, 138.4, 141.5, 149.8. TOF-MS *m*/*z*: 469.0959 (Calcd for $C_{20}H_{22}N_4NaO_4S_2$: 469.0975).

4.5 Aromatase inhibition assay

Aromatase inhibitory activity was evaluated using the modified method of Stressor et al..[29] The experiment was performed using the Gentest kit. The activity of aromatase enzyme

(CYP19) is indicated by the conversion of the fluorometric substrate, *O*-benzyl fluorescein benzyl ester (DBF), to the fluorescein product. Initially, 100 µL of cofactor (containing 78.4 µL of 50 mM phosphate buffer (pH 7.4); 20 µL of 20x NADPH-generating system (26 mM $NADP^+$, 66 mM glucose-6-phosphate, and 66 mM $MgCl_2$); and 1.6 µL of 100 U/mL glucose-6-phosphate dehydrogenase) were added into a 96-well black plate and preincubated for 10 min in 37 °C water bath. Subsequently, 100 µL of enzyme/substrate mixture containing 77.3 µL of 50 mM phosphate buffer (pH 7.4); 12.5 µL of 16 pmol/mL CYP19; 0.2 µL of 0.2 mM DBF, and 10 µL of tested compound or negative control (10% DMSO) or positive control (letrozole) were added to initiate the reaction. Then, fluorescence signal was recorded (excitation wavelength of 490 nm and emission wavelength of 530 nm) with cutoff 515 nm. The measured absorbance values were used to calculate % inhibition according to the equation (2). The compounds giving the % inhibition greater than 50 were further investigated to obtain their IC_{50} values.

$$\%\ inhibition = 100 - [(sample - blank)/(DMSO - blank)\ \text{Ã—}\ 100] \qquad (2)$$

4.6 Cytotoxicity assay

The cytotoxic activity of compounds (**9-26**) was tested using hormone-dependent breast cancer cell line (T47-D) and normal embryonic lung cell line (MRC-5). T47-D cells were grown in RPMI-1640 medium supplemented with 2 mM L-gluthamine, 100 U/mL penicillin-streptomycin, 0.2 U/mL insulin, 4.5 g/L glucose and 10% FBS whereas MRC-5 cells were grown in DMEM medium supplemented with 100 U/mL penicillin streptomycin and 10% FBS. Briefly, the cells suspended in the corresponding culture medium were inoculated in 96-well microtiter plates (Corning Inc., NY, USA) at a density of 10,000-20,000 cells per well, and then incubated at 37 °C under a humidified atmosphere with 95% air and 5% CO_2 for 24 h. An equal volume of additional medium containing either the serial dilutions of the tested compounds, positive control (etoposide and/or doxorubicin) or negative control (DMSO) was added to the desired final concentrations. The microtiter plates were further incubated for 48 h. Cell viability in each well was determined by staining with MTT assay.[30-32] The MTT solution (10 mL/100 mL medium) was added to all wells of the assay, and the plates were incubated for 2-4 h. Subsequently, DMSO was added to dissolve the resulting formazan by sonication. The plates were read on a microplate reader (Molecular Devices, USA) using a test wavelength of 550 nm and a reference wavelength of 650 nm.

The IC_{50} value was determined as the compound concentration that inhibited cell growth by 50%. The compounds exhibited IC_{50} > 50 µg/mL were considered as noncytotoxic.

4.7 Molecular Docking

Crystal structure of the target protein, human placental aromatase co-crystallized with natural substrate ASD, was retrieved from RSCB protein data bank (PDB ID: 3EQM, http://www.rcsb.org/). The preparation of the protein was initially performed by adding essential hydrogen atoms and repairing missing side chains, using the WHAT IF web server version 10.1.[33] Subsequently, non-polar hydrogen atoms were merged, Gasteiger atomic charges were assigned, and atom type of the protein structures were specified using AutoDock Tools version 1.5.6..[34,35] The chemical structures of the investigated ligands (**9**-**26**) were drawn using Marvin Sketch version 6.1.4,[36] and were geometrically optimized by Gaussian 09[37] using Becke's three-parameter hybrid method with the Lee-Yang-Parr correlation functional (B3LYP) together with the 6-31g(d) basis set. The geometrically optimized compounds then were prepared by merging non-polar hydrogen atoms, assigning partial atomic charge, and defining rotatable bonds using AutoDock Tools version 1.5.6.[34,35] Molecular docking simulation was conducted using AutoDock Vina, as a part of the PyRx 0.8 software.[38] The grid boxes sizing 25 × 25 × 25 A° were generated and the center of binding cavity was allocated using x, y and z coordinates of 85.9275, 54.2004, and 46.0769, respectively. The validation of docking protocol was performed by redocking of the co-crystallized ligand ASD to the aromatase protein. The accuracy of the docking protocol was evaluated by RMSD value, which was calculated by the difference between original and redocking poses using the Chimera software.[39] Docking poses of the investigated compounds were visualized using PyMOL,[40] and two-dimensional ligand-protein interaction diagrams were generated using PoseView (http://proteins.plus).[41]

4.8 QSAR

Data set

To obtain distribution of data points, the experimental activity (IC_{50} values) of the compounds were converted to pIC_{50} values by taking the negative logarithm to the base of 10 (-log IC_{50}). Herein, the inactive compound **23** (IC_{50} > 12.5 µM) were excluded from the data set. Finally, a set of 17 compounds were included for model construction.

Molecular structure optimization and descriptor calculation

Geometrical optimization was performed to obtain the low-energy conformers that were used as input files for descriptor extraction. The initial optimization with semi-empirical Austin Model 1 (AM1) level was performed followed by the density functional theory (DFT) calculation using the Becke's three-parameter hybrid method with the Lee-Yang-Parr correlation functional (B3LYP) together with the 6-31g(d) level using Gaussian 09.[37] A set of quantum chemical descriptors were subsequently extracted from the optimized structures using an in-house developed script (i.e., mean absolute atomic charge (Q_m), total energy (E_{total}), total dipole moment (μ), highest occupied molecular orbital energy (E_{HOMO}), lowest unoccupied molecular orbital energy (E_{LUMO}), energy difference of HOMO and LUMO (HOMO-LUMO$_{Gap}$), electron affinify (EA), ionization potential (IP), Mulliken electronegativity (χ), hardness (η), softness (S), electrophilic index (ω_i), and electrophilicity (ω)). Additionally, the optimized structures were underwent the calculation to obtain a set of 3,224 molecular descriptors using Dragon software (version 5.5).[42] The obtained molecular descriptors included 22 classes i.e., Constitutional descriptors, Topological descriptors, Walk and path counts, Connectivity indices, Information indices, 2D autocorrelation, Edge adjacency indices, Burden eigenvalues, Topological charge indices, Eigenvalue-based indices, Randic molecular profiles, Geometrical descriptors, RDF descriptors, 3D-MoRSE descriptors, WHIM descriptors, GETAWAY descriptors, Functional group counts, Atom-centred fragments, Charge descriptors, Molecular properties, 2D binary fingerprints and 2D frequency fingerprints.

Feature selection

Initially, correlation-based feature selection was performed to filter a set of relevant descriptors from the whole large set. Pearson's correlation coefficient (r) values were calculated for each pair of a descriptor and bioactivity (pIC$_{50}$). The descriptors whose $|r| \geq |0.7|$ then were selected, whereas the rest having $|r| < 0.7$ were excluded for further feature selection process. Subsequent feature selection was performed using stepwise multiple linear regression (MLR) algorithm as implemented in SPSS statistics 18.0 to obtain a final descriptor set for QSAR modelling.

Multivariate analysis using multiple linear regression

Multivariate analysis was performed to elucidate relationships of the selected descriptors and the compound's activity. Multiple linear regression (MLR) algorithm was performed using Waikato Environment for Knowledge Analysis (WEKA) version 3.4.5[43] to construct the QSAR model according equation (3), where selected descriptor values and pIC_{50} values were assigned as independent variables (X) and dependent variable (Y), respectively.

$$Y = B_0 + \sum B_n X_n \qquad (3)$$

where Y is the pIC_{50} values of compounds, B_0 is the intercept and B_n are the regression coefficient of descriptors X_n.

Data sampling

Data set was separated into 2 subsets (i.e., training set and testing set) by means of leave-one-out cross validation (LOO-CV). One compound was removed from the whole data set (N) to be used as the testing set (whose bioactivity was predicted) while the remaining compounds (N-1) were used as the training set (whose relationships between X and Y variables were learned). The same sampling process was continued until every compound in the data set was used as the testing set to predict its Y variable (activity).

Evaluating the performance of QSAR model

The predictive performance of the constructed QSAR model was assessed by two statistical parameters i.e., correlation coefficient (R) representing the predictive performance and root mean square error (RMSE) representing the predictive error of the model.

Acknowledgments

This project is financially supported by Srinakharinwirot University (grant no. 011/2562). Great supports from the annual budget grant (BE 2562-2563) of Mahidol University are appreciated. We are also indebted to Chulabhorn Research Institute for recording mass spectra and bioactivity testing.

References

1. Ahmad I, Shagufta. Recent developments in steroidal and nonsteroidal aromatase inhibitors for the chemoprevention of estrogen-dependent breast cancer. Eur J Med Chem. 2015;102:375–386.
2. Ghosh D, Lo J, Egbuta C. Recent progress in the discovery of next generation inhibitors of aromatase from the structure−function perspective. J Med Chem. 2016;59:5131–5148.
3. Yadav MR, Barmade MA, Tamboli RS, Murumkar PR. Developing steroidal aromatase inhibitors-an effective armament to win the battle against breast cancer. Eur J Med Chem. 2015;105:1–38.
4. Palmieri C, Patten DK, Januszewski A, Zucchini G, Howell SJ. Breast cancer: current and future endocrine therapies. Mol Cell Endocrinol. 2014;382:695–723.
5. Sainsbury R. The development of endocrine therapy for women with breast cancer. Cancer Treat Rev. 2013;39:507–517.
6. Adhikari N, Amin SA, Saha A, Jha T. Combating breast cancer with non-steroidal aromatase inhibitors (NSAIs): Understanding the chemico-biological interactions through comparative SAR/QSAR study. Eur J Med Chem. 2017;137:365–438.
7. Bruno RD, Njar VCO. Targeting cytochrome P450 enzymes: A new approach in anti-cancer drug development. Bioorg Med Chem. 2007;15: 5047–5060.
8. Lonning PE, Eikesdal HP. Aromatase inhibition 2013: clinical state of the art and questions that remain to be solved. Endocr Relat Cancer. 2013;20:R183–201
9. Sobral AF, Amaral C, Correia-da-Silva G, Teixeira N. Unravelling exemestane: from biology to clinical prospects. J Steroid Biochem Mol Biol. 2016;163:1–11.
10. Coates A, Keshaviah A, Thürlimann B, Mouridsen H, Mauriac L, Forbes JF, Paridaens R, Castiglione-Gertsch M, Gelber RD, Colleoni M, Láng I, Del Mastro L, Smith I, Chirgwin J, Nogaret JM, Pienkowski T, Wardley A Jakobsen, EH, Price KN, Goldhirsch A. Five years of letrozole compared with tamoxifen as initial adjuvant therapy for postmenopausal women with endocrine-responsive early breast cancer: update of study BIG 1–98. J Clin Oncol. 2007;25:486–492.
11. Amir W, Seruga B, Niraula S, Carlsson L, Ocaña A. Toxicity of adjuvant endocrine therapy in postmenopausal breast cancer patients: A systematic review and meta-analysis. J Natl Cancer Inst. 2011;103:1299–1309.

12. Zhao C, Rakesh KP, Ravidar L, Fang W-Y, Qin H-L. Pharmaceutical and medicinal significance of sulfur (SVI)-containing motifs for drug discovery: A critical review. Eur J Med Chem. 2019;162:679–734.
13. Hu L, Li ZR, Jiang JD, Boykin DW. Novel diaryl or heterocyclic sulfonamides as antimitotic agents. Anticancer agents Med Chem. 2008;8:739–745.
14. Khan FA, Mushtaq S, Naz S, Farooq U, Zaidi A, Bukhari SM, Rauf A, Mubarak MS. Sulfonamides as potential bioactive scaffolds. Curr Org Chem. 2018;22:818–830.
15. Ammazzalorso A, De Filippis B, Giampietro L, Amoroso R. *N*-acylsulfonamides: Synthetic routes and biological potential in medicinal chemistry. Chem Biol Drug Des. 2017;90:1094–1105.
16. Supuran CT. Special issue: Sulfonamides. Molecules. 2017;22:1642.
17. Saha T, Hossain MS, Saha D, Lahiri M, Talukdar P. Chloride-mediated apoptosis-inducing activity of bis(sulfonamide) anionophores. J Am Chem Soc. 2016;138:7558–7567.
18. Su B, Tian R, Darby MV, Brueggemeier RW. Novel sulfonanilide analogs decrease aromatase activity in breast cancer cells: Synthesis, biological evaluation, and ligand-based pharmacophore identification. J Med Chem 51 2008;51:1126–1135.
19. Matteo MD, Ammazzalorso A, Andreoli F, Caffa I, Filippis BD, Fantacuzzi M, Giampietro L, Maccallini C, Nencioni A, Parenti MD, Soncini D, Rio AD. Amoroso R. Synthesis and biological characterization of 3-(imidazol-1-ylmethyl)piperidine sulfonamides as aromatase inhibitors, Bioorg Med.Chem Lett. 2016;26:3192–3194.
20. Pingaew R, Prachayasittikul V, Mandi P, Nantasenamat C, Prachayasittikul S, Ruchirawat S, Prachayasittikul V. Synthesis and molecular docking of 1,2,3-triazole-based sulfonamides as aromatase inhibitors. Bioorg Med Chem. 2015;23:3472–3480.
21. Ghorab MM, Alsaid MS, Al-Ansary GH, Abdel-Latif GA, Abou El Ella DA. Analogue based drug design, synthesis, molecular docking and anticancer evaluation of novel chromene sulfonamide hybrids as aromatase inhibitors and apoptosis enhancers. Eur J Med Chem. 2016;124:946–958.

22. Pingaew R, Mandi P, Prachayasittikul V, Prachayasittikul S, Ruchirawat S, Prachayasittikul V. Synthesis, molecular docking, and QSAR study of sulfonamide-based indoles as aromatase inhibitors. Eur J Med Chem. 2018;143:1604–1615.
23. Ghorab MM, Alsaid MS, Samir N, Abdel-Latif GA, Soliman AM, Ragab FA, Abou El Ella DA. Aromatase inhibitors and apoptotic inducers: Design, synthesis, anticancer activity and molecular modeling studies of novel phenothiazine derivatives carrying sulfonamide moiety as hybrid molecules. Eur J Med Chem. 2017;134:304–315.
24. Caporuscio F, Rastelli G, Imbriano C, Del Rio A. Structure-based design of potent aromatase inhibitors by high-throughput docking. J Med Chem. 2011;54:4006–4017.
25. Pingaew R, Prachayasittikul V, Anuwongcharoen N, Prachayasittikul S, Ruchirawat S, Prachayasittikul V. Synthesis and molecular docking of N,N'-disubstituted thiourea derivatives as novel aromatase inhibitors. Bioorg Chem. 2018;79:171–178.
26. Kao Y-C, Korzekwa KR, Laughton CA, Chen S. Evaluation of the mechanism of aromatase cytochrome P450 A site-directed mutagenesis study. Eur J Biochem. 2001;268:243–251.
27. Loge C, Le Borgne M, Marchand P, Robert J-M, Le Baut G, Palzer M, Hartmann RW. Three-dimensional model of cytochrome P450 human aromatase. J. Enzyme Inhib Med Chem., 2005;20:581–585.
28. Wood PM, Woo LWL. Thomas MP. Mahon MF. Purohit A. Potter BVL. Aromatase and dual aromatase-steroid sulfatase inhibitors from the letrozole and vorozole Templates. ChemMedChem. 2011;6:1423–1438.
29. Stresser DM, Turner SD, McNamara J, Stocker P, Miller VP, Crespi CL, Patten CJ. A high-throughput screen to identify inhibitors of aromatase (CYP19). Anal Biochem. 2000;284:427–430.
30. Mosmann T. Rapid colorimetric assay for cellular growth and survival: application to proliferation and cytotoxicity assays. J Immunol Methods. 1983;65:55–63.
31. Tominaga H, Ishiyama M, Ohseto F, Sasamoto K, Hamamoto T, Suzuki K, Watanabe M. A water-soluble tetrazolium salt useful for colorimetric cell viability assay. Anal Commun. 1999;36:47–50.

32. Carmichael J, DeGraff WG, Gazdar AF, Minna JD, Mitchell JB. Evaluation of a tetrazolium-based semiautomated colorimetric assay: assessment of radiosensitivity. Cancer Res. 1987;47:943–946.
33. Vriend G. WHAT IF: A molecular modeling and drug design program. J Mol Graph. 1990;8:52–56.
34. Sanner MF. Python: a programming language for software integration and development. J Mol Graph Model. 1999;17:57–61.
35. Morris GM, Huey R, Lindstrom W, Sanner MF, Belew RK, Goodsell DS, Olson AJ. AutoDock4 and AutoDockTools4: Automated docking with selective receptor flexibility, J Comput Chem. 2009;30:2785–2791.
36. ChemAxon. Marvin Sketch Version 6.0, in, Budapest, Hungary, 2013.
37. Frisch MJ, Trucks GW, Schlegel HB, Scuseria GE, Robb MA, Cheeseman JR, Scalmani G, Barone V, Mennucci B, Petersson GA, Nakatsuji H, Caricato M, Li X, Hratchian HP, Izmaylov AF, Bloino J, Zheng G, Sonnenberg JL, Hada M, Ehara M, Toyota K, Fukuda R, Hasegawa J, Ishida M, Nakajima T, Honda Y, Kitao O, Nakai H, Vreven T, Jr. JAM, Peralta JE, Ogliaro F, Bearpark M, Heyd JJ, Brothers E, Kudin KN, Staroverov VN, Kobayashi R, Normand J, Raghavachari K, Rendell A, Burant JC, Iyengar SS, Tomasi J, Cossi M, Rega N, Millam JM, Klene M, Knox JE, Cross JB, Bakken V, Adamo C, Jaramillo J, Gomperts R, Stratmann RE, Yazyev O, Austin AJ, Cammi R, Pomelli C, Ochterski JW, Martin RL, Morokuma K, Zakrzewski VG, Voth GA, Salvador P, Dannenberg JJ, Dapprich S, Daniels AD, Farkas Ö, Foresman JB, Ortiz JV, Cioslowski J, Fox DJ. Gaussian Inc., Wallingford CT, 2009.
38. Dallakyan S. PyRx Version 0.8, 2013. http://pyrx.scripps.edu.
39. Pettersen EF, Goddard TD, Huang CC, Couch GS, Greenblatt DM, Meng EC, Ferrin TE. UCSF Chimera--a visualization system for exploratory research and analysis. J Comput Chem. 2004;25:1605–1612.
40. Delano W. PyMOL Release 0.99, DeLano Scientific LLC, Pala Alto, Ca, 2002.
41. Fährrolfes R, Bietz S, Flachsenberg F, Meyder A, Nittinger E, Otto T, Volkamer A, Rarey M. ProteinsPlus: a web portal for structure analysis of macromolecules. Nucleic Acids Res. 2017;45:W337–W343.

42. Talete. Dragon for Windows (Software for Molecular Descriptor Calculations). Version 5.5 [Computer Software]. Milan, Italy, in, 2007.

43. Witten IH, Frank E, Hall MA. Data Mining: Practical Machine Learning Tools and Techniques. (2nded.). San Francisco, CA: Morgan Kaufmann, in, 2011.

Supplementary data

Synthesis, molecular docking, and QSAR study of bis-sulfonamide derivatives as potential aromatase inhibitors

Ronnakorn Leechaisit, Ratchanok Pingaew*, Veda Prachayasittikul*, Apilak Worachartcheewan, Supaluk Prachayasittikul, Somsak Ruchirawat, Virapong Prachayasittikul

E-mail: ratchanok@swu.ac.th (R. Pingaew)

Tel: 662-649-5000 ext 18253; Fax: 662-260-0128

E-mail: veda.pra@mahidol.ac.th (V. Prachayasittikul)

Tel: 662-441-4376; Fax: 662-441-4380

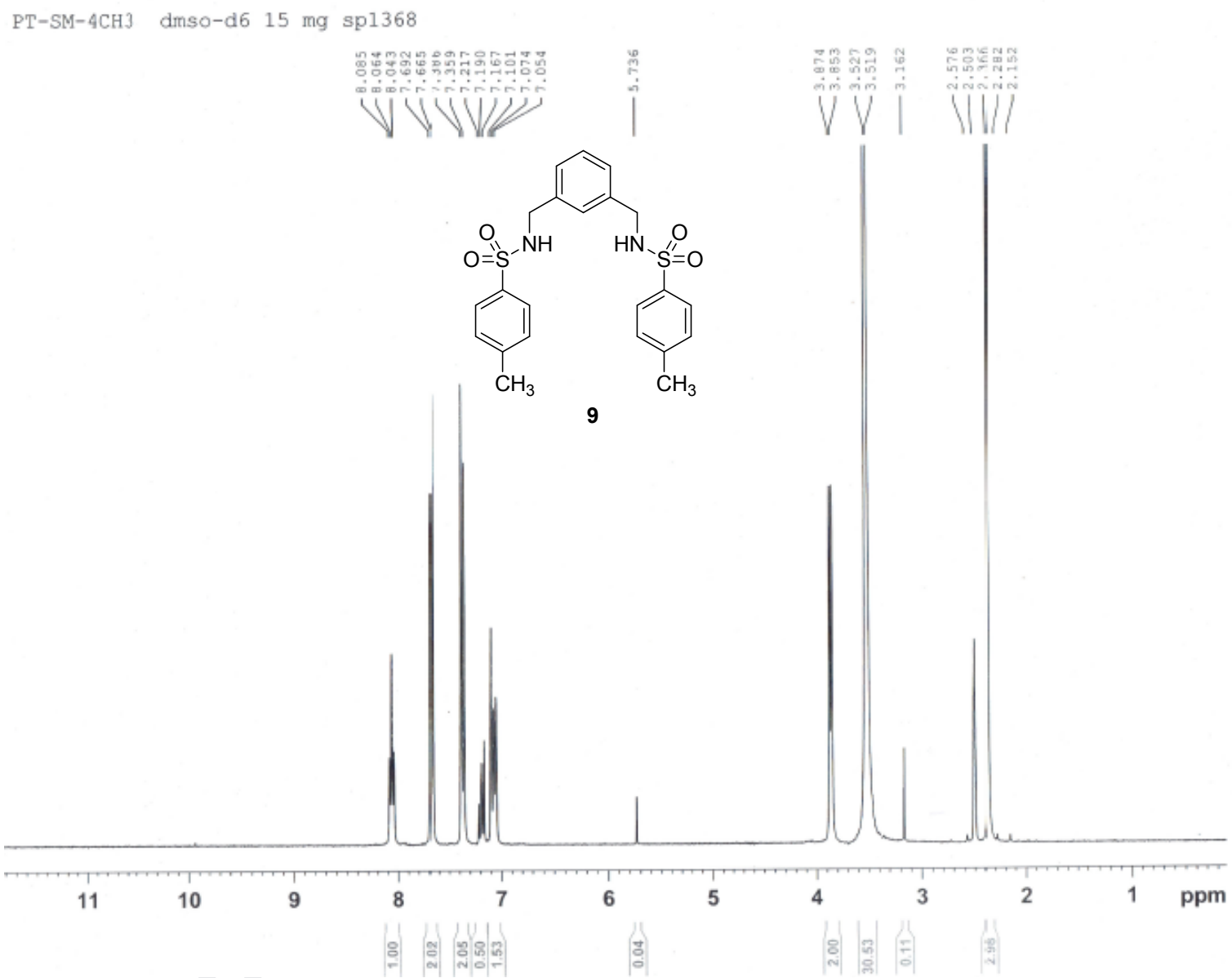

^{1}H NMR spectrum of compound **9** (DMSO-d_6)

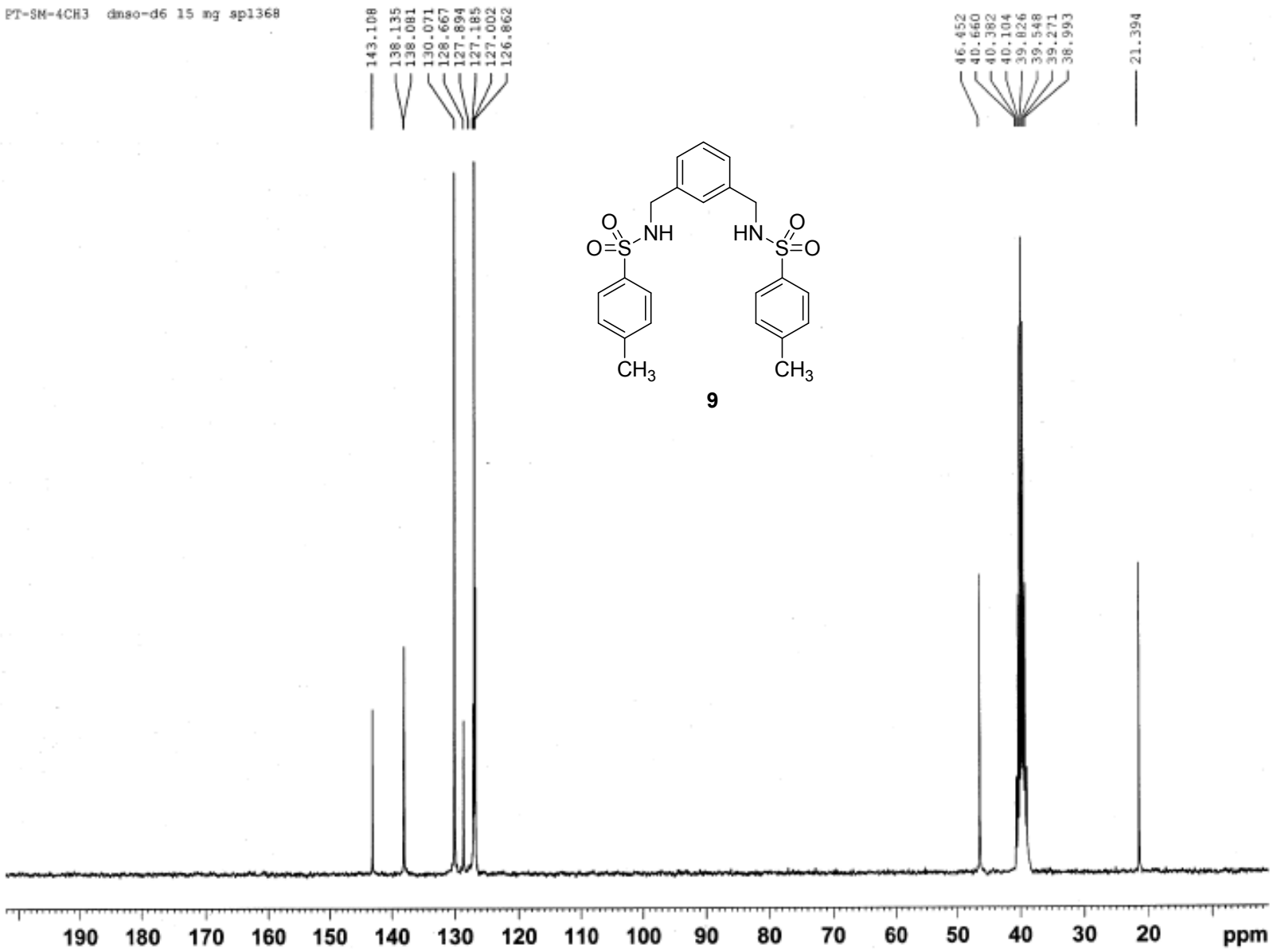

^{13}C NMR spectrum of compound **9** (DMSO-d_6)

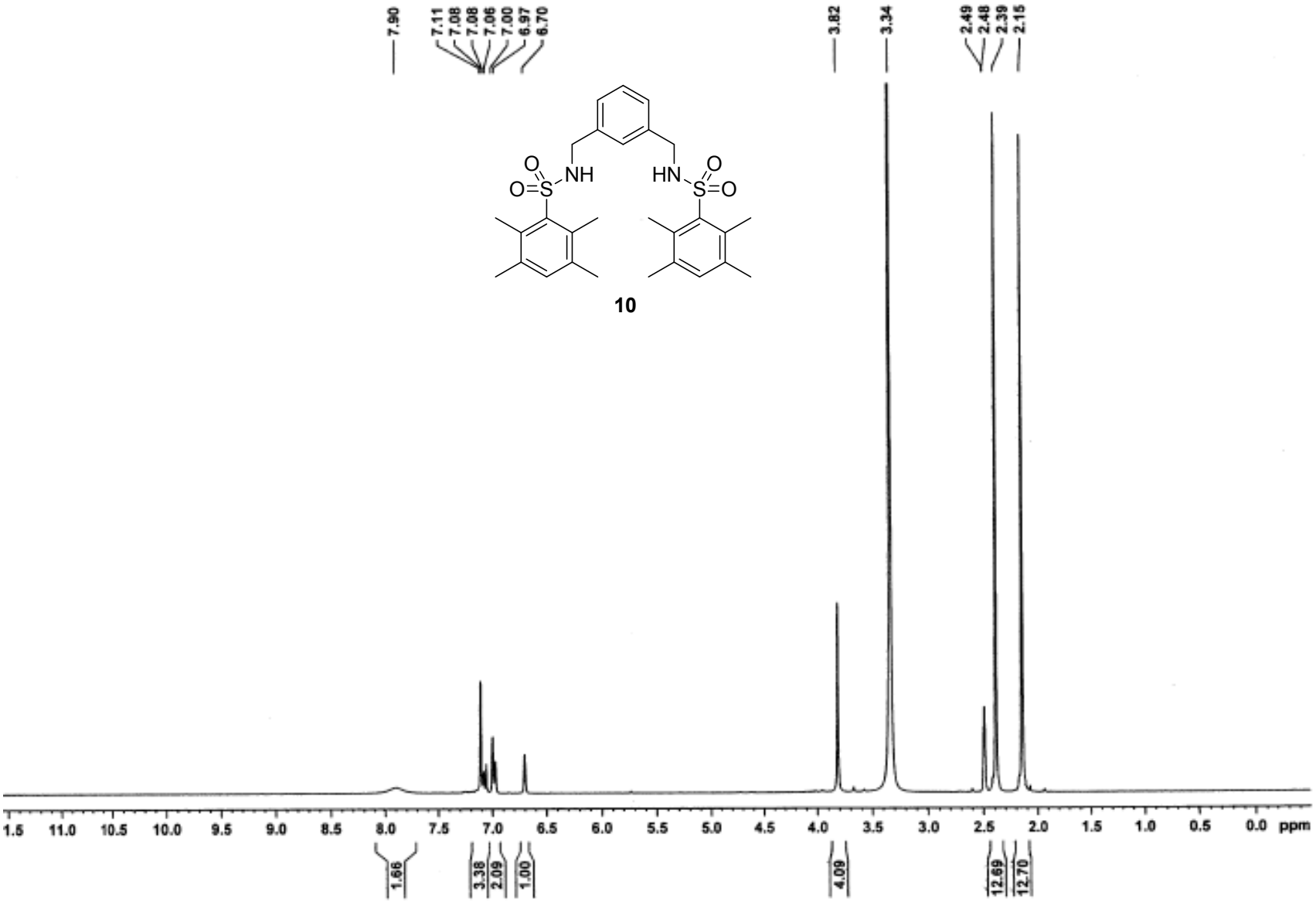

^{1}H NMR spectrum of compound **10** (DMSO-d_6)

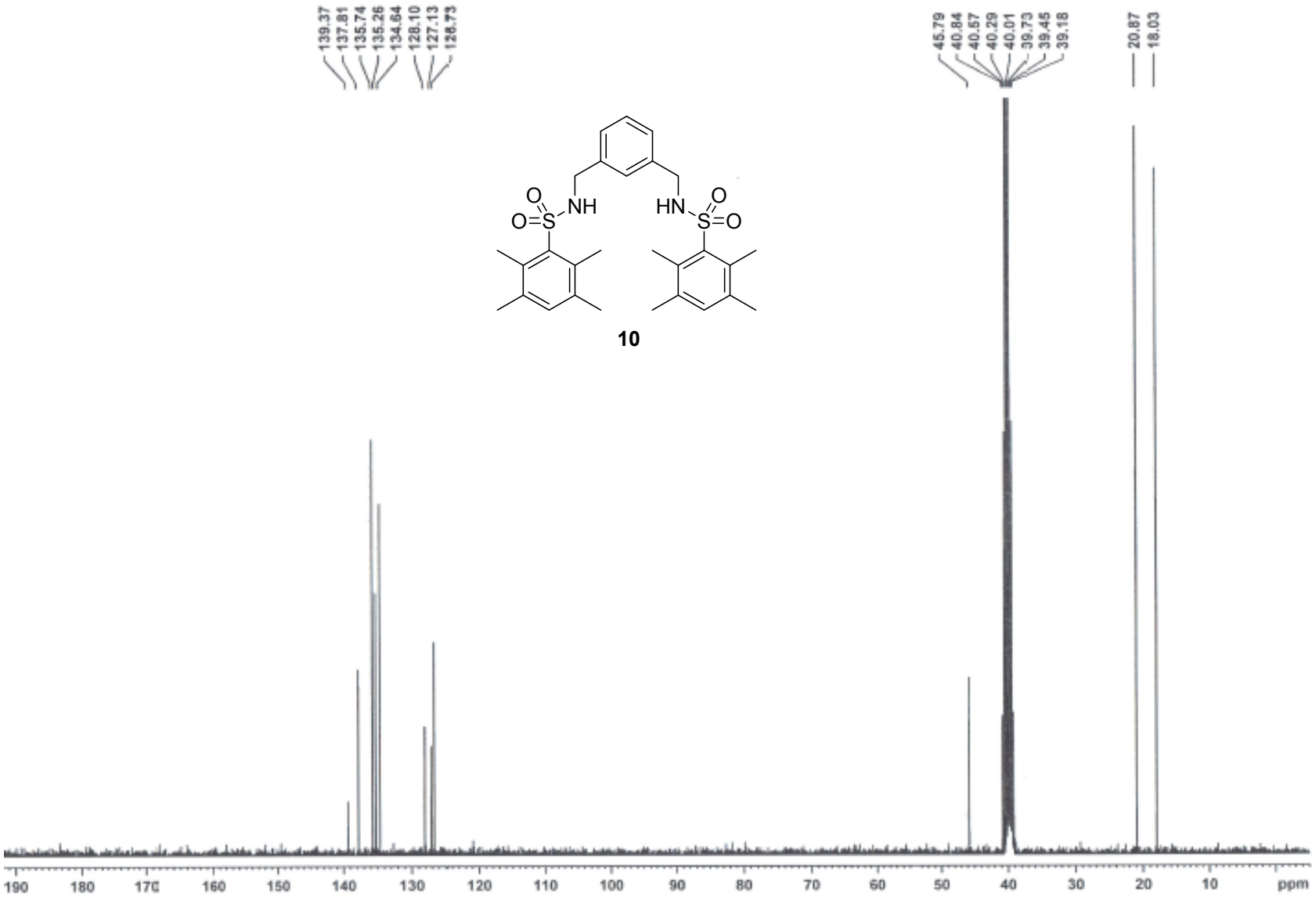

^{13}C NMR spectrum of compound **10** (DMSO-d_6)

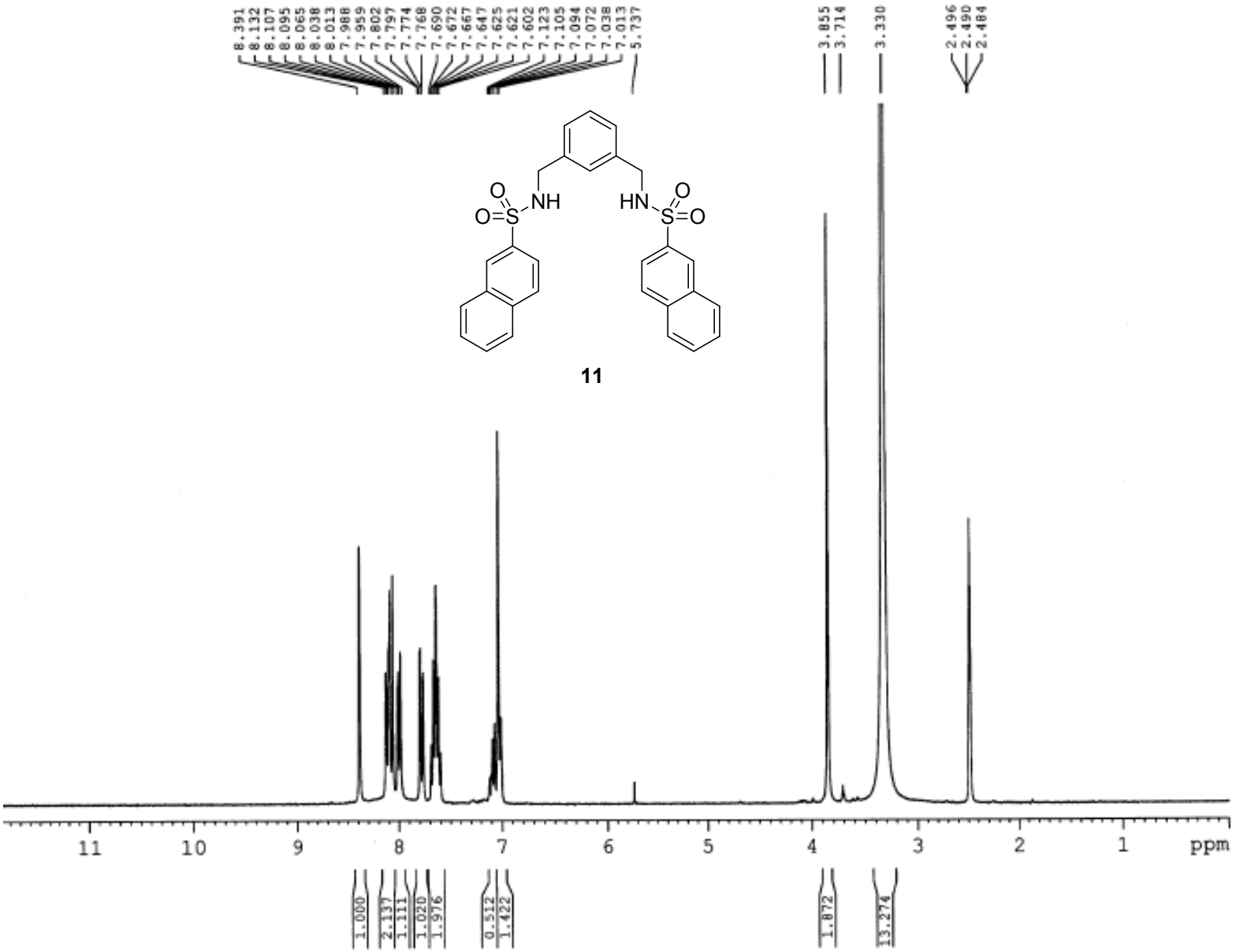

^{1}H NMR spectrum of compound **11** (DMSO-d_6)

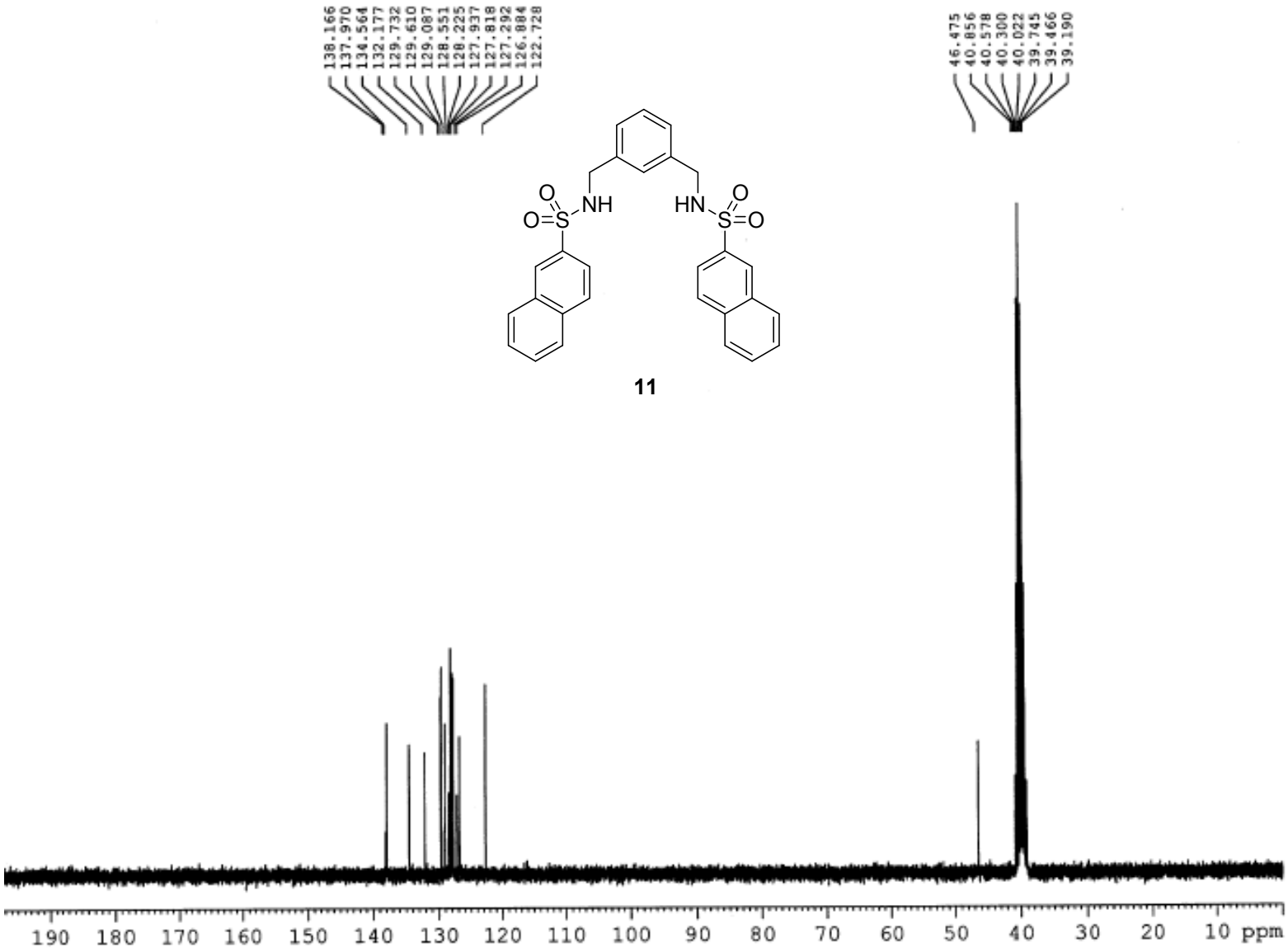

^{13}C NMR spectrum of compound **11** (DMSO-d_6)

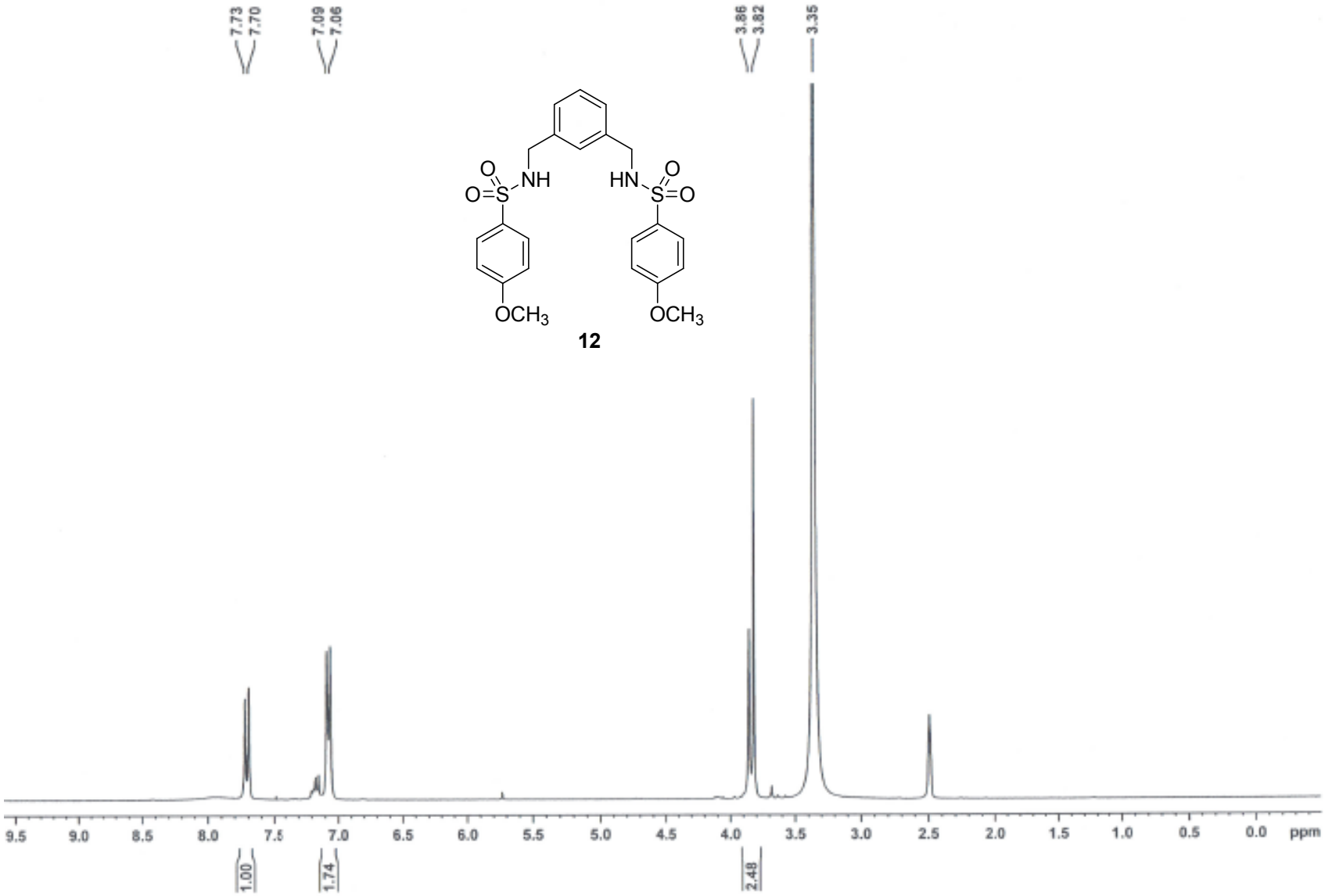

^{1}H NMR spectrum of compound **12** (DMSO-d_6)

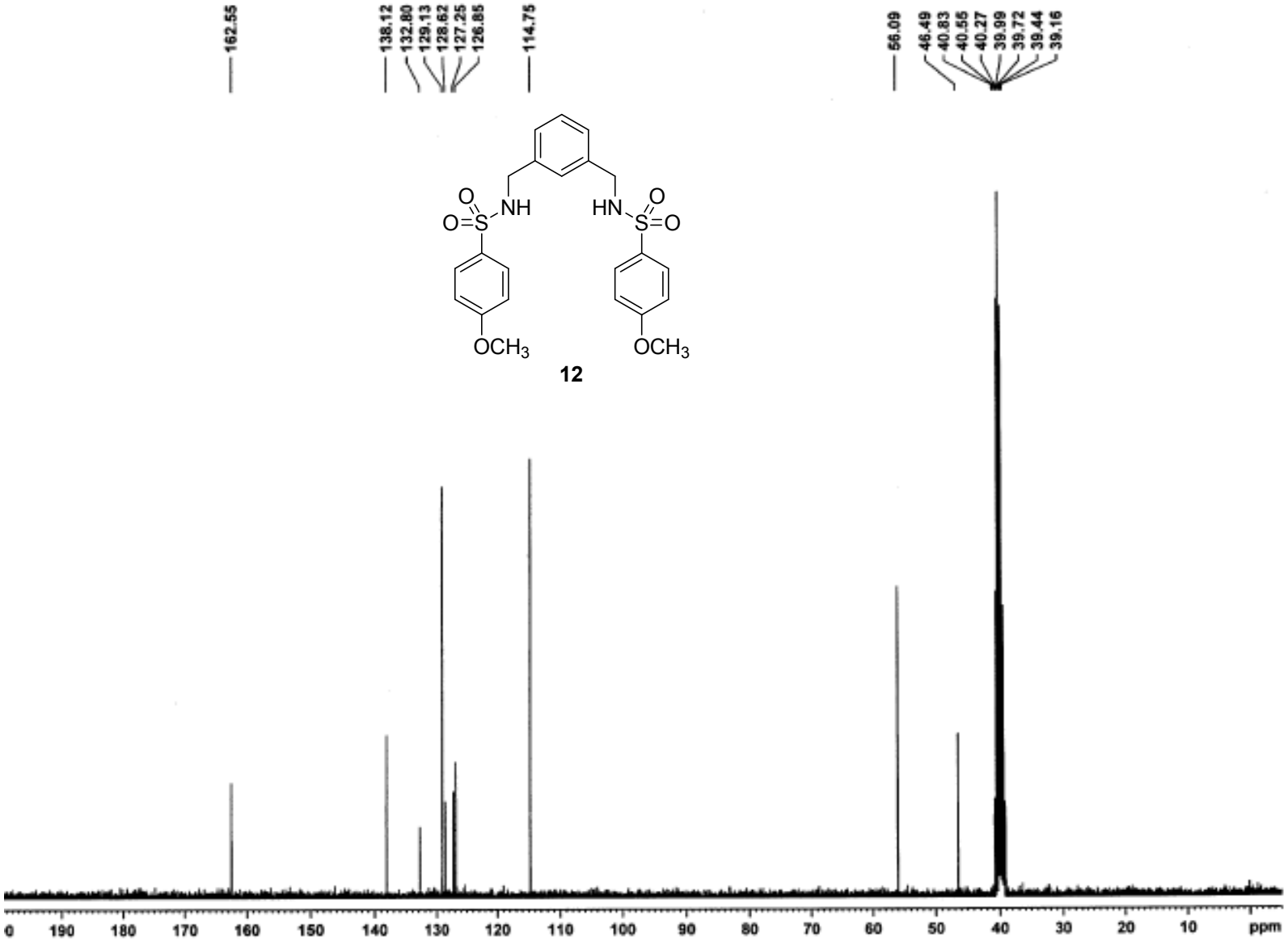

^{13}C NMR spectrum of compound **12** (DMSO-d_6)

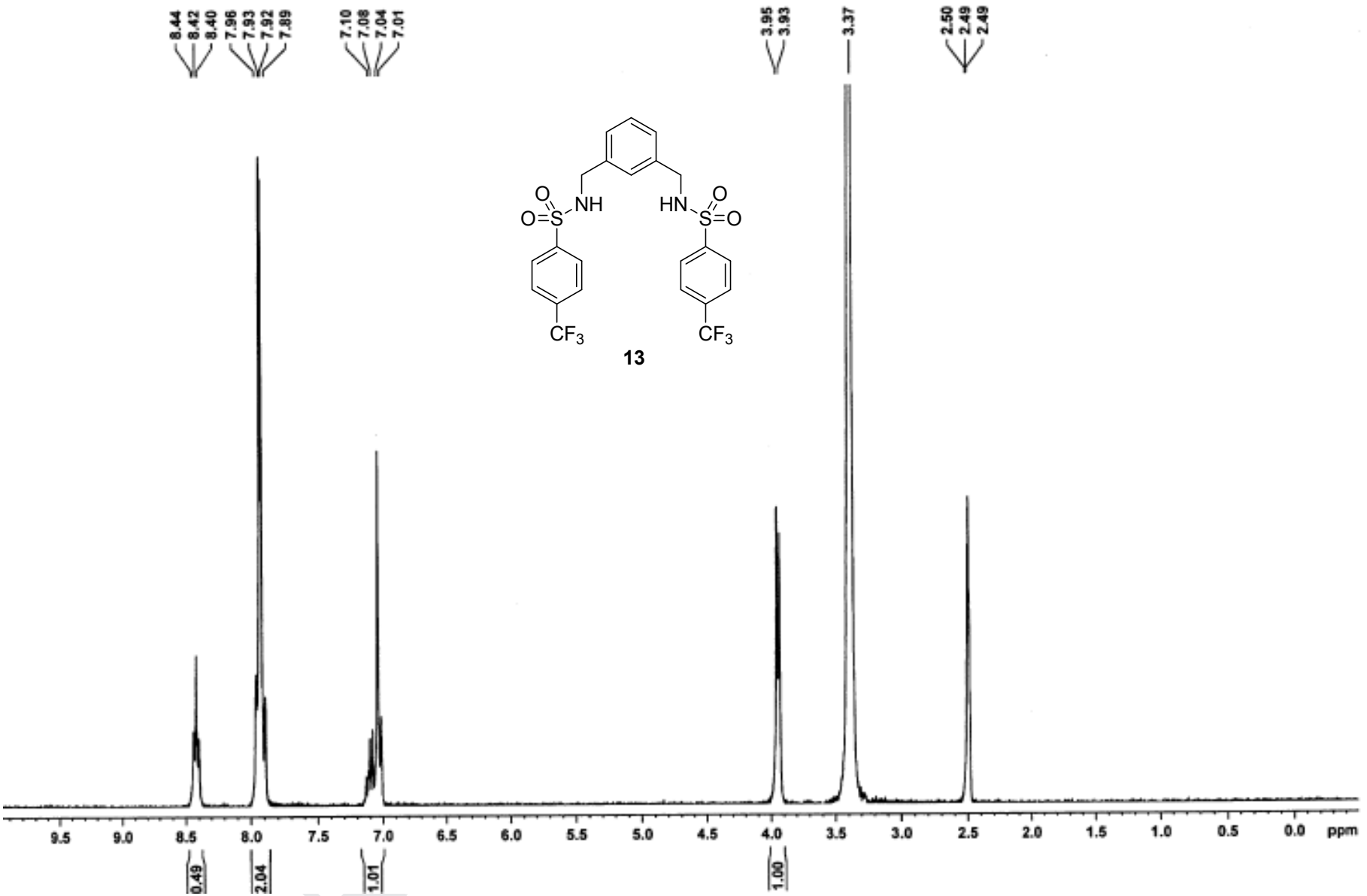

^{1}H NMR spectrum of compound **13** (DMSO-d_6)

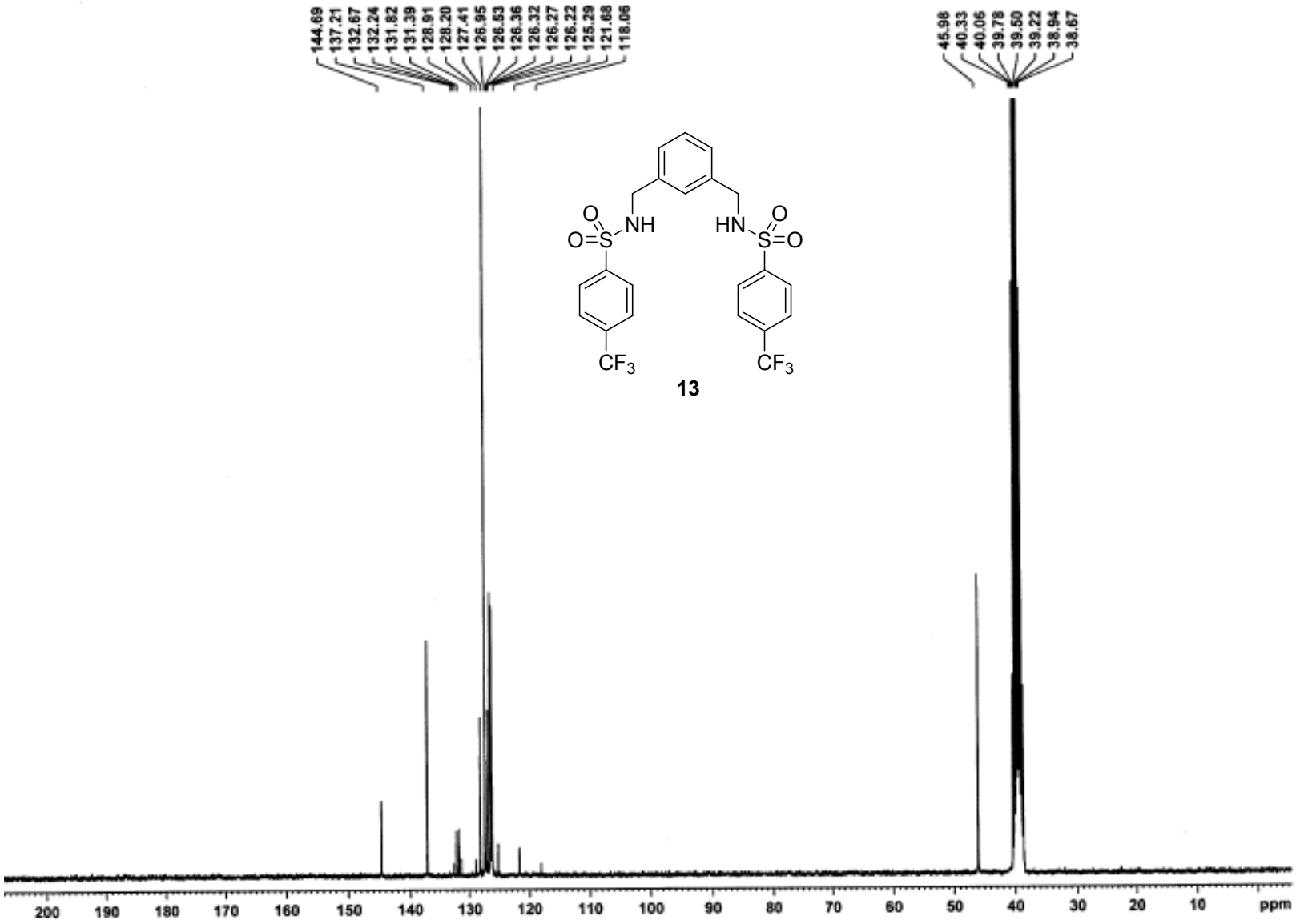

^{13}C NMR spectrum of compound **13** (DMSO-d_6)

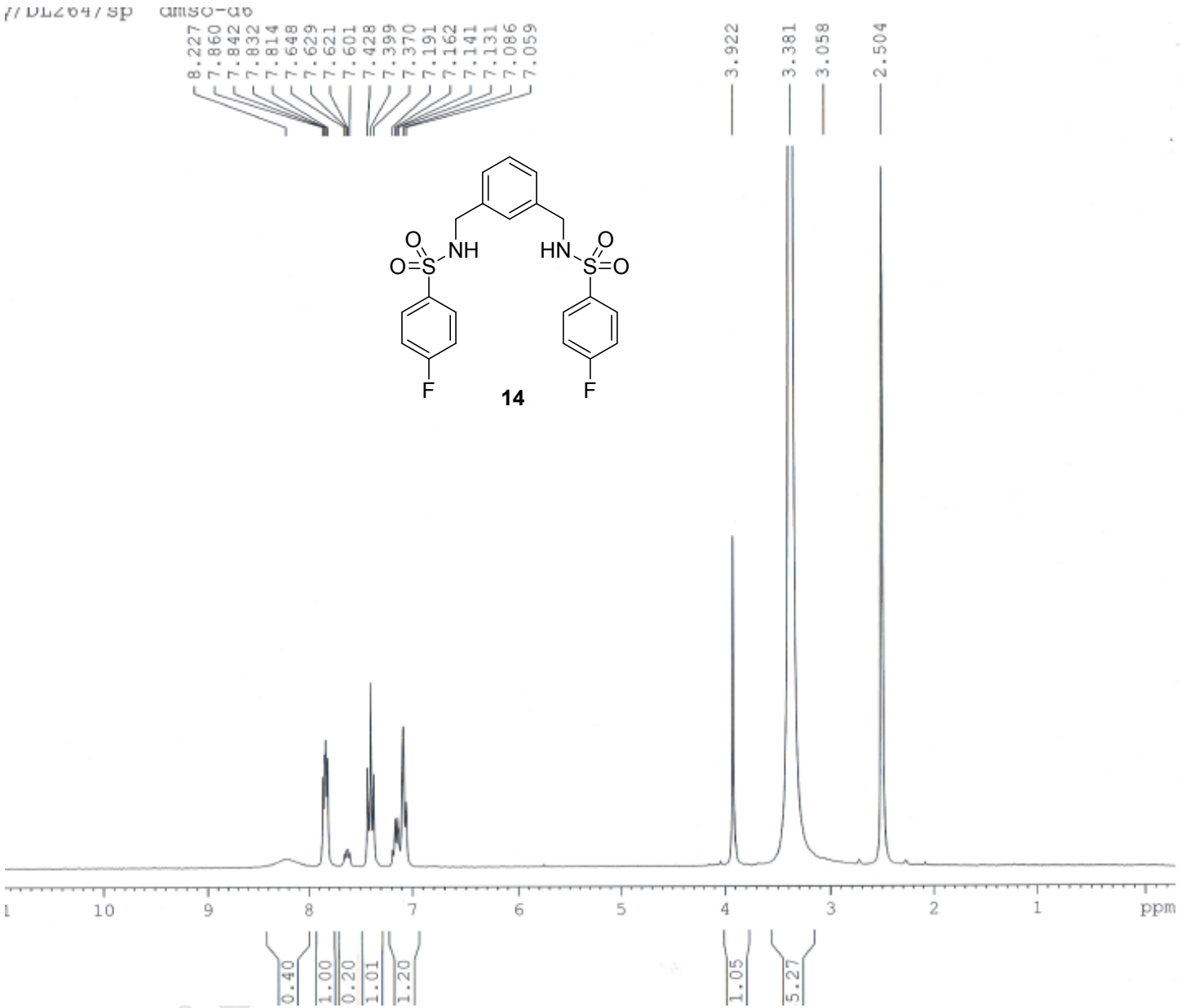

^{1}H NMR spectrum of compound **14** (DMSO-d_6)

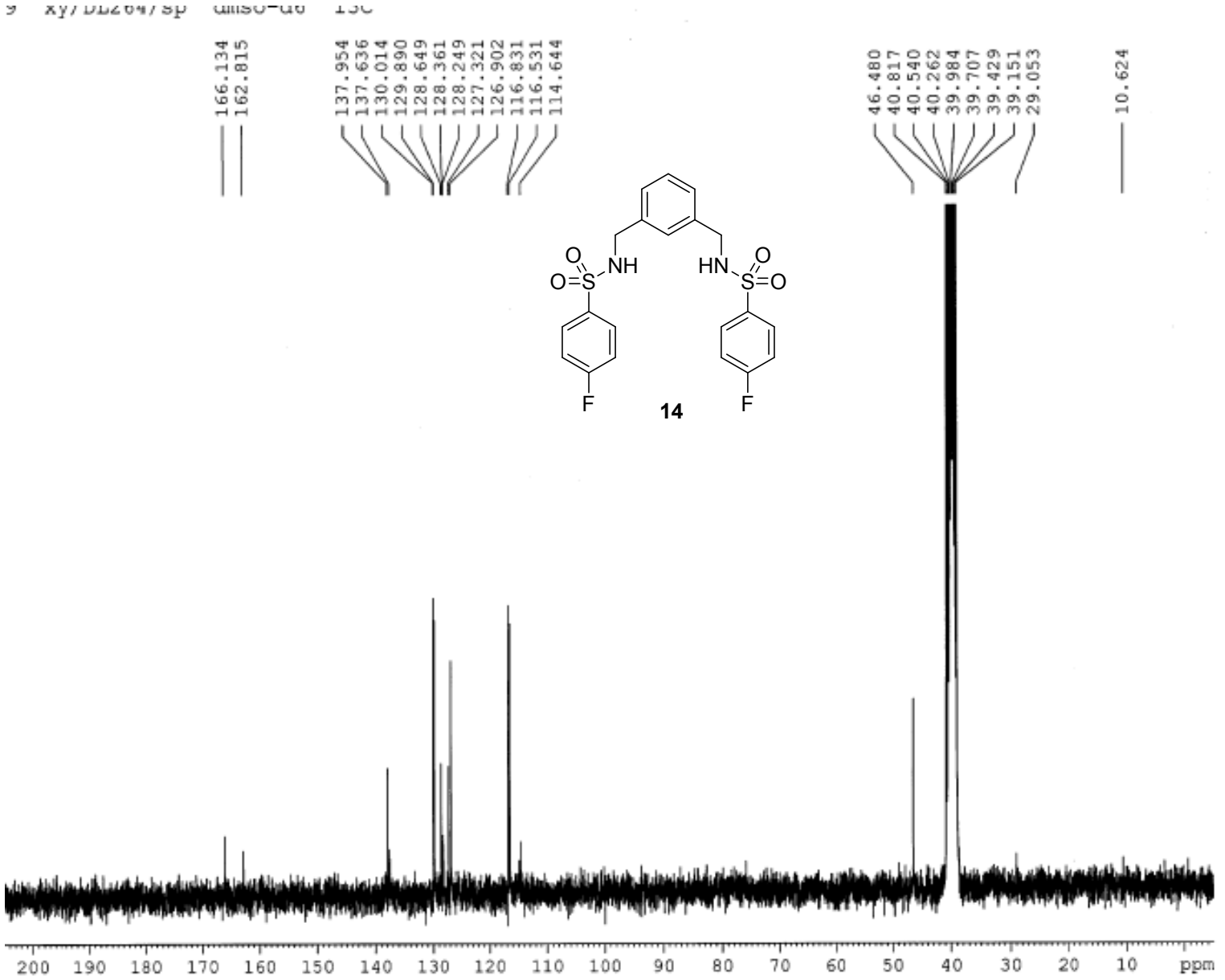

^{13}C NMR spectrum of compound **14** (DMSO-d_6)

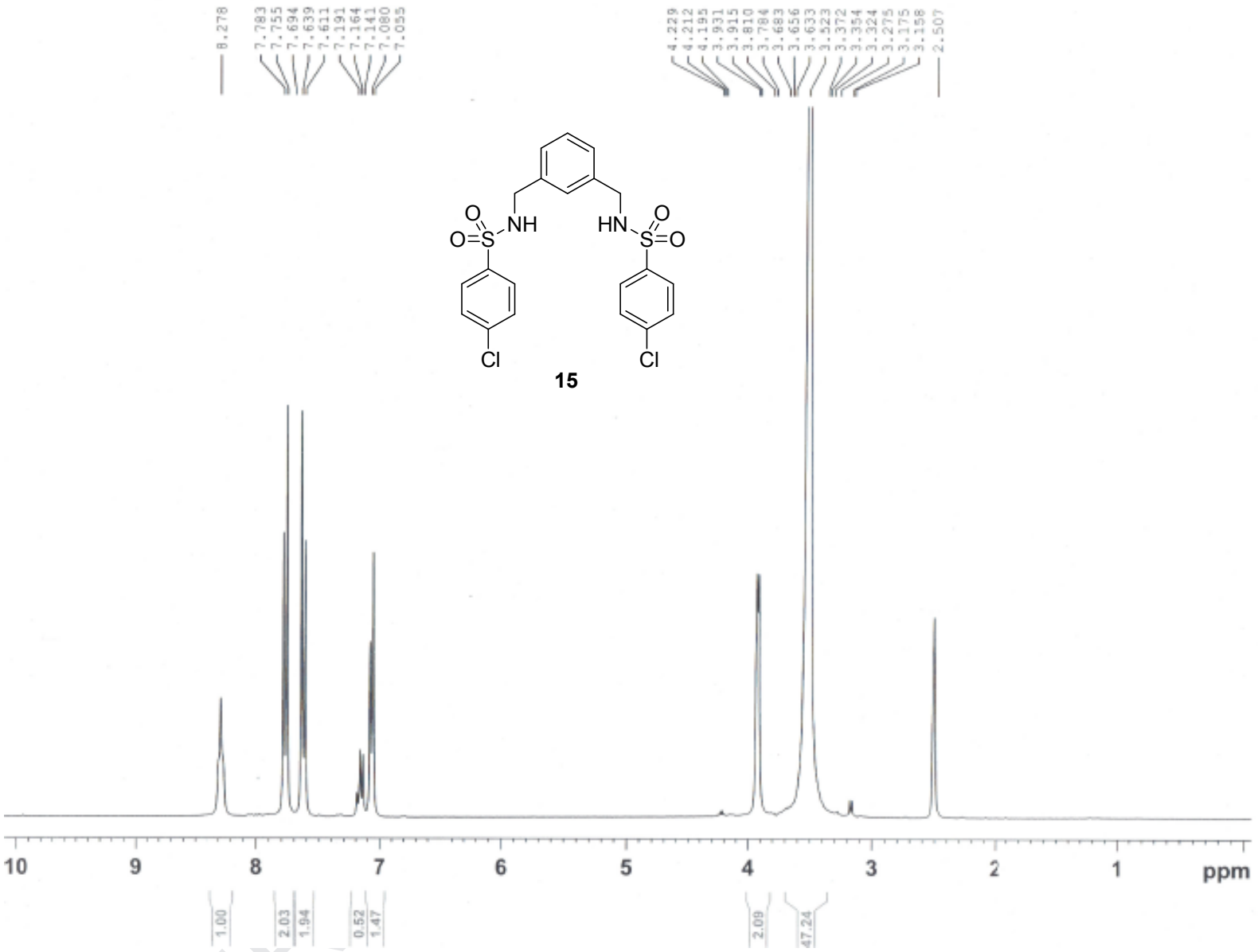

^{1}H NMR spectrum of compound **15** (DMSO-d_6)

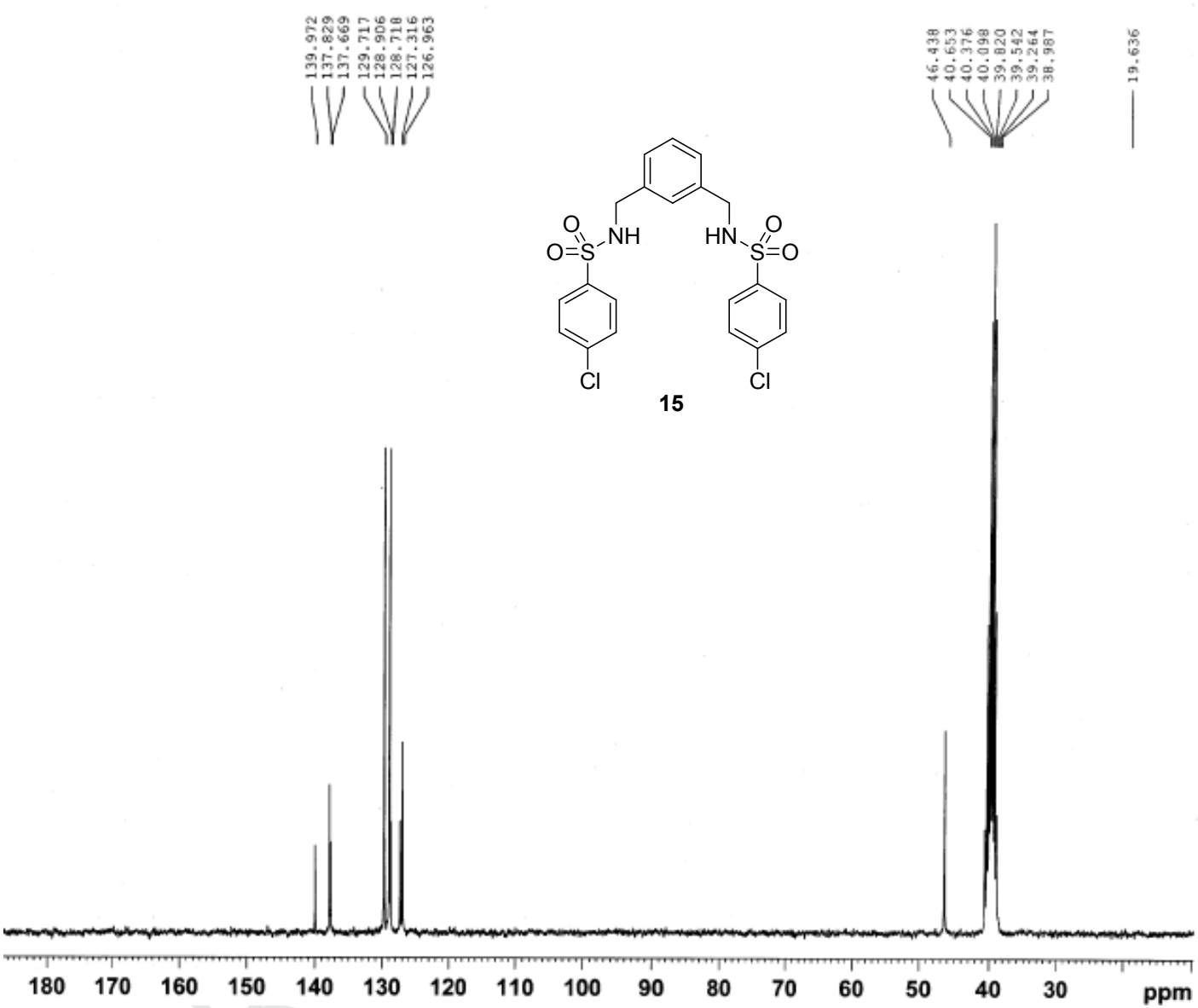

^{13}C NMR spectrum of compound **15** (DMSO-d_6)

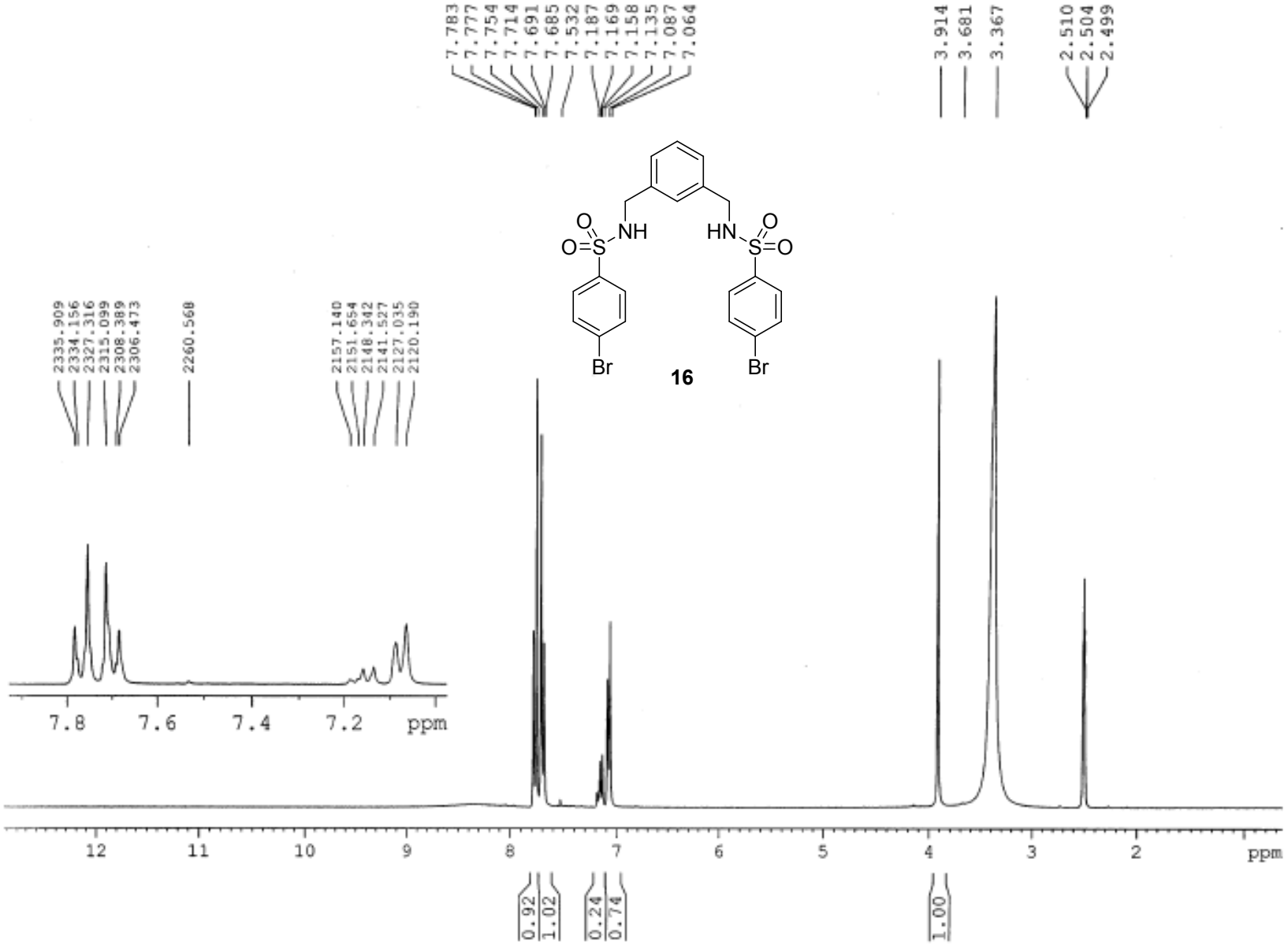

^{1}H NMR spectrum of compound **16** (DMSO-d_6)

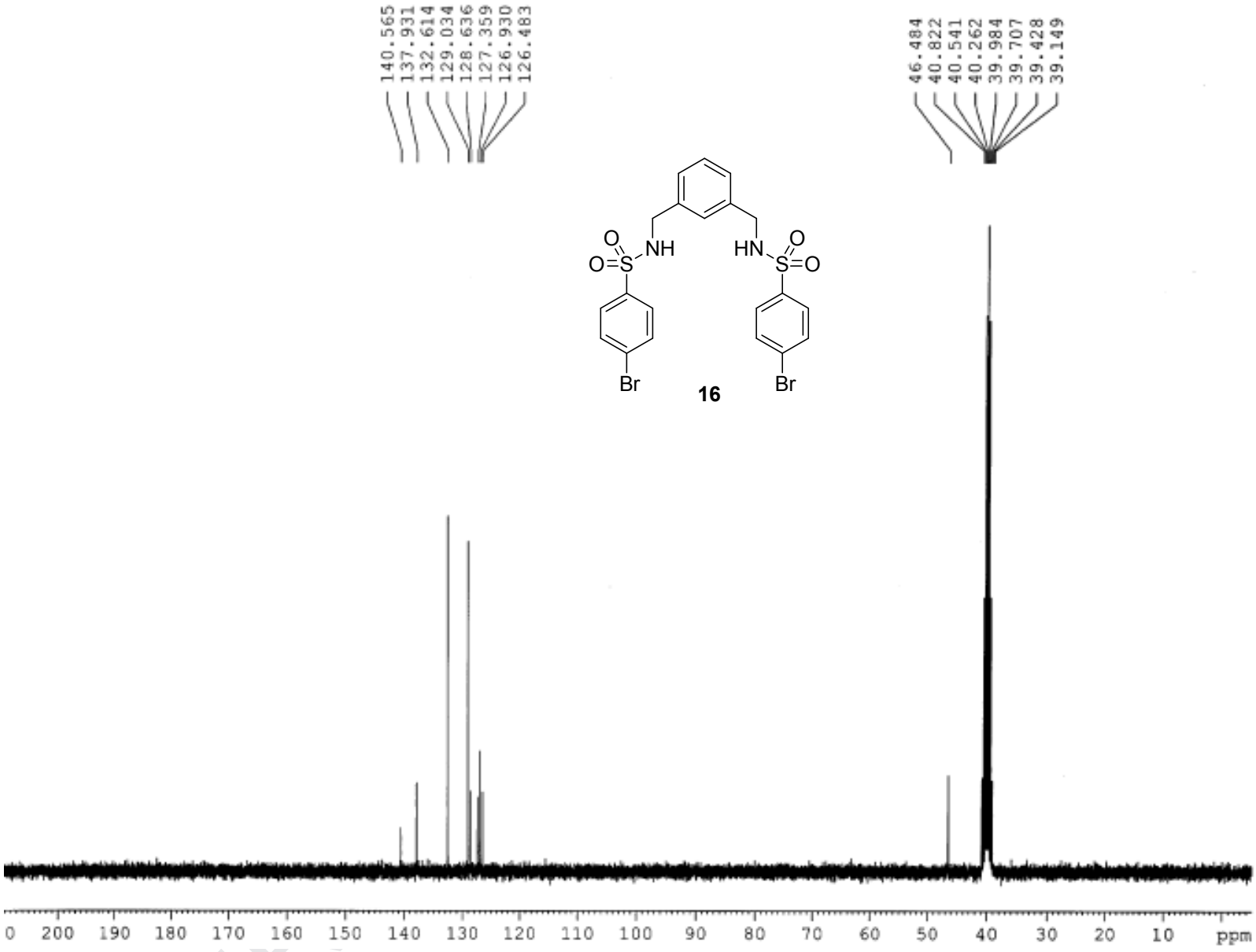

^{13}C NMR spectrum of compound **16** (DMSO-d_6)

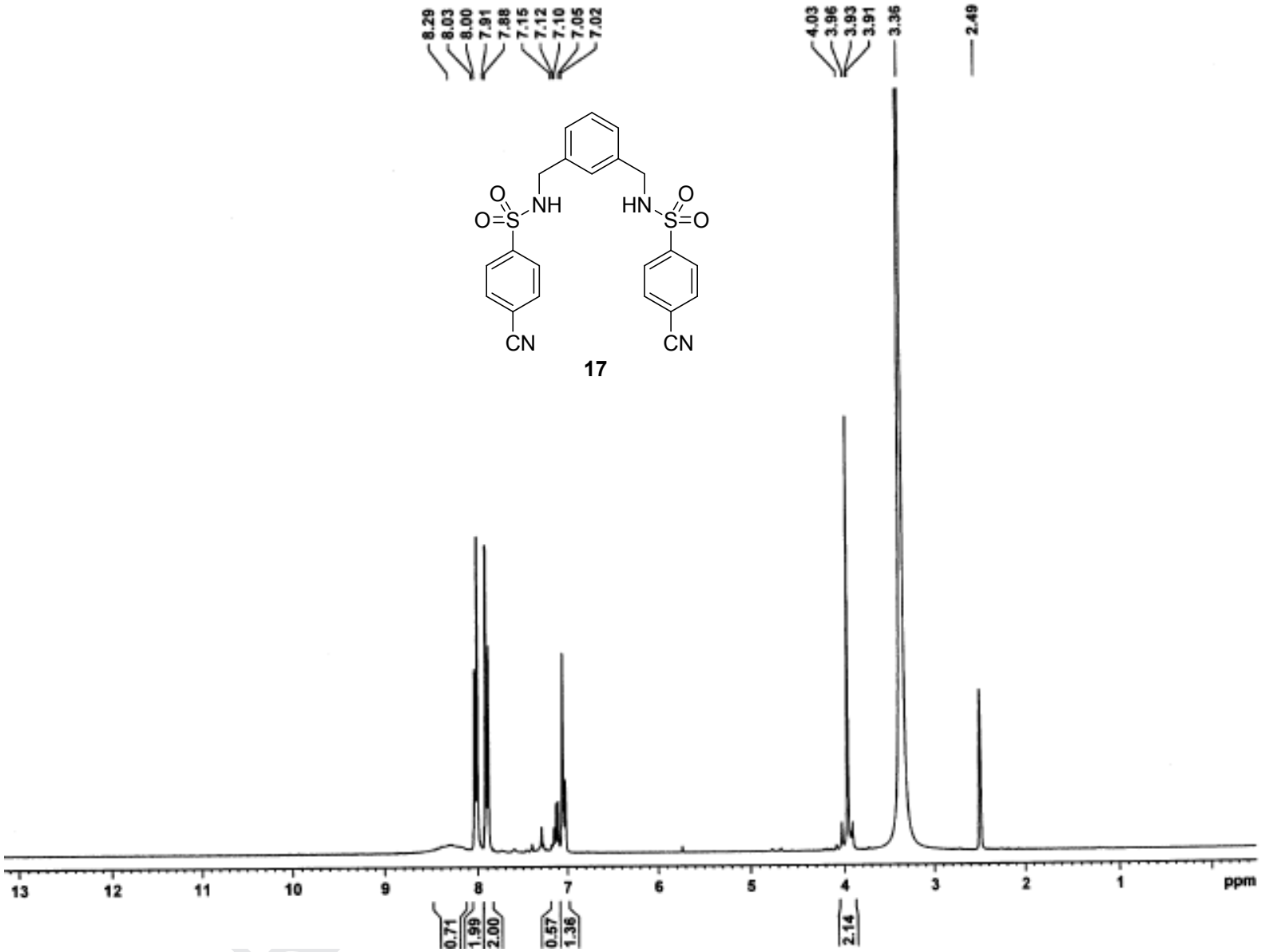

^{1}H NMR spectrum of compound **17** (DMSO-d_6)

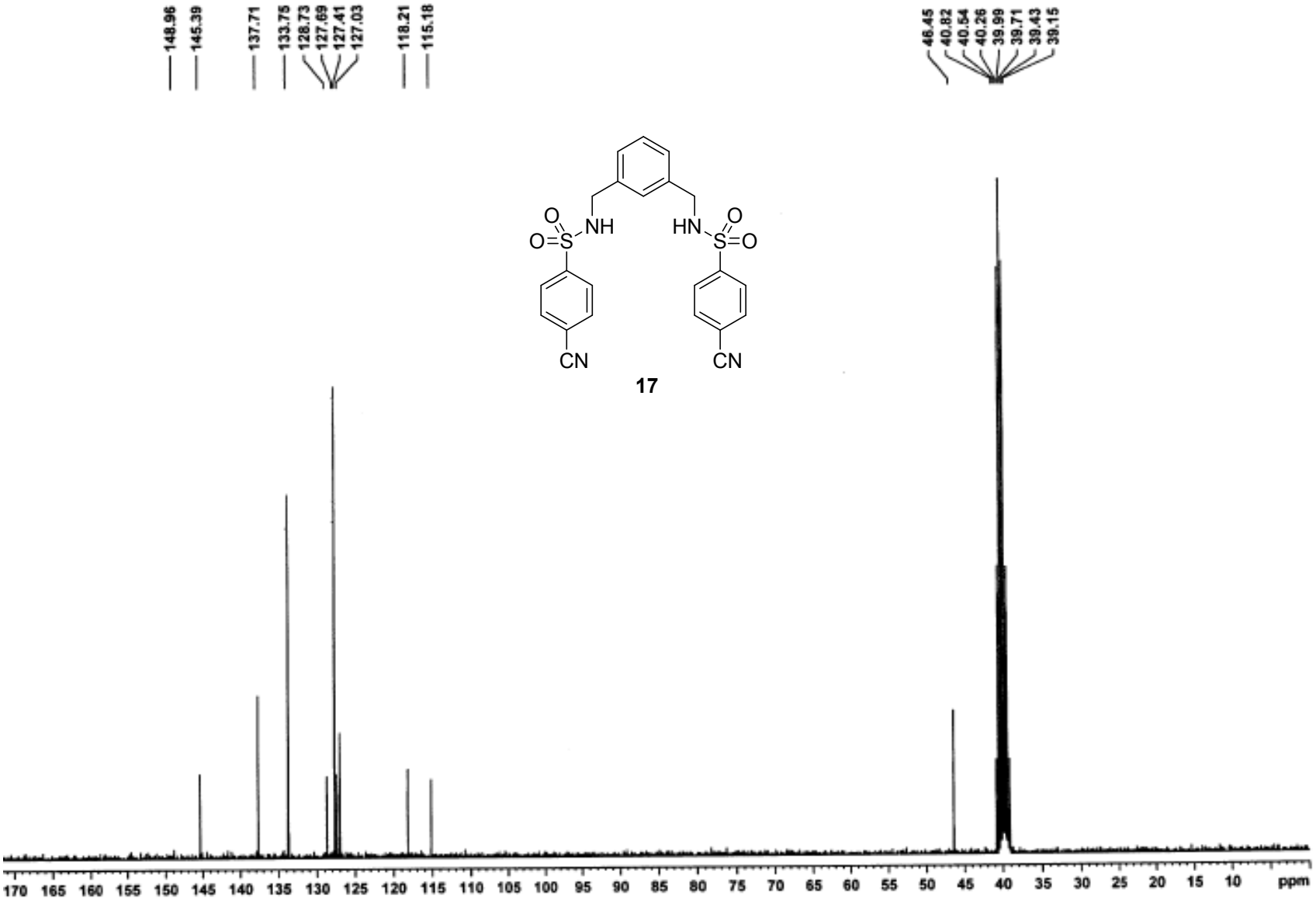

^{13}C NMR spectrum of compound **17** (DMSO-d_6)

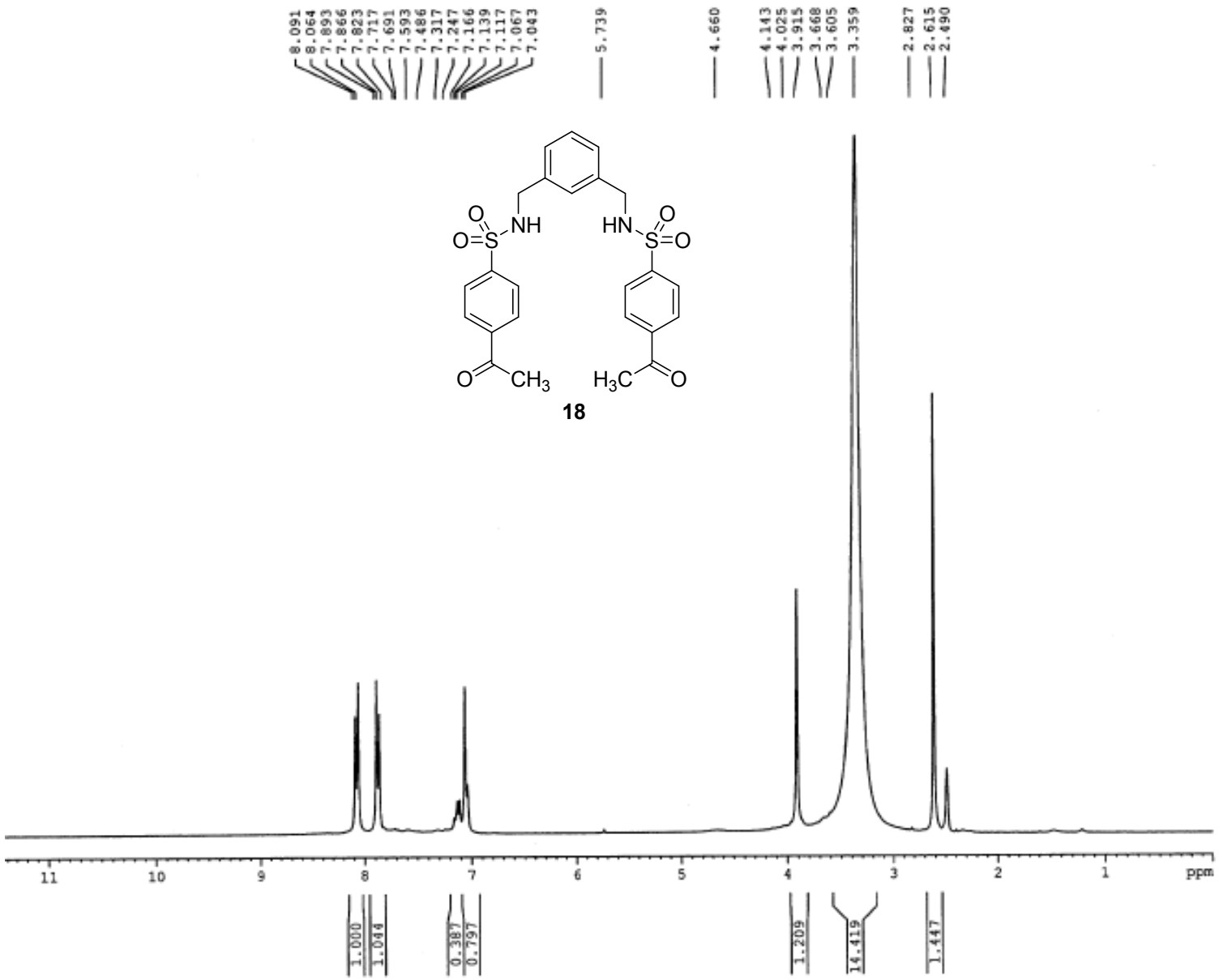

^{1}H NMR spectrum of compound **18** (DMSO-d_6)

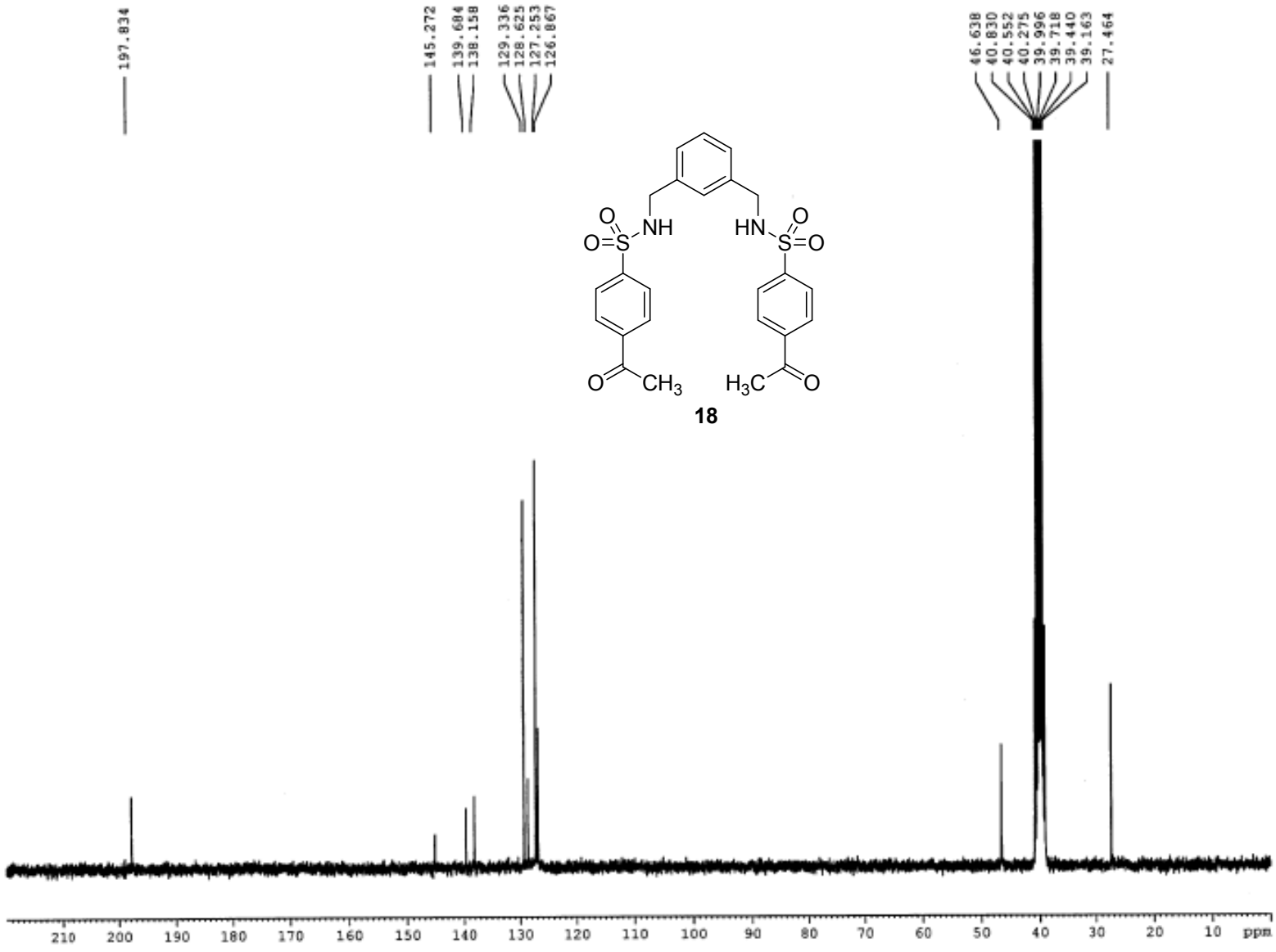

^{13}C NMR spectrum of compound **18** (DMSO-d_6)

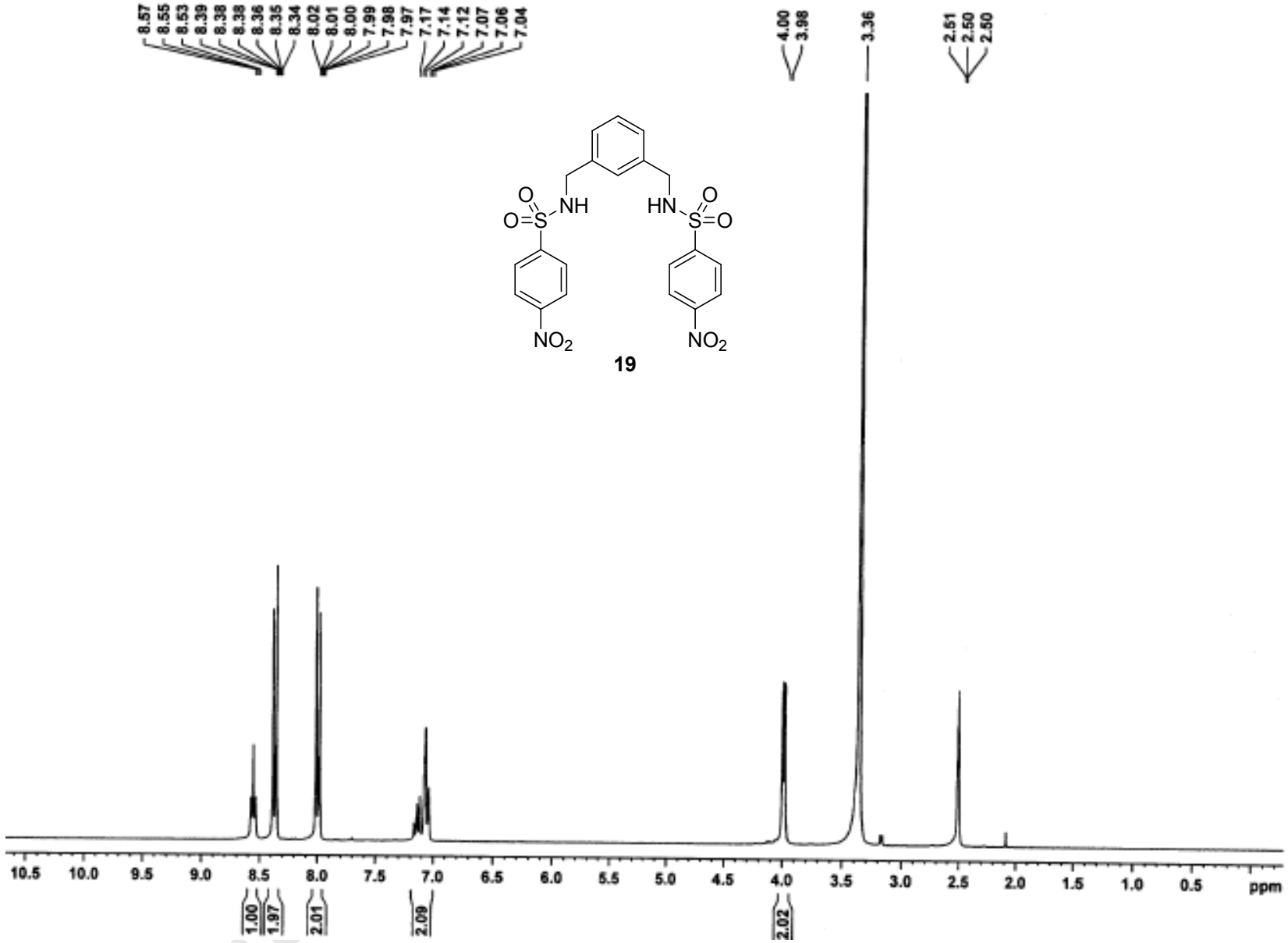

^{1}H NMR spectrum of compound **19** (DMSO-d_6)

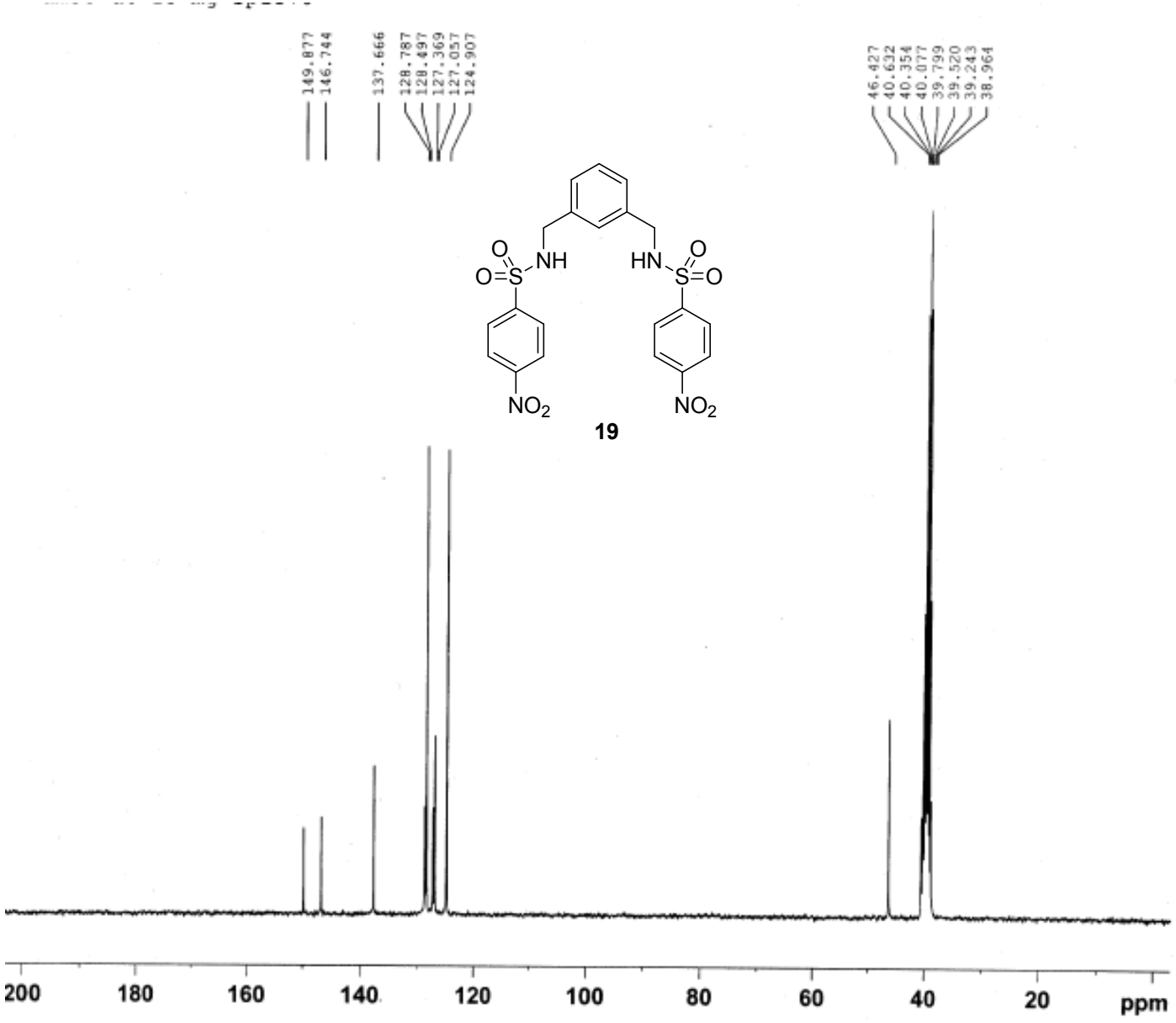

^{13}C NMR spectrum of compound **19** (DMSO-d_6)

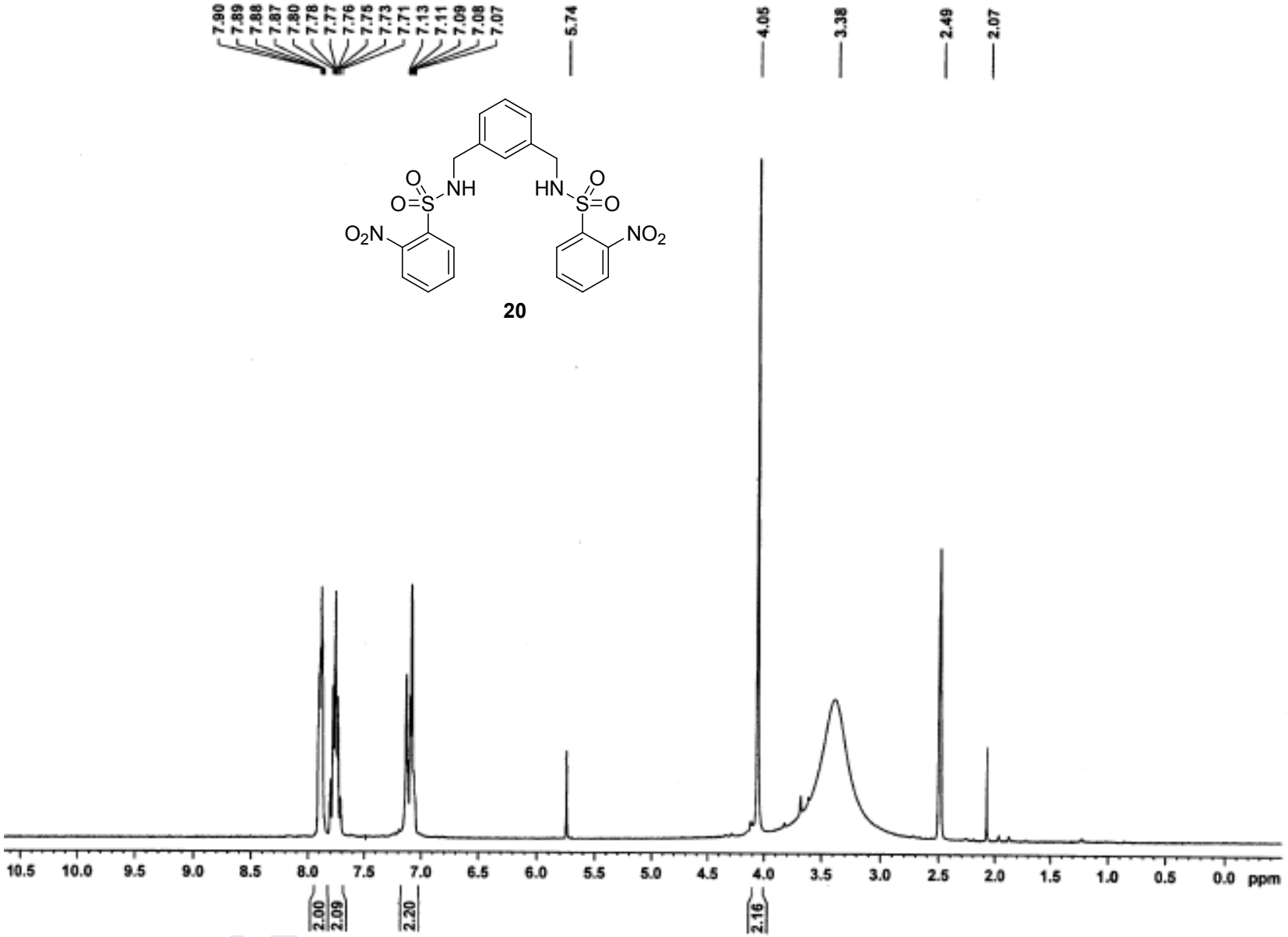

20

^{1}H NMR spectrum of compound **20** (DMSO-d_6)

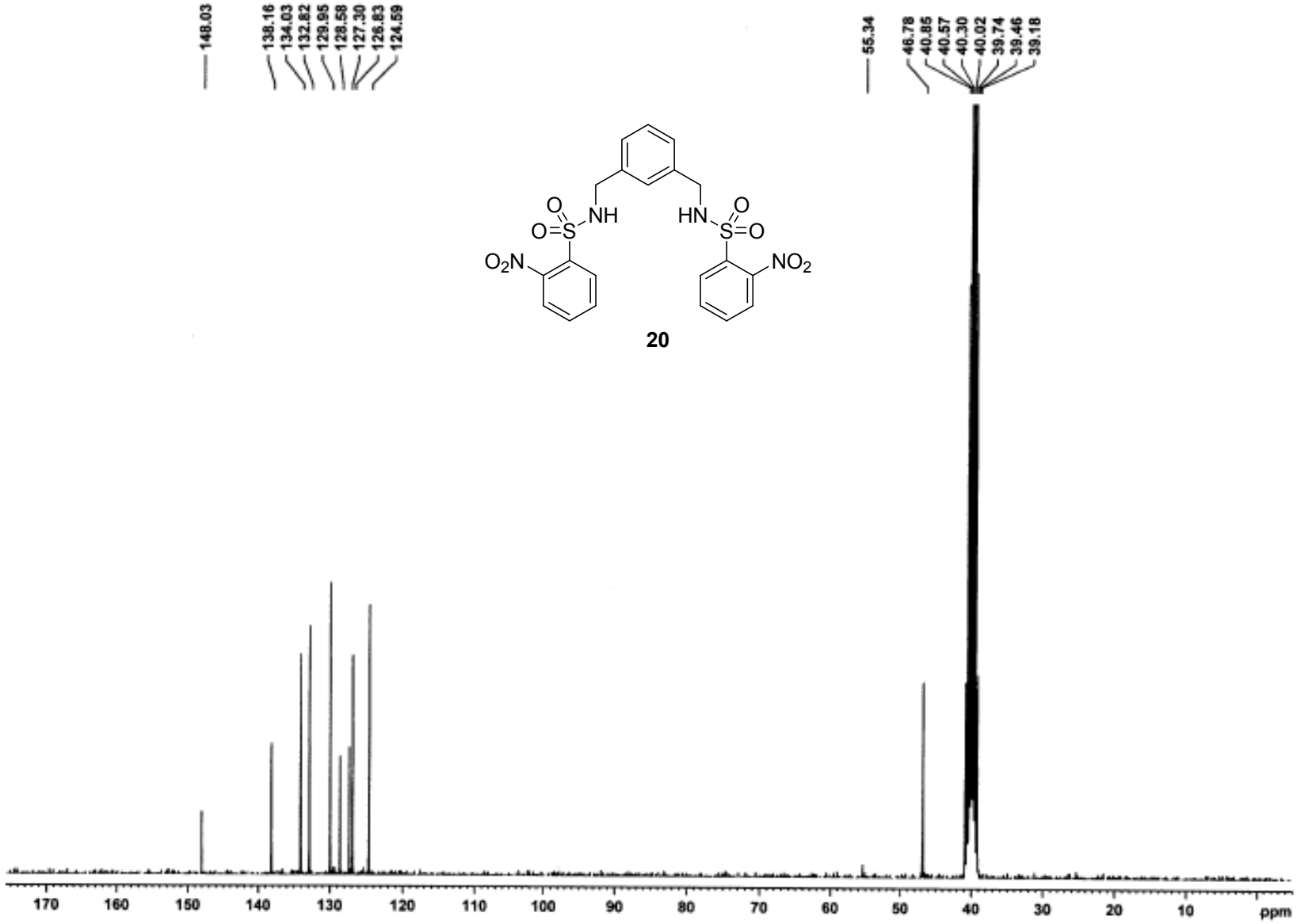

^{13}C NMR spectrum of compound **20** (DMSO-d_6)

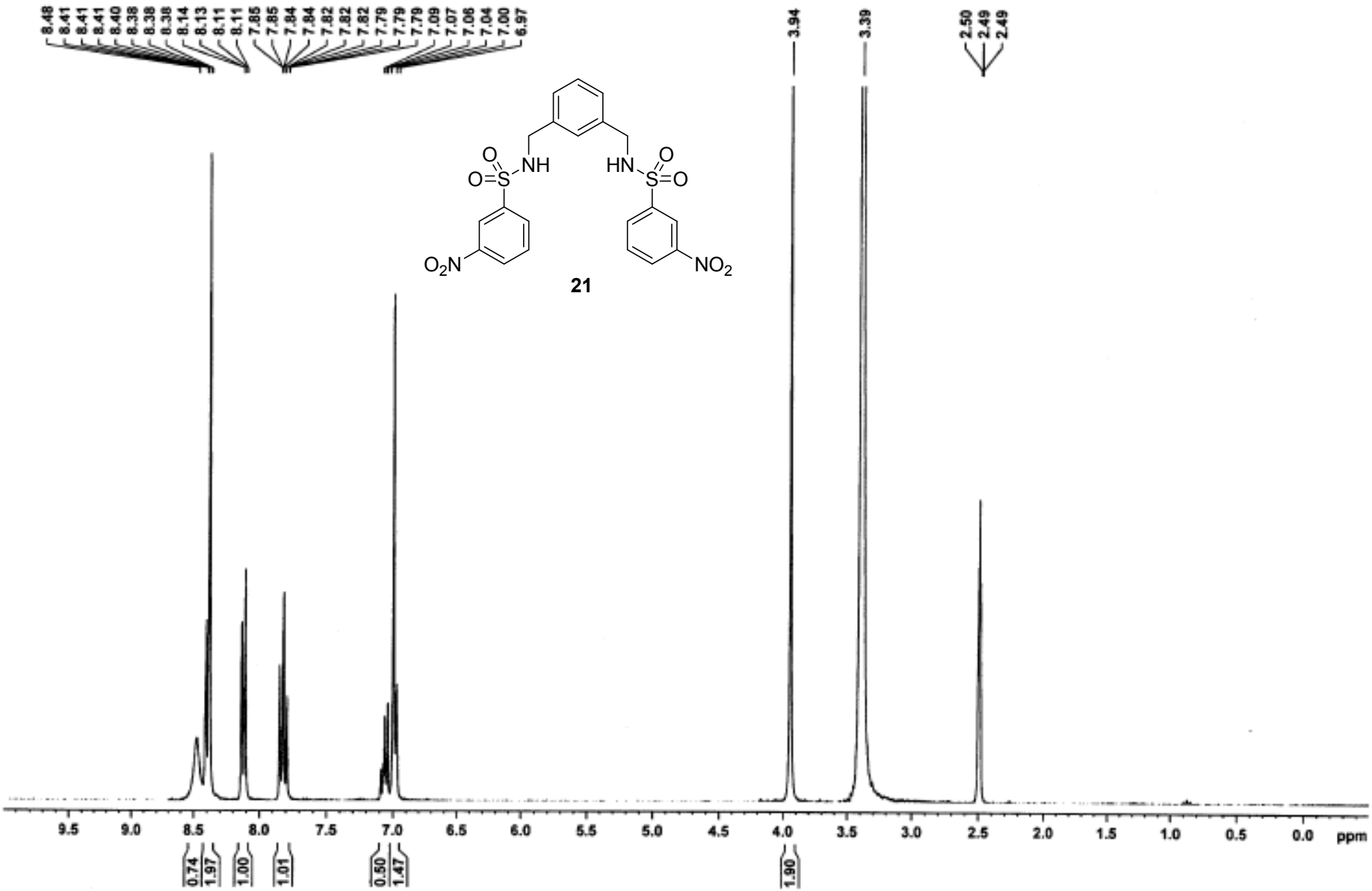

^{1}H NMR spectrum of compound **21** (DMSO-d_6)

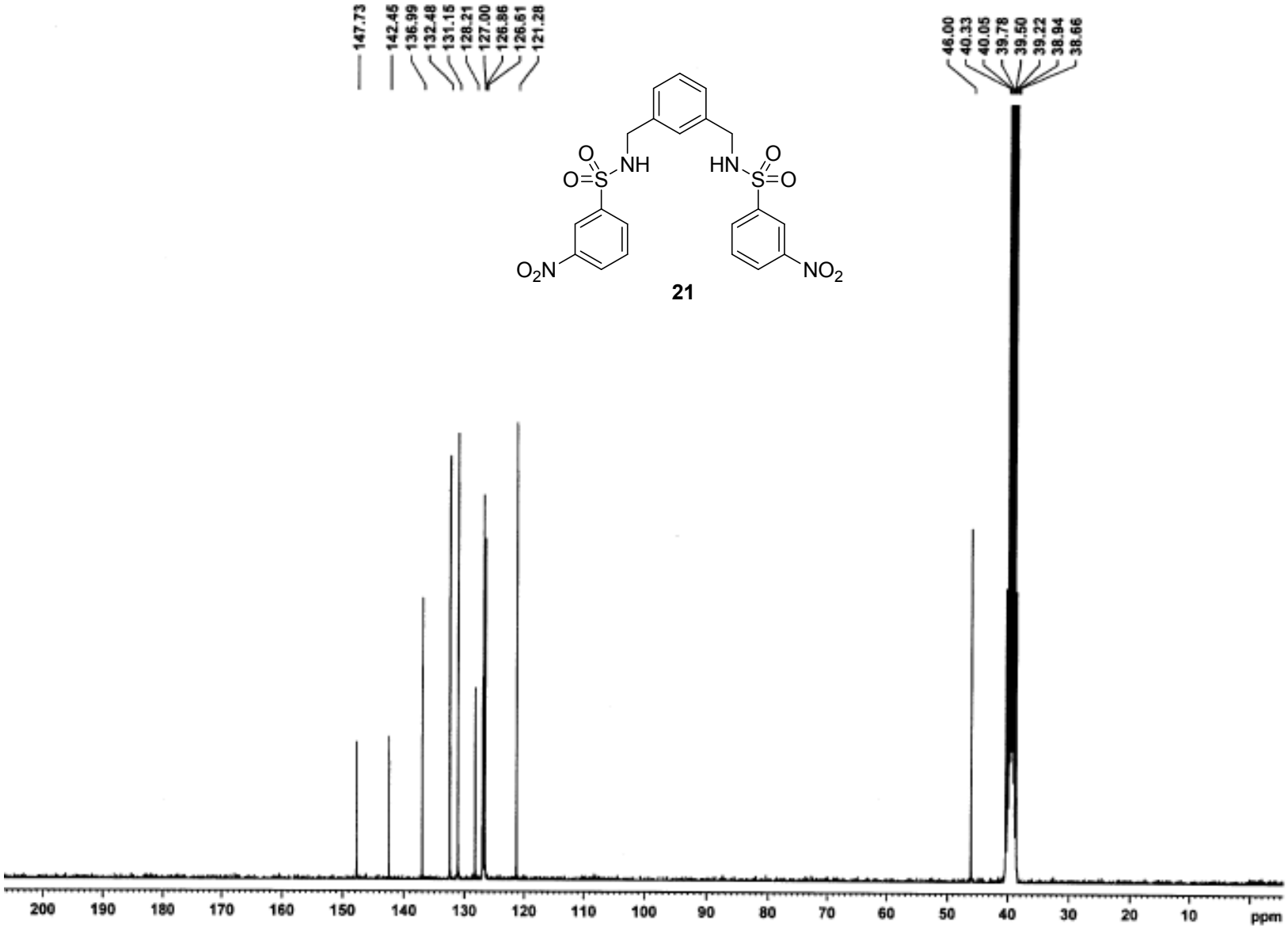

^{13}C NMR spectrum of compound **21** (DMSO-d_6)

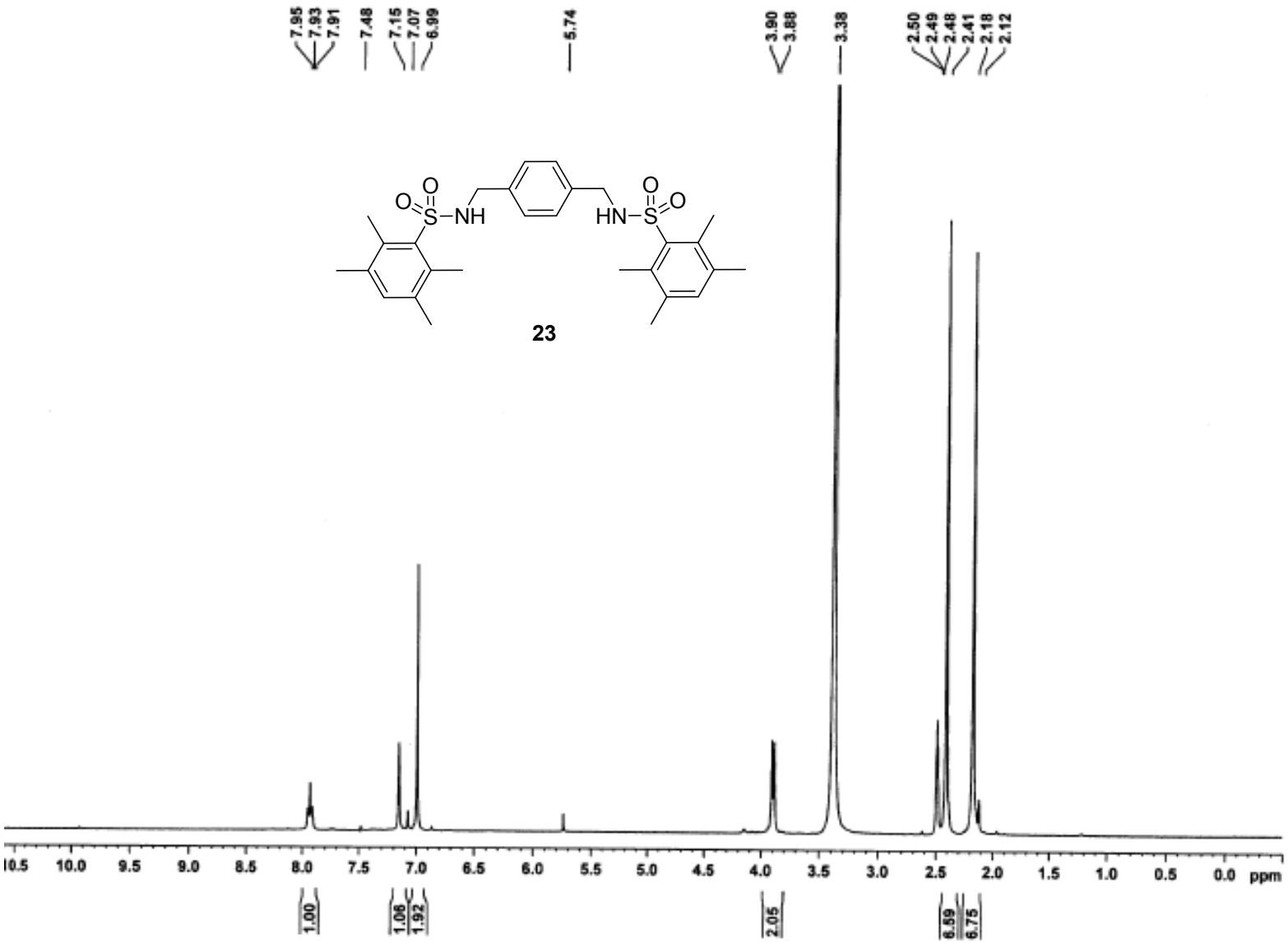

^{1}H NMR spectrum of compound **23** (DMSO-d_6)

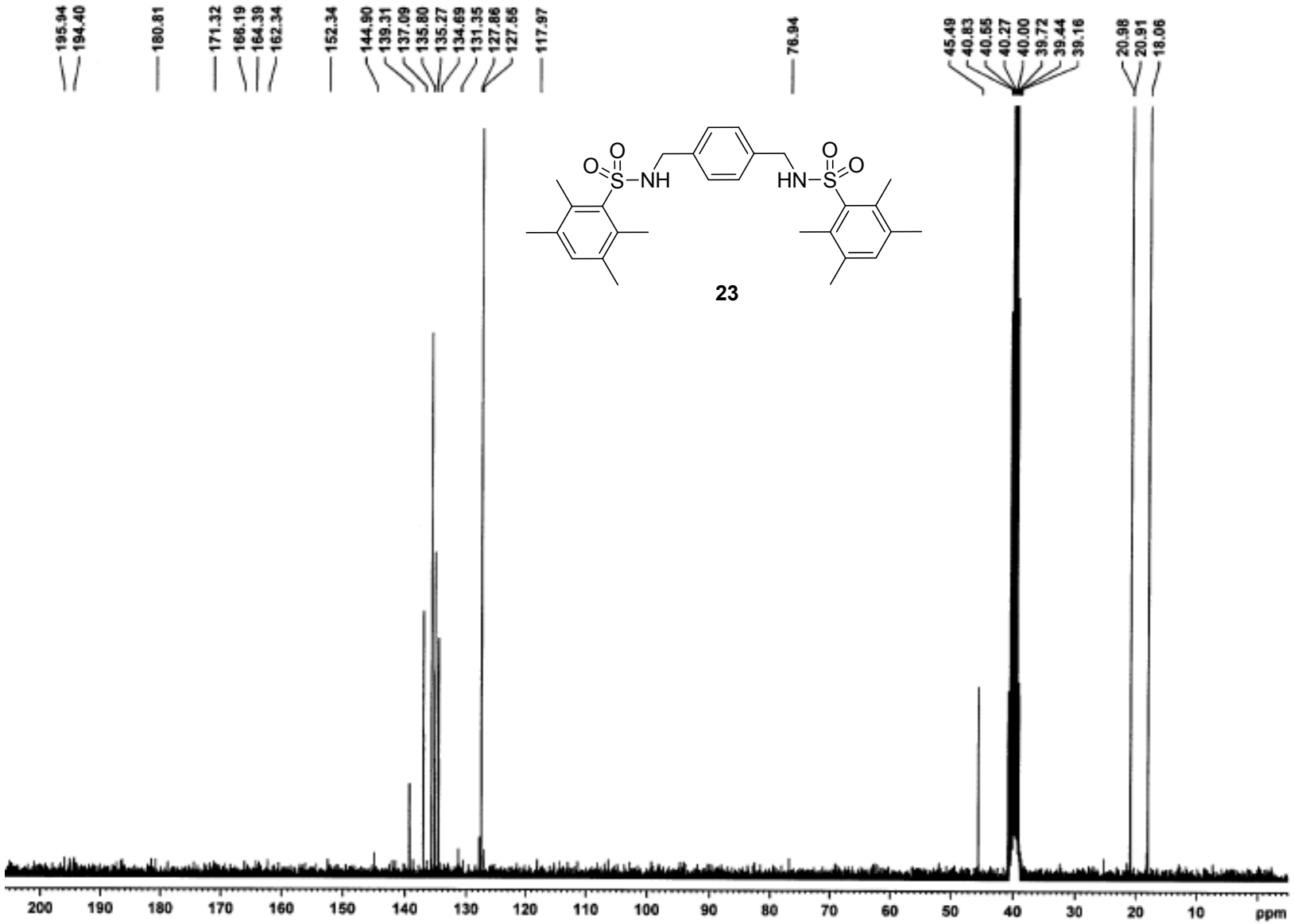

^{13}C NMR spectrum of compound **23** (DMSO-d_6)

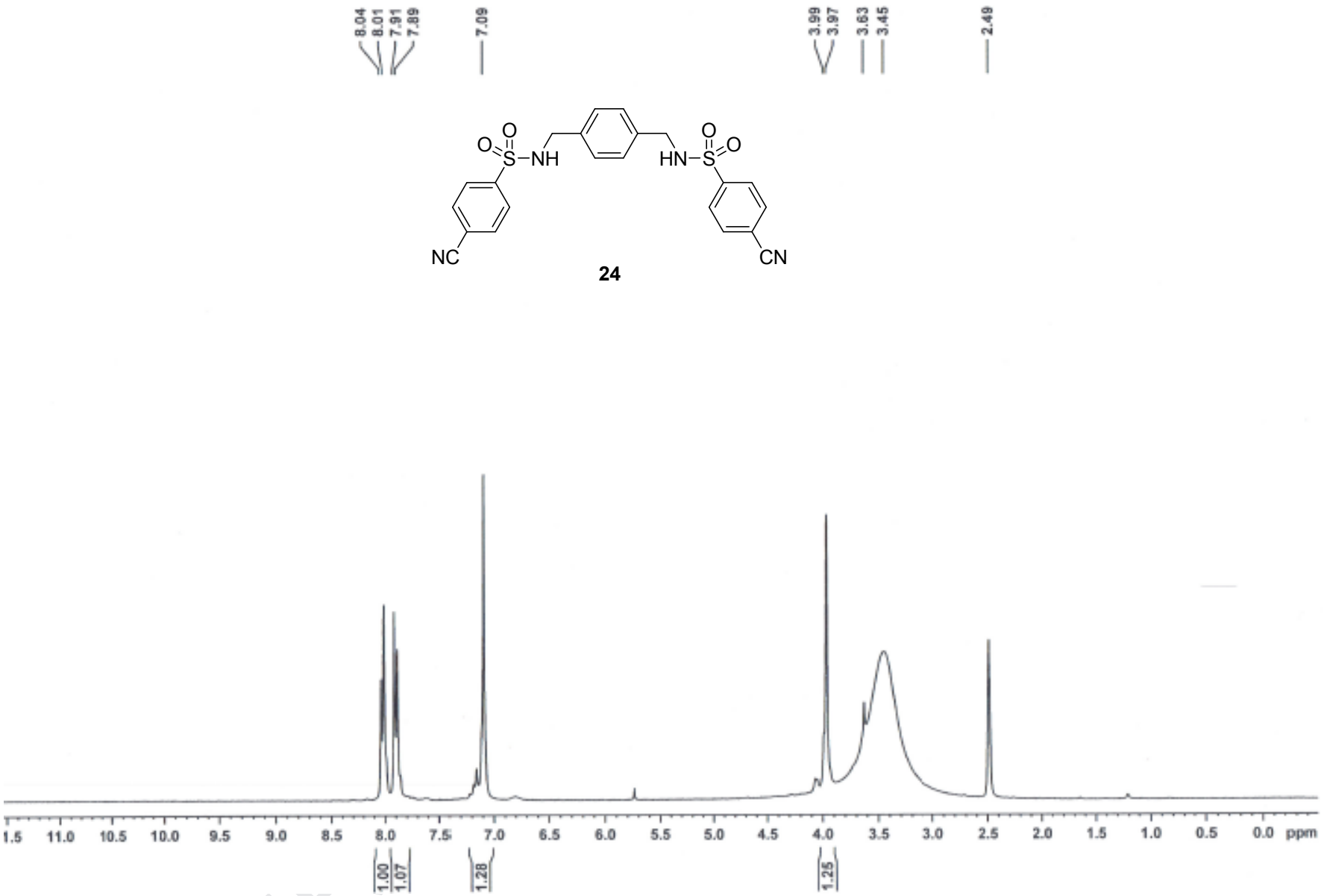

^{1}H NMR spectrum of compound **24** (DMSO-d_6)

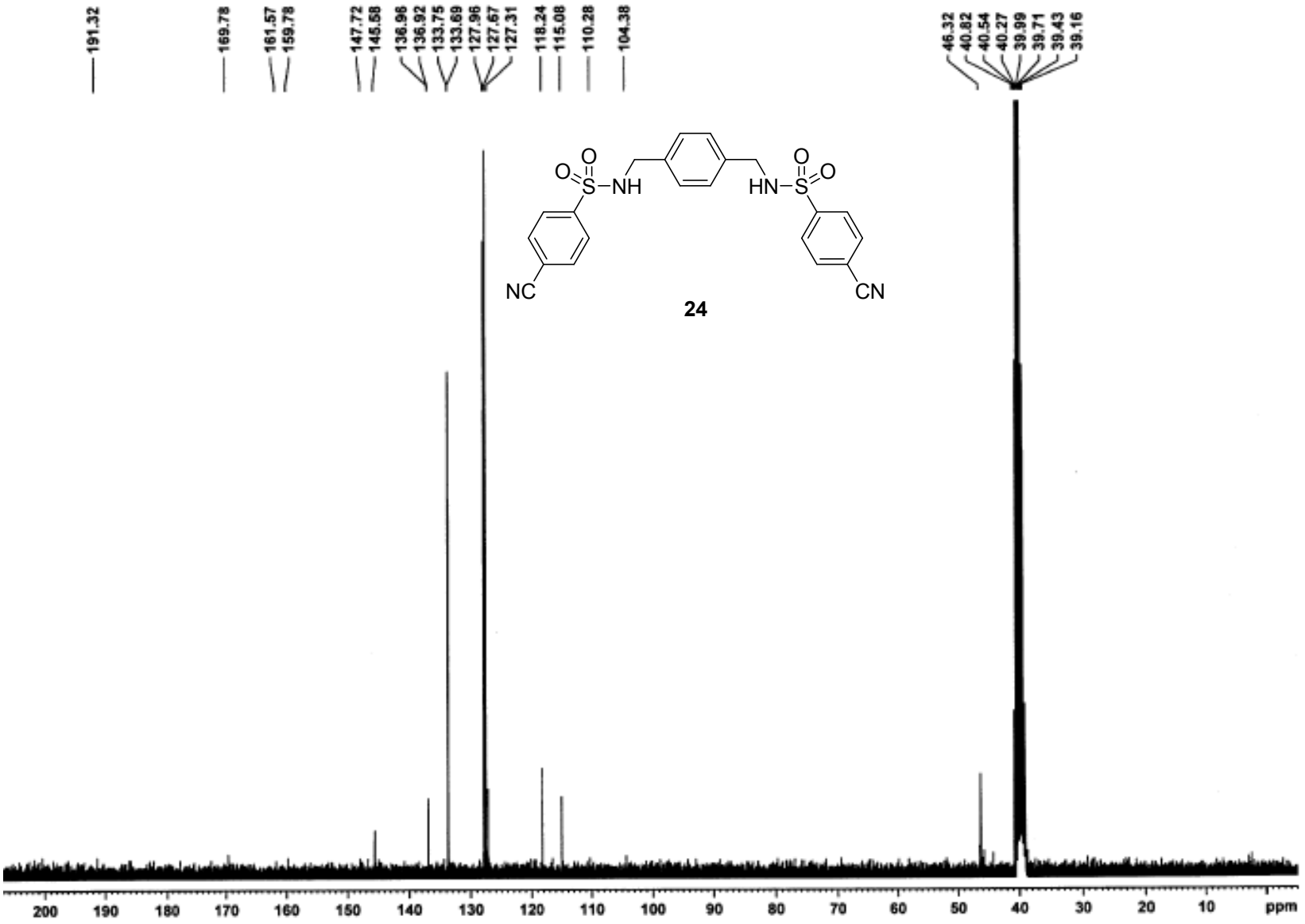

^{13}C NMR spectrum of compound **24** (DMSO-d_6)

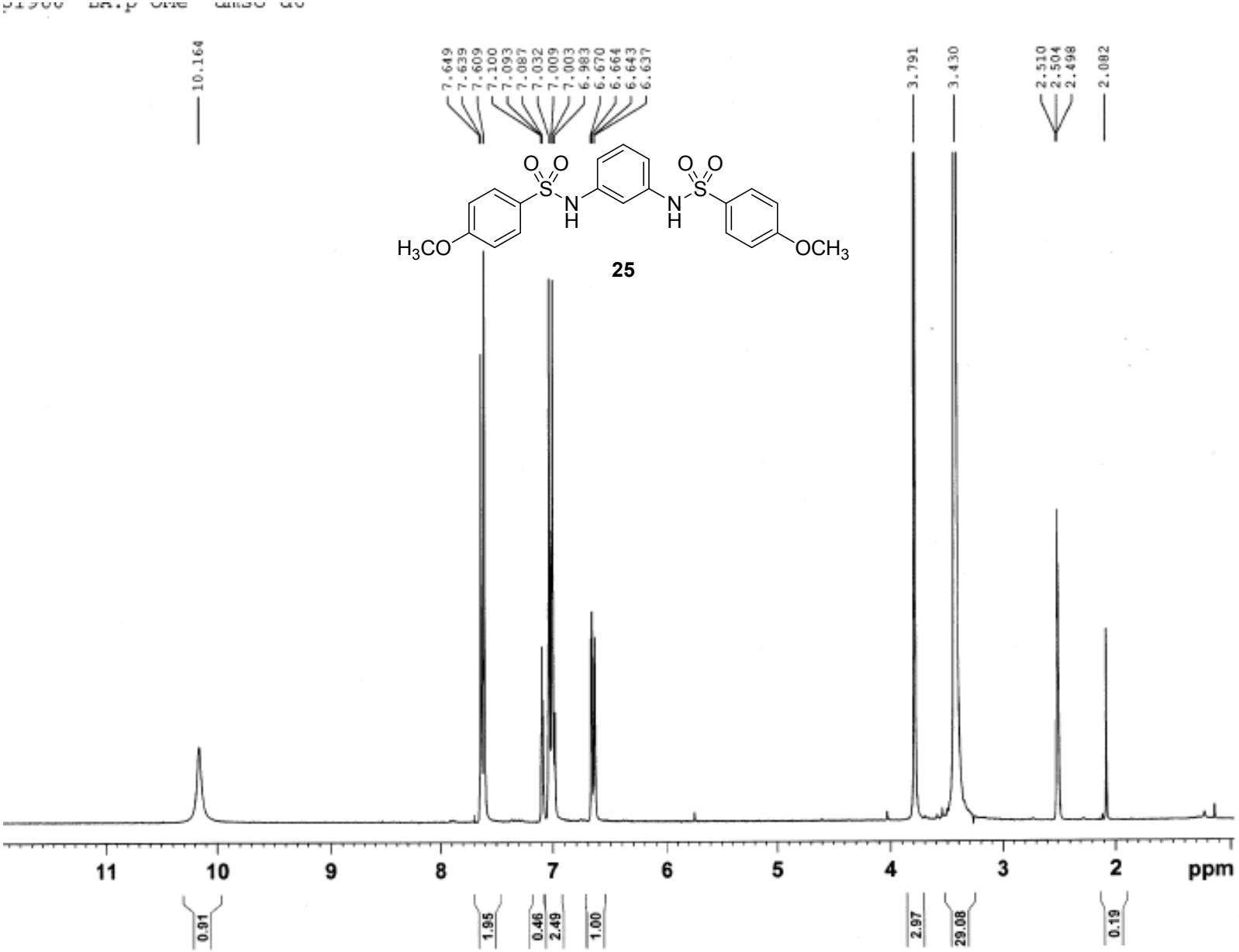

^{1}H NMR spectrum of compound **25** (DMSO-d_6)

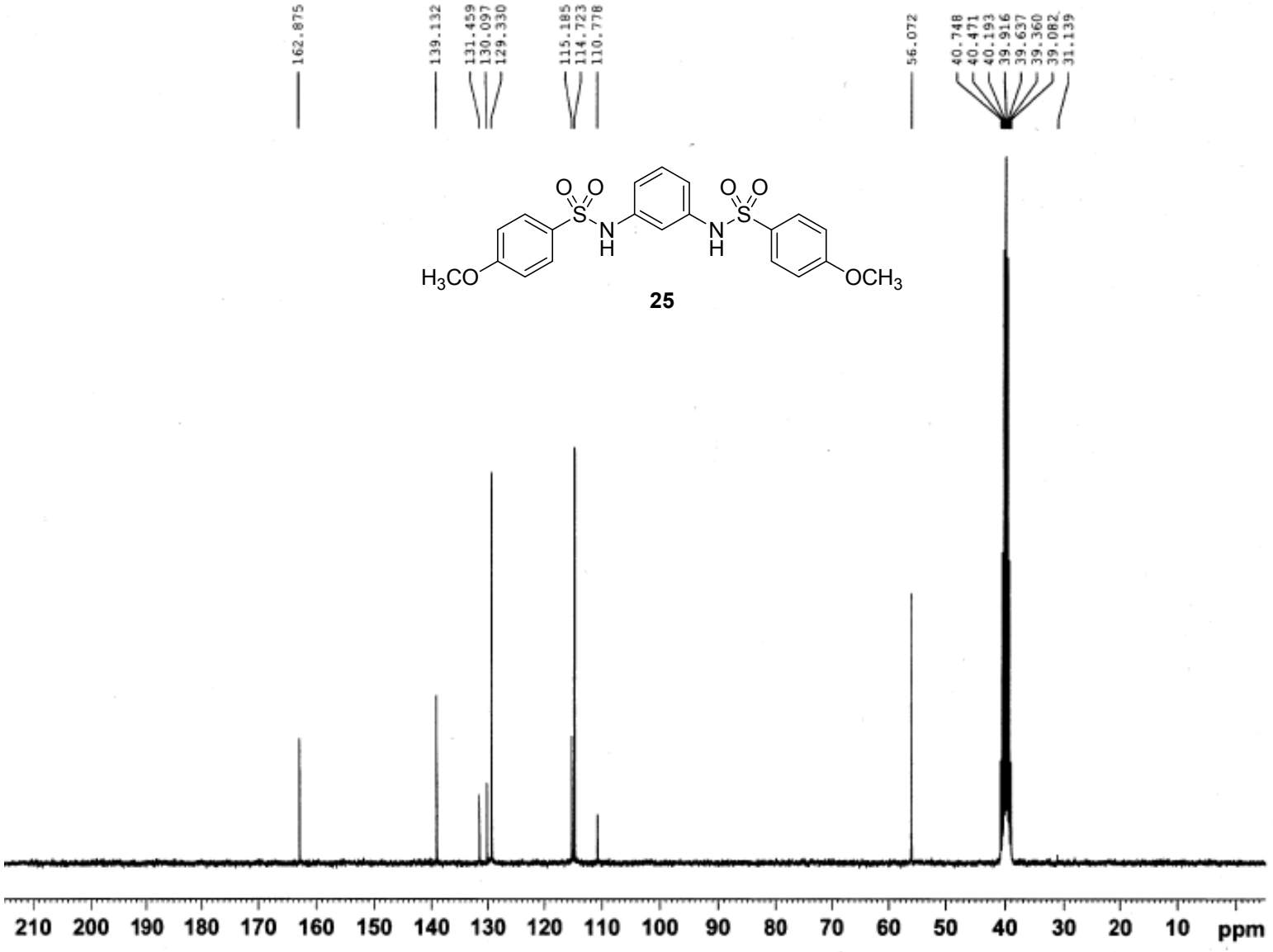

^{13}C NMR spectrum of compound **25** (DMSO-d_6)

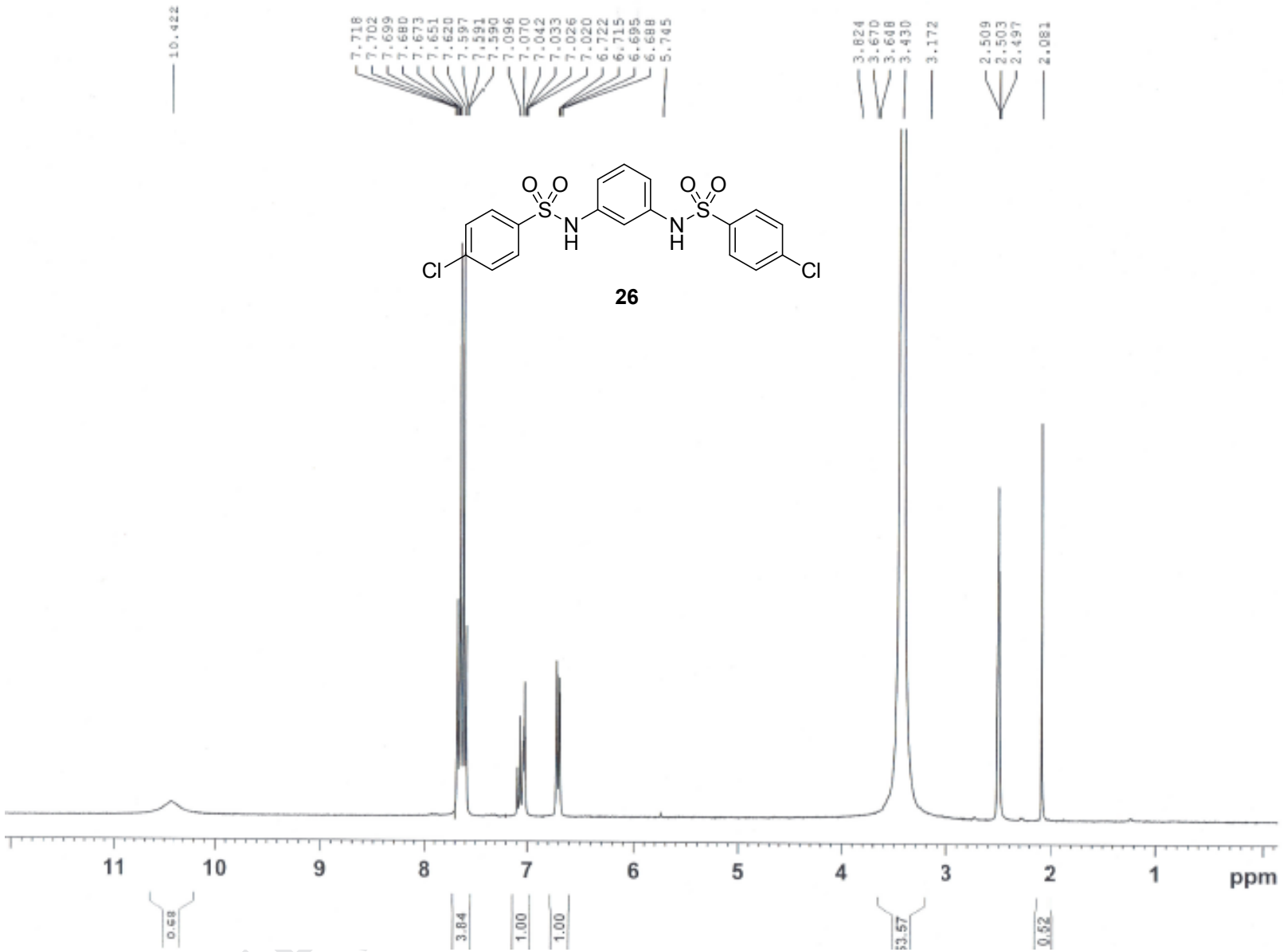

^{1}H NMR spectrum of compound **26** (DMSO-d_6)

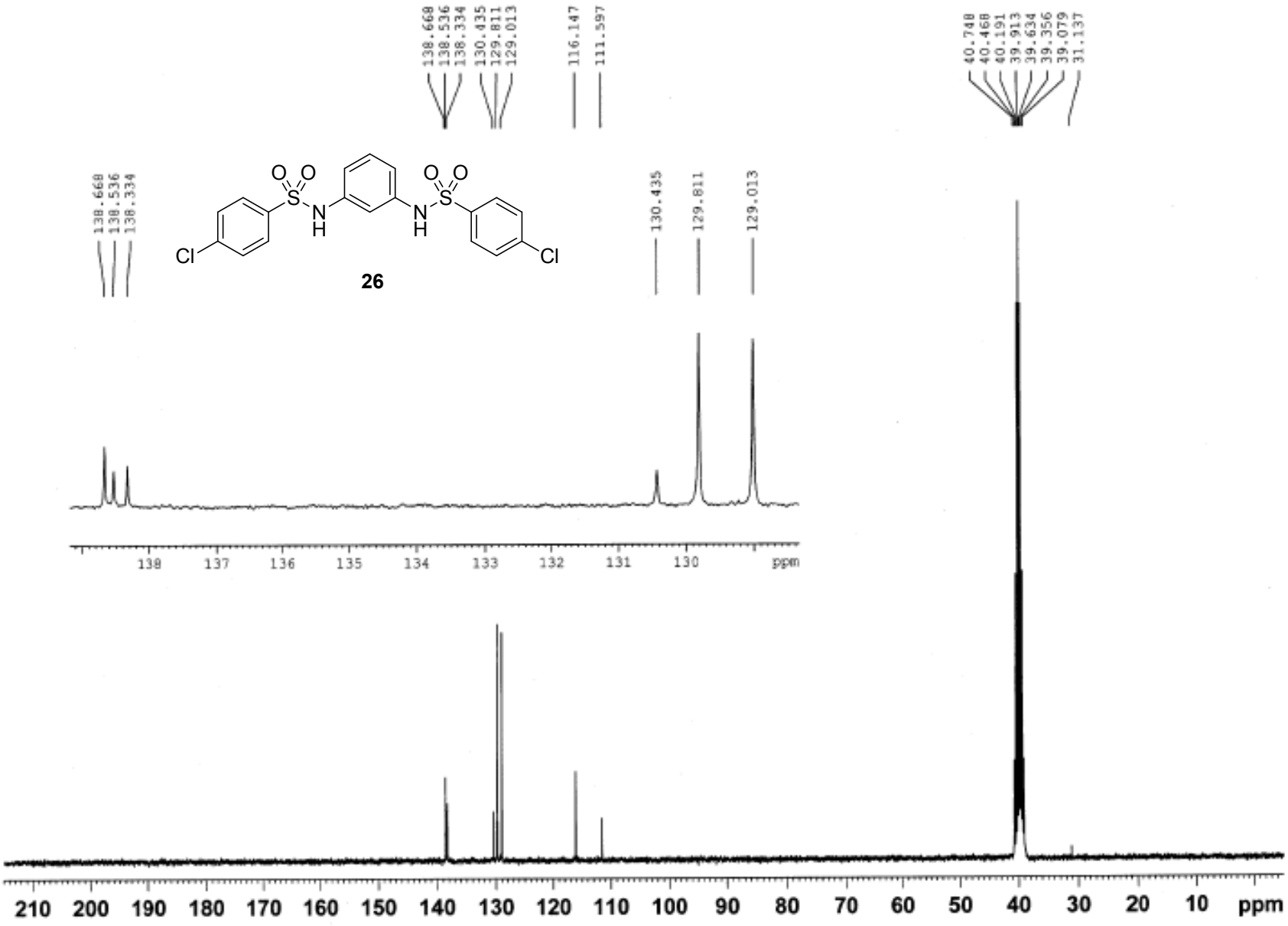

^{13}C NMR spectrum of compound **26** (DMSO-d_6)

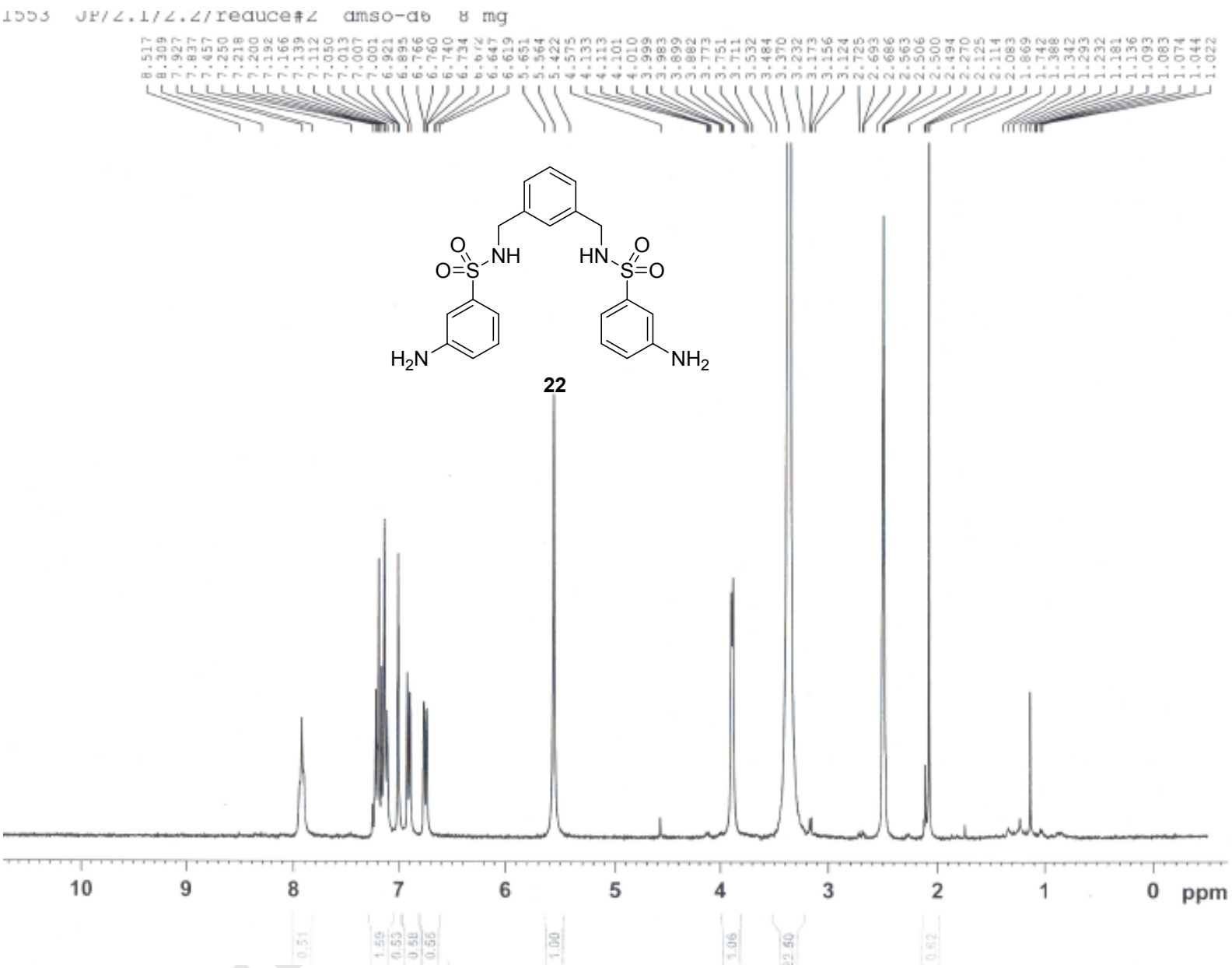

^{1}H NMR spectrum of compound **22** (DMSO-d_6)

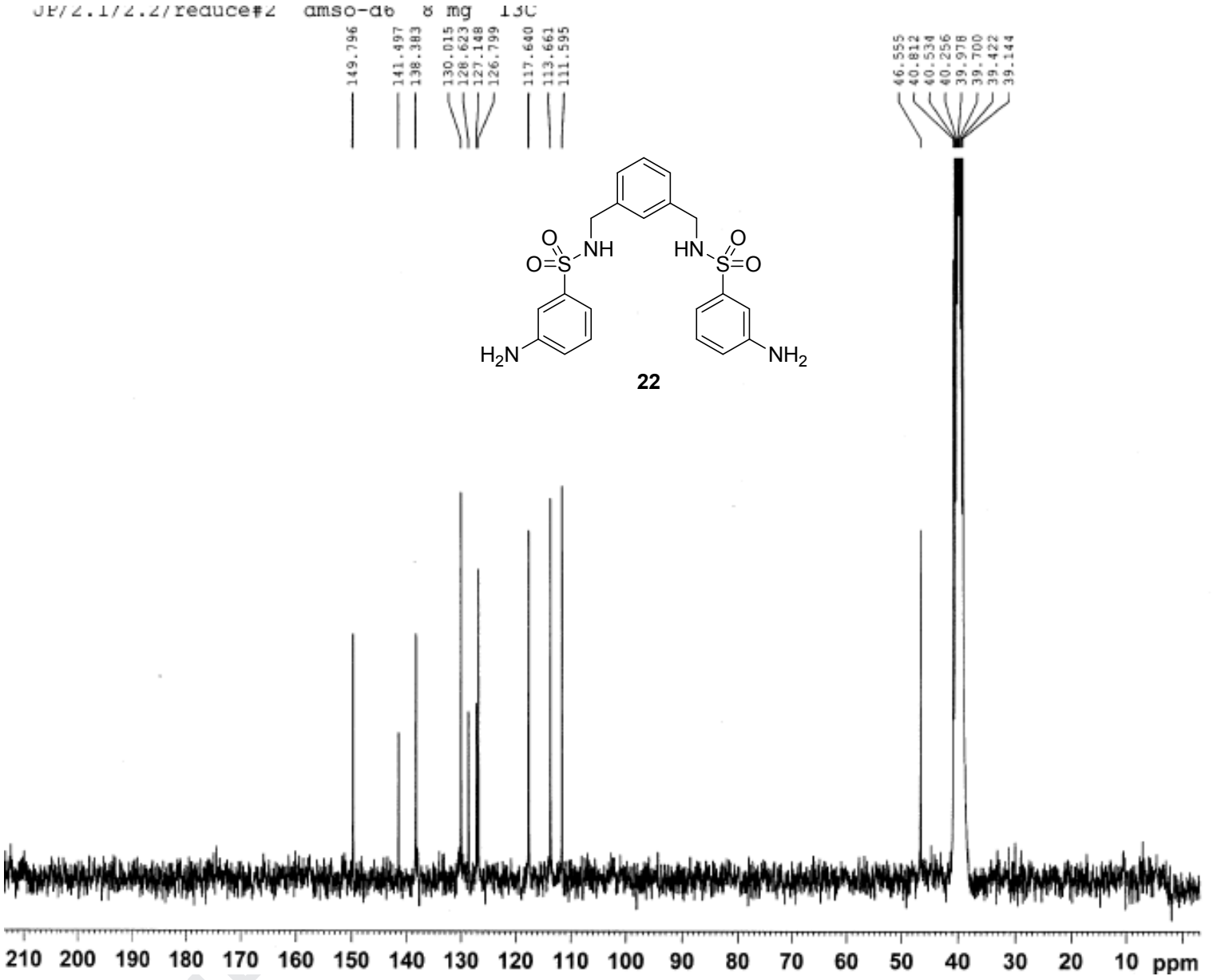

^{13}C NMR spectrum of compound **22** (DMSO-d_6)

▶ Eighteen bis-sulfonamides were synthesized.

▶ Seventeen bis-sulfonamides displayed aromatase inhibitory activity (IC_{50} = 0.05-11.6 μM).

▶ Chloro (**15**, IC_{50} = 50 nM) and bromo **(16**, IC_{50} = 60 nM**)** analogs are promising inhibitors with high safety index.

▶ Molecular docking and QSAR were studied.

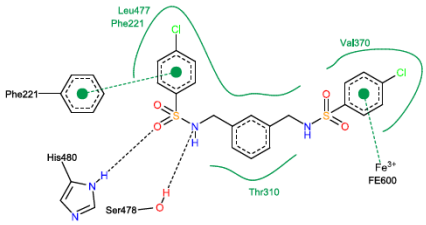

Compound **15**: aromatase inhibitory activity
IC_{50} = 50 nM; SI = 1370

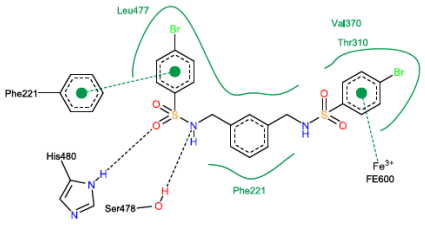

Compound **16**: aromatase inhibitory activity
IC_{50} = 60 nM; SI = > 1451